Managing Soybean Iron Deficiency Chlorosis with Agronomics, Economics, and Remote Sensing

A THESIS SUBMITTED TO THE FACULTY OF THE UNIVERSITY OF MINNESOTA BY

Maykon Junior da Silva

IN PARTIAL FULFILLMENT OF THE REQUIREMENTS FOR THE DEGREE OF MASTER OF SCIENCE

Adviser:

Dr. Seth Naeve

March 2023

Acknowledgements

First and foremost, I would like to express my sincere gratitude to my advisor Dr. Seth L. Naeve for the endless support during my M.S. studies and related research. Thank you for providing me guidance and extensive opportunities that contributed immensely to my personal and professional development. I will always be grateful for your willingness to help, teach, and listen. Your passion and dedication towards soybean research are something I will always carry with me.

I am also grateful for my committee members, Dr. Daniel Kaiser, Dr. Jeffrey Coulter, and Dr. Joe Knight for serving on my committee, and for their insightful comments and suggestions on this thesis. In addition, I would like to thank the Minnesota Soybean Research and Promotion Council for funding this project.

A very special thanks to all members of the Naeve Lab for their contributions. The lab technicians (Victor L. Guimera, Dimitri von Ruckert, Mitchel Johnson), MAST students (Maiquel P. Pes, Regina Stacke, Junior Somavilla, Fabiano Schirmer, and Lucas Zaqueo), researchers (Jill M. Garvin and Jesse Christenson), and visitor's professor Anibal Cerrudo. I am deeply grateful to all of you. This project could not have been completed without your hard work and support.

Lastly, I would like to thank all the good friends I have made in Minnesota over the years. Your friendship made me feel welcomed and have brightened my time in the US.

Dedication

It is with genuine gratitude and warm regard that I dedicate this thesis to my family, whose good examples have taught me to work hard for the things that I aspire to achieve. A special feeling of recognition to my mother, Cleunice Lisete Schappo, father, Junior Roberto da Silva, brother, Matheus Roberto da Silva, sister, Isabella Cristina Bullow, grandfather, Elvino Schappo, grandmother, Ilse Maria Schappo, and stepfather, Vanderlei Bullow. I also dedicate this work and give special thanks to my girlfriend Hanna Floistad, who has been a constant source of support and encouragement during the challenges of graduate school and life. I am truly thankful for having you in my life.

Abstract

Iron deficiency chlorosis (IDC) is a major yield-limiting factor for soybean [*Glycine max* (L.)] grown on high pH calcareous soils. In soybean, IDC is caused by a lack of soluble (Fe^{2+}) iron to the plants, with symptoms characterized by interveinal chlorosis of the leaves and stunting of the growth. In order to overcome the problem and ensure profitability, effective and economical solutions are needed. This study examined the effectiveness and interactive effects between three of the most often used management strategies for soybean IDC across a range of IDC stress levels: varietal tolerance [highly tolerant (HT) and moderately tolerant (MT)], iron chelate rates (0, 2.24 and 4.48 kg Fe-EDDHA ha^{-1}) and seeding densities (309,000 and 433,000 seeds ha^{-1}). Given that there is a trade-off in cost and yield relative to the adoption of each of these management strategies, profitability and economic risk analysis were performed to evaluate the impact of variety selection, seeding densities, and iron chelate rates on economic returns. Overall, our findings determined that planting a HT variety, applying Fe-EDDHA in-furrow at planting, and increasing the seeding rate were all effective at minimizing yield losses due to IDC. For every one-point increase in IDC severity measured by our environmental index (EI), the HT variety yielded 0.21 Mg ha^{-1} more, on average, than the MT variety. A similar trend was observed with iron chelate application. As IDC became very severe (EI of 4, for example), yield improvements averaging 1.4 and 1.7 Mg ha^{-1} were observed with soil applications of 2.24 and 4.48 kg Fe-EDDHA ha^{-1}, respectively, compared to the untreated plots. Although a smaller effect was observed with increased seeding rates (150 kg ha^{-1} yield increase with 433,000 seeds ha^{-1} relative to 309,000 seeds ha^{-1}), this effect was consistent across environments and treatment combinations. For profitability and economic risk analysis, environments were classified into low-moderate and severe IDC based on their EI. Our economic risk analysis showed that the best option in terms of risk to reward for low-moderate IDC conditions was the HT variety with 2.24 kg Fe-EDDHA ha^{-1} at 309,000 seeds ha^{-1}. Conversely, when IDC was severe, the single best alternative for IDC management considering the amount of risk per unit of reward was the HT variety with 4.48 kg Fe-EDDHA ha^{-1} planted at 433,000 seeds ha^{-1}, which provided a sharpe ratio only 0.02 points lower than the optimum portfolio. Because IDC most frequently occurs in

complex and discontinuous patterns, creating low, moderate, and severe areas interspaced within a field, growers very often do not know the extent of these areas and amount of yield loss being caused by this abiotic stress. Thus, this study also investigated the utility of UAV-based vegetation indices for estimating grain yield of soybean grown under IDC stress conditions as a tool to aid growers, researchers, industry and policy makers with crop management, market planning, market research, and policy writing. Results from this study showed that in-field assessment of IDC symptoms using vegetation indices (VI's) generated from UAV imagery is more precise, objective, and efficient than ground-based methods such as visual chlorosis scores and ground-based canopy sensing tools such as Crop Circle™. In addition, we found that NDVI provides the highest predictive power for yield estimation at R1, while NDRE provided the most accurate yield estimations at R5.5. These two VI's were then used as explanatory variables for yield prediction model development using linear regression. Performance analysis showed that NDRE at R5.5 was more accurate in predicting yield than NDVI at R1, but the overall performance of both models could have been better when validated with testing data. As such, an alternative approach was proposed to improve yield forecasting accuracy. A path analysis was performed to identify the cause-and-effect relationship between VI's and grain yield, which indicated NDRE at R5.5, OSAVI at R5.5, and NDVI at R1 as most relevant for yield estimation. These VI's were used as predictors in a regression tree algorithm, which was able to predict soybean yield with a relatively low RMSE (0.53 Mg ha^{-1}) and MAE (0.45 Mg ha^{-1}), while explaining more than 93% of the yield variability. Results from this study can help soybean growers increase productivity, improve economic returns while controlling economic risk, and provide an advantage when it comes to agricultural decision making.

Table of Contents

List of Tables

List of Figures

Chapter 1. Literature Review

1.1 Soybean Production Worldwide and in the USA

Soybean [*Glycine max* (L.) Merrill] is a leguminous plant in the Fabaceae family and is extremely valuable for livestock feed and human diets, primarily due to its protein-rich meal, and as an oilseed crop for many food ingredients and industrial uses (Clemente and Cahoon, 2009; Vogel et al., 2021). Typically, soybean seeds contain around 36% protein, 19% oil, 28% carbohydrates, and 4% mineral elements, but the expression of these contents can vary significantly based on genotype by environment interactions (Gopalan et al., 1974; SOPA, 2002; Pipolo, 2002). Native to Eastern Asia, soybean domestication occurred around 5000 years ago from its wild ancestor *Glycine soja* Sieb. & Zuccc. (Carter et al., 2004; Hymowitz, 2004; Qiu and Chang 2010). In view of the concerted efforts in domestication, breeding improvements, and enhanced agronomic practices, soybean has become the major contributor to the world's oilseed production (Anderson et al., 2019).

In the 2020/2021 marketing year, soybean alone accounted for 60% of the global oilseed production (619.2 million metric tons, MMT), while other crops such as rapeseed, sunflower, and peanut accounted for 11%, 9%, and 8%, respectively (USDA-FAS, 2021). Currently, soybean is grown on 127.9 million hectares (ha) worldwide, with a total annual production of 366.2 MMT (USDA-FAS, 2021). Brazil, USA, and Argentina are the leading countries in soybean production, holding a respective share of 38%, 31%, and 13% of global production (Table 1-1). Together, these three countries contribute 82% of the annual soybean production and 70% of the harvested area globally (USDA-FAS, 2021).

Farmers in North America first cultivated soybean as early as 1765, using cultivars brought by sailors from China (Qiu and Chang, 2010; Gaonkar and Rosentrater, 2019). Before the early 1950's, soybean was grown in the US as a soil nitrogen builder and forage crop (Anderson et al., 2019). Then, two main factors triggered soybean production on an increasingly large scale in the country: a) an explosion in livestock and poultry production due to low-cost soybean meal availability, and b) the recognition of its value as a source of vegetable oil (Brar and Carter, 1993). Between 1970 and 2021, soybean planting in the US expanded more than 85%, increasing from 17.1 to 33.4 million hectares harvested (USDA-

FAS, 2021). Currently, soybean is the second most relevant US grain crop regarding area planted with a total market value of US$45.7 billion (Soystats, 2022).

Along with the increase in planted and harvested acreage, a change in the geography of soybean production occurred. As breeding programs began developing new varieties that demanded shorter growing periods and were more tolerant of drier conditions, soybean production expanded northward and westward ("U.S. Soy: International Buyer's Guide", 2006). Presently, the top ten producing states in the US are Illinois, Iowa, Minnesota, Indiana, Nebraska, Missouri, Ohio, South Dakota, North Dakota, and Kansas (USDA-NASS, 2021). As shown in Table 2-2, more than 80% of the US soybean production occurs in the midwestern United States.

As soybean has been extensively grown in areas of the Midwest, where high calcium carbonate content and high pH are intrinsic properties of the soil, significant yield losses have been reported due to Iron Deficiency Chlorosis (IDC) (Inskeep and Bloom, 1984; Rogovska et al., 2007; Goos and Johnson, 2000; Helms et al., 2010; Hansen et al., 2003). Using a geographic information system with maps of soil pH, Hansen et al. (2004) mapped the area where IDC is expected to be a problem in North Central US. The authors estimated the total area of soybean grown under IDC-prone soils to be approximately 1.8 million hectares in the region encompassing the states of North and South Dakota, Minnesota, and Iowa. In addition, a 160% expansion in soybean acreage was verified between 1970 and 2002 in this region, which is a clear demonstration of how IDC has become a major problem for soybean grown in the Upper Midwest (Hansen et al., 2004).

1.2 Soybean Iron Deficiency Chlorosis

Iron (Fe) is the fourth most abundant mineral element in the crust of the Earth, and in fact, IDC is not associated with a shortage of Fe in the soil (Stucki et al., 1988; Hansen et al., 2003). The form of iron present in the soil solution is what determines availability for plant uptake, and consequently, the incidence of IDC (Inskeep and Bloom, 1987; Marschner and Romheld, 1994). Soybean plants preferentially take up the soluble/reduced form of iron [Fe^{2+} or ferrous iron] (Kaiser and Bloom, 2018). When iron becomes less soluble in the soil, i.e. present in its ferric [Fe^{3+}] form, plants cannot absorb it (Naeve, 2004). Without a sufficient supply of iron, the synthesis of chlorophyll, necessary for

photosynthesis, is restricted, resulting in IDC development, a common symptom of iron deficiency (Goos and Johnson, 2000; Gambel et al., 2014).

In soybean, IDC is characterized by interveinal chlorosis (leaves that are yellow with dark green veins) and overall stunting of growth (Hansen et al., 2003; Inskeep and Bloom, 1987). Typically, IDC symptoms appear as early as when the first trifoliate leaf appears and can persist until maturity if IDC is severe but are most common from V2 to V4 developmental stages (Inskeep and Bloom, 1987; Caviness and Fehr, 1981; Niebur and Fehr, 1981). Since iron is not translocated from older to younger tissues, new growth is most affected in soybean plants (Ham and Dowdy, 1978; Karlen et al., 1982; Sojka et al., 1986; Sadler et al., 1991; Zhang et al., 1996; Burton et al., 1998). Under extreme conditions, IDC symptoms can include necrosis which progresses from the edges of the leaves to the entire leaflets decreasing the amount of leaf tissue available for photosynthesis, and may even lead to plant death (Wiersma, 2005; Goos and Johnson, 2000; Caliskan, 2008; Rodriguez-Lucena et al., 2009; Liesch et al., 2011; Kandel, 2014).

There are two major mechanisms that plants have developed to increase their ability to take up iron when Fe bioavailability is low: strategy I and strategy II (Marschner et al., 1986). As a strategy I plant, soybean relies on three adaptive components to maintain sufficient iron levels in its tissues (Romheld, 1987; Jolley et al., 1996). First, soybean plants activate a membrane-bound H^+-ATPase that releases protons into the rhizosphere to promote its acidification and thus increase the solubility of ferric chelates (Romheld et al., 1984; Santi and Schmidt, 2009). Once these Fe^{3+} chelates have been solubilized, ferric iron is reduced to soluble ferrous iron with the aid of a ferric reductase enzyme, encoded by the FRO2 (Ferric Reductase Oxidase 2) gene (Beinfait et al., 1985; Tipton and Thowsen, 1983). Following the reduction of insoluble ferric iron to soluble ferrous iron, Fe^{2+} is imported into epidermal cells via an iron uptake transporter encoded by the IRT1 (Iron-Regulated Transporter 1) gene (Kim and Guerinot, 2007). After iron has entered the root, it moves through the xylem chelated with nicotianamine and citrate (Hell and Stephen, 2003). Other reducing agents and organic chemical compounds are also extruded by soybean roots under iron deficiency and have been reported to be directly involved in iron acquisition (Clemens and Weber, 2016) yet the biochemical mechanism by which they influence iron nutrition is not fully understood (Joeng et al., 2017).

However, several soil physical and chemical properties and their interactions can modify the solubility of Fe in the soil or limit the success of plant-mediated iron reduction mechanisms by creating an environment that impairs their effectivity (Inskeep and Bloom, 1987; Hansen et al., 2003). Factors such as soluble salt concentration, soil moisture content, levels of calcium carbonates, soil pH, and residual soil nitrate can significantly influence the incidence and severity of IDC (Morris et al., 1990; Rogovska et al., 2007; Bloom et al., 2011; Liesch et al., 2012).

1.3 Environmental Factors that Promote IDC

Different from Strategy II species that transport insoluble Fe^{3+} into the root cells as an entire ferrated (Fe^{3+}) phytosiderophore complex [Fe(III)-PS], soybean, as a Strategy I plant, transports soluble Fe^{2+} into the roots (Rohmheld, 1987). In alkaline soils, with pH ranging from 7.4 to 8.5, iron precipitates as Fe hydroxides [$Fe(OH)_x$], lowering its solubility. Previous research has shown that the solubility of iron is reduced a thousand-fold for every unit increment in soil pH (Latimer, 1952; Lucena, 2003). The combination of high pH with the low solubility of these Fe precipitates significantly reduces iron availability for plant uptake, promoting deficiencies (Ortiz et al., 2007; Schenkeveld et al., 2008; Rodriguez et al., 2010; Kobayashi and Nishizawa, 2012; Lucena and Hernandez-Apaolaza, 2017).

Another soil factor contributing to IDC expression is high concentrations of calcium carbonates, measured as calcium carbonate equivalent (CCE), in the soil (Bloom, 1987). Calcareous soils are prone to IDC because carbonate, when in the soil solution, acts as lime, raising the soil pH and oxidizing ferrous iron (Fe^{2+}) to ferric iron (Fe^{3+}). In addition, carbonate also function as a buffer against plant-mediated iron reduction mechanisms, neutralizing the H^+ protons and organic acids excreted from the roots, thus inhibiting the reduction of Fe^{3+} to Fe^{2+} (Kaiser et al., 2011; Hansen et al., 2003). In the soil, carbonate levels are determined by two major processes: a) dissociation of calcium carbonates into Ca^{2+} and CO_3^{-2} (carbonate) under high soil moisture content, and b) by extrusion from roots when nitrate is available in excess in the soil (Hansen et al., 2003; Merry et al., 2021). Therefore, residual nitrate (NO_3^-) in the soil also exacerbates the severity of IDC (Silva and Uchida, 2000; Kaiser et al., 2011). When NO_3^- is excessively

available in the soil, nodule development and N_2 fixation are reduced and thus N acquisition relies on mineral soil N absorption (Gibson and Harper, 1985). During NO_3^- assimilation, a differential uptake of anions and cations occurs (Aktas and Van Egmond, 1979; Lucena, 2000). Consequently, instead of releasing H^+ ions, soybean roots extrude HCO_3^- into the soil medium to balance intracellular charge (Wiersma, 2010). In the soil, HCO_3^- also shows a buffering effect, neutralizing the protons released from the roots that were meant to acidify the rhizosphere and reduce ferric iron to ferrous iron (Inskeep and Bloom, 1987).

Several factors can influence the amount of nitrate present in the soil, including carryover from the previous crop, mineralization of organic N, and denitrification (Broom et al., 2011). Denitrification is affected by soil moisture and temperature. Low soil temperature and low soil moisture content can greatly lower denitrification, resulting in higher NO_3^- levels at the time of soybean planting (Hilton et al., 1994). However, if nitrate carryover from the previous crop is low, soil temperature is relatively high, and early season soil moisture is substantial, soil nitrate concentrations can be reduced, minimizing its effect on IDC incidence and severity (Bloom et al., 2011).

The generation of HCO_3^- in the soil is also affected by excess soil moisture. Water saturated soils are prone to IDC because filling of soil pores reduces the rate of gas diffusion in the soil medium (Inskeep and Bloom, 1997). This decrease in gas exchange results in accumulation of CO_2 produced through respiration. When trapped in the soil solution, CO_2 is dissolved to carbonic acid (H_2CO_3) and at alkaline pH's, protons are donated to H_2CO_3 ion exchange sites increasing bicarbonate levels in the soil (Inskeep and Bloom, 1986). As mentioned above, buffering caused by HCO_3^- can limit the conversion of unavailable ferric iron to readily available ferrous iron, a necessary step in Fe uptake by soybean plants (Lucena, 2000).

High concentration of soluble salts has also been suggested to have a role in IDC incidence. Dahiya and Singh (1979) found that an increase in salt levels decreases iron availability in the soil for plant uptake. The relationship between IDC and soluble salts was also studied by Franzen and Richardson (2008), who verified that higher amounts of soluble salts stress the plant and exacerbate IDC.

Iron deficiency chlorosis is a major yield-limiting stress for soybean cultivated in southwest, south central, west central, and northwest Minnesota (Kaiser and Bloom, 2018). In these regions, soybean IDC is predominantly found in shallow depressions and on the rims of potholes, where higher concentrations of calcium carbonates and salts accumulated because of evaporation of large amounts of water from when the soils were wet prairies (Naeve, 2004; Kaiser and Bloom, 2018). While soils with a pH higher than 7.5, carbonate levels higher than 5%, and salt concentrations higher than 1 mmhos/cm are good indicators of high IDC risk, predicting IDC through soil testing is difficult and imprecise. Therefore, the best method to predict IDC is from past history (Naeve, 2004).

A study conducted by Hansen et al. (2003) in western Minnesota indicated that IDC is a common and economically important issue in 99% of farms that responded their survey. These soybean growers indicated that 24% of their crop was affected by IDC. The average yield losses in those areas were reported to be 0.8 Mg ha^{-1}. Similar yield reductions caused by IDC were also reported by Inskeep and Bloom (1987). Froechlich and Fehr (1981) evaluated the relationship between agronomic performance and the amount of IDC that soybean cultivars could sustain when grown on calcareous soils and observed a 20% yield reduction for every one-point increase in chlorosis scores at the V3 phenological stage on a five-point visual severity scoring. In such rating system, a score of 1 indicates zero chlorosis apparent, a score of 2 indicates slight chlorosis, a score of 3 indicates moderate chlorosis, a score of 4 indicates intense chlorosis, and a score of 5 indicates severe chlorosis with some necrosis.

Although the costs associated with yield losses due to IDC can vary substantially with the value of the crop, the amount of area planted in a given year, and the severity of IDC symptomology (Merry et al., 2021), it was estimated that IDC costs soybean producers approximately $260 million a year in the United States (Peiffer et al., 2012). Since even minor IDC symptoms may result in significant yield reductions, management strategies are extremely important when it comes to decreasing the severity and duration of symptoms throughout the growing season (Niebur and Fehr, 1981).

1.4 Management Strategies for Soybean Iron Deficiency Chlorosis

In the same 2002 survey conducted by Hansen et al. (2003), soybean growers in the Upper Midwest indicated the adoption of the following strategies to manage IDC: variety selection (90%); seeding management comprising seeding rate, row spacing, and planting date (42%); artificial drainage (33%); tillage (16%); and fertility management including foliar and soil applications and seed treatments (11%). Several of these management practices have been reported to prevent or reduce the drastic losses caused by IDC.

Planting varieties with improved tolerance has long been suggested as the most important and most practical strategy to manage iron chlorosis (Niebur and Fehr, 1981; Goos and Johson, 2000; Wiersma, 2005; Naeve and Rehm, 2006; Helms et al., 2010; Kaiser et al., 2014). Soybean varieties vary widely in how they respond to IDC, with some being highly susceptible and others being exceptionally tolerant (Dobbles, 2020). Soybean varieties with high resistance to IDC possess an increased capacity to reduce Fe^{3+} to Fe^{2+}, enhancing iron uptake (O'Rourke et al., 2007). In a study comparing management strategies to prevent IDC in soybean, Kaiser et al. (2014) verified that the tolerant variety outyielded the susceptible variety by 34% when IDC was severe. In addition, the authors found that in terms of risk, planting the high resistance cultivar alone appeared to be as good as planting the low resistance cultivar with any of the other IDC treatments tested (oat as a companion crop and Fe-EDDHA in-furrow).

Fertility management through the application of different sources of Fe to control IDC has previously been studied, but effectiveness can vary substantially across environments and cultivars (Wiersma, 2005). Chelated Fe fertilizers are commonly utilized in IDC-prone fields to alleviate symptoms and avoid losses (Gamble et al., 2014; Goos & Johnson, 2001; Helms et al., 2010; Kaiser et al., 2014; Wiersma, 2007). Iron chelates are synthetic or naturally derived products of high stability as Fe fertilizers that make iron readily available to plants (Wittwer et al., 1965; Lucena-Rodriguez and Apaolaza-Hernandez, 2010). Chemically, a chelating compound binds the metal ion (cations) through multiple sites, protecting the nutrient from precipitation, thus maintaining its availability for a longer period (Augustin, 2019).

The three common chelated forms of iron are Fe-EDTA (ethylene diamine tetraacetic acid), Fe-DTPA (diethylene triamine phentaacetic acid), and Fe-EDDHA

(ethylenediamine-*N*,*N′*-di[(*ortho*-hydroxyphenyl) acetic acid]), differing in their ability to hold iron in solution, therefore keeping iron soluble and available in the soil (Lucena et al., 1992). Nonphenolic chelates, such as Fe-EDTA have been reported to not increase soybean yield in IDC-prone areas (Lucena, 2003). According to Lindsay (1972), Fe-EDTA becomes unstable and loses its capacity to maintain Fe availability when applied in calcareous soils with a pH above 6.5. Therefore, since Fe-EDTA efficiency is significantly lowered under these conditions, its use is recommended only under mild chlorotic conditions in fertigation or foliar applications (Abadia et al., 2011; Rodriguez-Lucena et al., 2009).

On the contrary, Fe-EDDHA and Fe-DTPA have been reported to increase grain yield of soybeans grown in calcareous soils (Lucena, 2003). Kaiser et al. (2014) found that in-furrow Fe-EDDHA application at a rate of 3.36 kg ha^{-1} significantly increased the yield of a susceptible variety under moderate to severe IDC conditions. Gamble et al. (2014) evaluated the effectiveness of Fe-EDDHA in controlling IDC in soybean grown in high pH soils of Alabama and verified that all Fe-EDDHA treatments (2.2, 3.4, and 4.5 kg product ha^{-1}) were effective at reducing IDC symptoms under severe conditions. The authors also verified that the application of 4.5 kg product ha^{-1} significantly increased grain yield when supplied in-furrow or as a foliar spray through a split application at planting and at V3 developmental stage. Soil-applied Fe-EDDHA treatments have also been found to prevent IDC and increase grain yield in soybeans by Penas et al. (1990) and Schenkeveld et al. (2007). As opposed to what happens with Fe-EDTA, Fe-EDDHA is stable at pH's ranging from 4 to 9, thus it can maintain iron availability for plant uptake under severe IDC conditions (Lindsay and Schwab, 1982). Soygreen® AST™ is one example of a Fe-EDDHA product, containing 1.8% Fe in a liquid iron solution (CHS Inc., 2022).

Seed-applied Fe-EDDHA (as a seed coating) has been found to increase soybean yield under IDC conditions. Wiersma (2007) verified a 15% increase in soybean yield with seed-applied Fe-EDDHA under mild to moderate iron deficiency. Promising yield improvement results for Fe-EDDHA applied as a seed coating have also been reported by Karkosh et al. (1988) and Liesch et al. (2011). Other studies, however, have shown little or no yield response in soybean with Fe-EDDHA either as a seedcoat (Good and Johnson, 2000) or in-furrow (Wiersma, 2005). The success of iron chelate application is associated with the rate used and the buffering capacity of the soil (Merry et al., 2021). Under high

buffering conditions, suboptimal iron chelate rates provide only short-term IDC control, which may result in Fe-deficiency symptoms reappearing and negatively impacting harvestable grain yield (Wiersma, 2007).

Research using foliar applications of iron has shown varying levels of success. Goos and Johnson (2000) found a consistent yield increase using foliar iron applications (two sprays of 1.1 kg ha^{-1} of Fe-EDTA, one at V1-V2 and the other at V4-V5) on all three cultivars tested (one more susceptible and two more tolerant to IDC) at one of four sites studied, with an average yield increment of 300 kg ha^{-1} at the responsive site. In a controlled environment, Rodriguez-Lucena et al. (2010) compared five synthetic iron chelates and ten natural complexes for their ability to correct Fe deficiency in Fe-susceptible plants. The authors observed a significant improvement in chlorophyll synthesis and a reduction in chlorotic symptoms when all five synthetic chelates were applied through foliar sprays. Contrarily, foliar Fe treatments have been reported by Chatterjee et al. (2017) to not be effective in controlling IDC when applied to soybeans grown under severe IDC conditions, indicating that iron fertilizers supplied in the form of foliar applications might have a positive effect on symptom recovery but do not significantly increase grain yield. Similar findings have been reported by Hecht-Bucholz and Ortmann (1982), Franzen et al. (2003), and Lingenfelser et al. (2005). These inconsistencies in response to foliar applications of iron may be associated with a physical challenge this management strategy faces. At early growth stages, soybean leaves are relatively small, resulting in a low leaf area, which reduces their capacity to absorb the iron for recovery (Merry et al., 2021).

While providing soybean plants with a chelated form of iron may help overcome the effects of IDC, the cost associated with the product restricts its widespread application (Dobbles, 2020). Historically, iron chelates such as Fe-EDDHA were considered very expensive, and thus their application was not cost-effective (Wiersma, 2005). However, driven by innovations in the manufacturing process of Fe-EDDHA, a new and form of Fe-EDDHA (Soygreen®, a dry water soluble powder with 6% iron in the form of Fe-EDDHA) entered the market in 2006, reducing the cost to soybean farmers (Gaspar, 2010; Kaiser et al., 2014). Applying this type of product as a liquid suspension in-furrow at planting is considered a practical option to soybean growers in central and western Minnesota due to

the widespread availability of planters equipped with technology for similar applications on other crops (Kaiser et al., 2014).

Increasing seeding rate (or plant population) also represents a viable option to minimize the effects of IDC in soybean fields. According to Naeve (2004), more attention has been given to this management strategy by farmers and researchers after two fortuitous events occurred in the late 1990's: a) soybean farmers noticed that a green strip would be formed throughout the fields where air seeders overlapped, increasing the plant population in those areas, and b) researchers at North Dakota State University verified that one single plot had IDC greatly alleviated because of a planting error that ended up doubling the seeding rate of a susceptible variety (Goos and Johnson, 2001).

To confirm this observation, Goos and Johnson (2001) planted a susceptible variety at three different seeding rates in 1999: 185,000 (half of the recommended plant population for soybean grown in 76-cm rows in North Dakota), 370,000 (recommended plant population), and 740,000 (twice the recommended plant population) seeds ha^{-1}. They found that increasing the seeding rate significantly reduced IDC symptoms and increased grain yield. Compared to the recommended seeding rate for North Dakota, planting a higher population of plants led to an average of 586 to 942 kg ha^{-1} yield increase across sites on chlorosis-producing soils. In the following year, Goos and Johnson (2001) tested three varieties (two tolerant to IDC and one susceptible to IDC) at two seeding rates (370,000 and 740,000 seeds ha^{-1}) and verified that increased seeding rate increased grain yield of all cultivars in two of the four sites.

Other studies have also found a positive yield effect from increased seeding rate on soybeans grown in chlorotic areas (Wiersma, 2007; Lingenfelser et al., 2005). Wiersma (2007) verified that soybean yield increased linearly as seeding densities were increased for all three varieties tested under severe IDC conditions. However, the author pointed out that the more susceptible cultivars showed a greater response to higher plant populations than the tolerant one, indicating that varieties respond differently to increases in plant population. Naeve (2006) also evaluated the effects of increased seeding rates on alleviating IDC symptoms and improving yield across chlorosis-prone environments but reported inconsistent results. While increasing seeding densities from 432,000 to 926,000

seeds ha^{-1} increased yield by 16% on average and decreased IDC scores, these findings were reported to be small and confounded by environmental interactions.

The mechanism behind the plant population effect is thought to be associated with the release of H^+ ions and mobilization of phenolic compounds into the rhizosphere that occurs when soybeans are grown in Fe-limiting conditions (Naeve, 2004). When the seeding rate is increased (the number of seeds per unit of row is larger), soybean roots exploit soil substrate that is occupied by roots of neighboring plants, raising the amount of root mass per unit volume of soil (Bohm, 1977). This increased rooting of soil volume results in an increased reductive capacity and acidification of the rhizosphere, enhancing iron availability and acquisition (Rengel and Marschner, 2005). From a farmer's standpoint, the practice of using different plant populations in affected vs. non-affected areas of a field can be efficiently achieved by mapping the hotspot and non-hotspot areas in the tractor's GPS and varying the plant density with variable-rate seeding equipment (Gaspar, 2010).

Excessive levels of soil NO_3^- and excess soil moisture, as discussed previously, have been observed to increase the incidence and severity of Fe chlorosis in soybeans grown in calcareous soils (Aktas and Van Egmond, 1979; Wiersma, 2010; Bloom et al., 2011). Based on that knowledge, another management strategy that can produce positive results, both in terms of improving IDC scores and reducing yield losses, is growing a companion crop to take up excess soil nitrate and avoid bicarbonate buildup by reducing excess soil moisture (Naeve, 2006; Bloom et al., 2011; Kaiser et al., 2014). Small grains, such as oat (*Avena sativa* L.), have been interplanted with soybean as a potential more economically feasible alternative for IDC mitigation due to their susceptibility to glyphosate and relative low cost, which enables their termination at the time of early season weed control (Naeve, 2006; Kaiser et al., 2014). However, the adoption of this management strategy adds risks related to termination timing, usually targeted at 25 cm for oat (Kaiser et al., 2011). If terminated too early, the oat will not remove enough nitrate or moisture from the soil, resulting in a reduced, little lasting positive effect and potentially leading to chlorotic soybeans after glyphosate application (Naeve, 2006). If terminated beyond the optimal time, the oat can compete with soybeans for sunlight, nutrients, and water, resulting in yield reductions (Bloom et al., 2011; Kaiser et al., 2014).

Reducing other forms of stress to the soybean plant is also important when managing IDC. Weed control with glyphosate herbicides is less stressful than with some of the preplant and in-season herbicides because glyphosate can cause less damage to soybean plants (Kaiser et al., 2011). Potentially damaging soybean cyst nematode levels are widely distributed across important soybean producing regions and research has indicated that nematodes are frequently present in greater quantities in soils with high pH (Francl 1993; Rogovska et al., 2006; Pedersen et al., 2010; Melakeberhan et al., 2013). According to Dobbles (2020), the likelihood of SCN and IDC co-occurring in a farmer's field is high, making symptoms more severe. Other soybean diseases and pests also must be treated based on recommended thresholds to reduce plant stress as much as possible (Kaiser and Bloom, 2018).

1.5 Economics of Managing IDC

As discussed previously, various studies have been conducted to evaluate the effectiveness of different management strategies in controlling IDC in soybean. Few, however, have assessed the economic feasibility of their approaches. In addition, the studies that have included grain prices and input costs into their analysis are relatively out-of-date since grain prices and input costs have significantly changed over time.

Wiersma (2005) evaluated the economic feasibility of managing IDC with varieties (tolerant vs. susceptible) and with the application of different rates of iron chelates (Fe-EDDHA) and found that applying increased amounts of Fe-EDDHA was environment- and cultivar-specific. For the susceptible cultivar in a moderate to severe IDC environment, significant yield increases were verified for every increase in Fe-EDDHA unit rate. Based on a regression analysis, the author proposed that soybean growers would have to receive roughly \$0.12 per kilogram of grain to equal the cost of every increment (kg) of applied Fe-EDDHA costing \$24.26 kg^{-1}. Therefore, any additional increment of Fe-EDDHA ranging from 0 to 11.2 kg ha^{-1} would at the minimum cover the cost of the product once the soybean price is greater than \$0.12 kg^{-1}. However, the same yield increases were not verified for the tolerant variety, suggesting that the soybean price would have to be higher, approximately \$0.33 kg^{-1}, to equal the cost of each Fe-EDDHA increment. Based on these findings, the author concluded that Fe-EDDHA application would not be economically

feasible for resistant varieties unless extremely harsh IDC conditions prevailed, and that less costly iron chelates were needed.

Historically, soil applications of chelated forms of iron were very costly, which economically forbade their use. However, in 2006, a new Fe-EDDHA product termed Soygreen® was released into the market. Soygreen® is a dry, water-soluble powder that contains 6% of iron in the form of EDDHA. The price of Soygreen® was previously reported to be \$24.7 ha^{-1} (\$10.00 $acre^{-1}$) to \$34.6 ha^{-1} (\$14.00 $acre^{-1}$) (Gaspar, 2010). Currently, average grower price for Soygreen® is \$16.5 kg^{-1}, which for a full rate of 3.36 kg ha^{-1} results in a total of \$55.5 ha^{-1} (CHS company represtative, personal communication, 2022). Using Soygreen® as the Fe-EDDHA form on the seed at the time of planting, Kaiser et al. (2014) found that Fe-EDDHA would be economically feasible, in contrast to the findings reported by Wiersma (2005). At the time of their study, 3.36 kg Fe-EDDHA ha^{-1} cost US\$12.20 and the soybean price was US\$367 Mg^{-1}. Based on these grain prices and input costs, a 33 kg ha^{-1} increase in soybean yield would be required for Fe-EDDHA application to be profitable. Given that all increments in grain yield were 0.1 Mg ha^{-1} or greater, the iron chelate (Soygreen®) used in their research was indicated to be economically feasible for soybean growers (Kaiser et al., 2014).

1.6 Tables

Table 1-1. Soybean production (Million Metric Tons), harvested area (Million hectares), and yield (Megagram per hectare) of the top three producing countries in 2021.

Country	Production (MMT)	Harvested area (M ha)	Yield (Mg ha^{-1})
Brazil	138	38.9	3.55
USA	115	33.4	3.43
Argentina	46.2	16.5	2.81
Global	**366**	**128**	**2.86**

Data from USDA, FAS, 2021.

Table 1-2. Soybean production (Million Metric Tons), harvested area (Million hectares), and yield (Megagram per hectare) of the top ten producing states in the USA in 2021.

State	Production (MMT)	Harvested area (M ha)	Yield (Mg ha^{-1})
Illinois	18.30	4.25	4.30
Iowa	16.91	4.06	4.17
Minnesota	9.69	3.07	3.16
Nebraska	9.54	2.25	4.24
Indiana	9.13	2.28	4.00
Missouri	7.53	2.29	3.30
Ohio	7.50	1.97	3.80
South Dakota	5.86	2.18	2.69
Kansas	5.16	1.94	2.66
North Dakota	4.94	2.88	1.71

Data from USDA, FAS, 2021.

Chapter 2. Soybean Iron Deficiency Chlorosis Management Strategies for High Yield and Profitability

2.1 Summary

Iron Deficiency Chlorosis (IDC) is a major yield-limiting factor for soybean [*Glycine max* (L.) Merr.] grown on the calcareous soils of the US Upper Midwest. During the 2021 and 2022 growing seasons, ten on-farm, small-plot, research trials were established on IDC-prone fields in Western Minnesota to evaluate the effectiveness and profitability of three of the most often used management strategies for IDC from a system's approach: variety selection, seeding rates, and iron chelate application. Three Fe-EDDHA rates (0, 2.24, and 4.48 kg Soygreen® ha^{-1}) were applied in-furrow at the time of planting either a highly tolerant (HT) or a moderately tolerant (MT) variety at 309,000 and 433,000 seeds ha^{-1}. Nitrogen was broadcast above the row to create a range of IDC symptomology. Visual chlorosis scores (VCS) were assessed as a method for measuring the severity of symptoms. Iron deficiency chlorosis occurred at all environments, varying in intensity from low to severe. Planting a HT variety, applying Fe-EDDHA in-furrow at planting, and increasing the seeding rate were effective at minimizing yield losses due to IDC. Larger yield responses were found for varieties and Fe-EDDHA rates as chlorosis symptoms increased, but their utilization tended to increase yields even in environments where IDC was low to moderate. Although the effects of Fe-EDDHA application were greater for the MT variety compared to the HT one, Fe-EDDHA application on the HT variety produced the highest yields. Consistent positive effects on yield (150 kg ha^{-1}) with increased seeding rates across environments and treatment combinations were observed. Profitability and economic risk analysis showed that the best option for the low-moderate IDC conditions tested was the HT variety with 2.24 kg Fe-EDDHA ha^{-1} at 309,000 seeds ha^{-1}. Conversely, when IDC was severe, a combination of increased management strategies resulted in both lowest risk and highest risk-to-reward. If using a portfolio of strategies with variable rate technology is not feasible from a farmer's standpoint, the HT variety with 4.48 kg Fe-EDDHA ha^{-1} planted at 433,000 seeds ha^{-1} is the best single alternative for areas where IDC is severe.

Abbreviations: IDC, iron deficiency chlorosis; Fe-EDDHA, ethylene diamine tetraacetic acid; SOM, soil organic matter; HT, highly tolerant; MT, moderately tolerant; CCE, calcium carbonate equivalent; EC, electrical conductivity; HCO_3^{2-}, carbonate; VCS, visual chlorosis scores.

2.2 Introduction

Iron Deficiency Chlorosis (IDC) is a major nutrient stress and economically relevant management disorder for soybean [*Glycine max* (L.)] grown in the calcareous soils of the North Central United States (Inskeep and Bloom, 1987; Franzen and Richardson, 2000). In this region, the total area of soybean grown on IDC-prone soils has been estimated to be 1.8 million hectares (Hansen et al., 2004), with associated yield losses totaling $165 million annually (Atencio et al., 2021). Although the name "Iron Deficiency Chlorosis" connotates a lack of Fe in the soil, this essential micronutrient is relatively abundant in all agricultural lands in the US (Stucki, 1988). Rather, iron is quite often present in a form [Ferric Fe or Fe(III)] that soybean plants cannot acquire from the soil (Stucki, 1988; Naeve, 2004). With a limited mobilization of this micronutrient, chlorophyll production, needed for photosynthesis, is greatly restricted resulting in IDC development (Goos and Johnson, 2000; Gambel et al., 2014). In soybean, IDC is characterized by interveinal yellowing of the leaves and stunting of the growth, both of which lead to significant yield reductions (Hansen et al., 2003; Inskeep and Bloom, 1987). It has been reported that even minor symptoms of IDC can decrease yields by up to 20%, and that severe manifestations could culminate in total crop failure (Froechlich and Fehr, 1981; Niebur and Fehr, 1981).

There are two major Fe acquisition strategies that plants have developed to increase their ability to take up iron upon Fe-deficient conditions: Strategy I and Strategy II (Marschner et al., 1986). As a Strategy I plant, soybean uses a multi-part, reduction-based mechanism to convert less soluble ferric iron to more soluble ferrous iron [Fe^{2+}]. In such a mechanism, protons and chelating substances are extruded into the rhizosphere to promote its acidification and to solubilize ferric chelates. Once solubilized, rhizospheric Fe^{3+} is reduced by a ferric reductase enzyme (Ferric Reductase Oxidase 2) located at the root's cell wall and can then be imported into the roots as Fe^{2+} via an iron uptake transporter

encoded by the IRT1 gene (Iron-Regulated Transporter 1) (Jeong et al., 2017). Alternatively, Strategy II plants (such as corn, and other graminaceous monocots) secrete a phytosiderophore into the rhizosphere that has high affinity to insoluble ferric iron, forming an iron-siderophore complex [Fe^{3+}-PS] that is entirely transported into the roots (Marschner and Romheld, 1994).

In the soil, a multitude of factors and their interactions can significantly influence the expression of IDC by changing the solubility of iron and/or limiting the effectiveness of plant-mediated iron acquisition mechanisms (Inskeep and Bloom, 1987; Hansen et al., 2003). Soils with a pH in the range of 7.2 to 8.5 precipitate iron in the form of Fe hydroxides [$Fe(OH)_x$]. The low solubility of Fe hydroxides in the soil solution leads to a low bioavailability of iron to the plants (Lindsay, 1979). Carbonates (CO_3^{2-}), found in calcareous parent materials, impair iron uptake in two ways. One way is acting as a strong base, increasing the soil pH, and oxidizing Fe^{2+} to Fe^{3+} (Lucena, 2000). Alternatively, CO_3^{2-} can function as a pH buffer, neutralizing the excreted acids and H^+ protons that were meant to acidify the rhizosphere, preventing the reduction of Fe^{3+} to Fe^{2+} (Hansen et al., 2003). Excessive nitrate (NO_3^-) availability and high soil moisture also increase IDC severity because both factors lead to a buildup of bicarbonates (HCO_3^-) in the soil (Silva and Uchida, 2000; Bloom et al., 2011a). The buffering capacity of HCO_3^- in the rhizosphere limits the conversion of unavailable ferric iron to readily available ferrous iron, a necessary step in Fe uptake by soybean plants (Aktas and van Egmond, 1979).

Due to the large impact of IDC on soybean production, growers have adopted various agronomic practices to avoid yield losses. Among the most widely used management strategies are cultivar selection, seeding management (comprising seeding rate and row spacing), and fertilizer application (including foliar and in-furrow application of iron chelates) (Hansen et al., 2003).

Planting varieties with improved tolerance has long been suggested as the most important and most practical strategy to manage chlorotic areas (Niebur and Fehr, 1981; Goos and Johnson, 2000; Wiersma, 2005; Helms et al., 2010). Soybean varieties with high tolerance to IDC can reduce Fe^{3+} to Fe^{2+} sooner and in larger amounts compared to less tolerant varieties (Ellsworth et al., 1998; O'Rourke et al., 2007). Even though varietal selection has generated the most consistent positive results, the most tolerant varieties can

experience yield reductions when severe IDC conditions prevail (Liesch et al., 2011; Froechlich and Fehr, 1981). Therefore, the best approach to manage severe IDC may be to pair tolerant varieties with other management strategies effective at minimizing losses.

Increasing the seeding rate has been proposed as another viable option to minimize the effects of IDC in soybean fields (Lingenfelser et al., 2005; Naeve, 2006; Wiersma, 2007). A larger number of plants per linear unit of row is presumed to result in an increased quantity of exudates (H^+ and organic acids) being released into the soil surrounding the roots, enhancing their reductive capacity, and converting greater amounts of non-available iron into a soybean-available form (Rengel and Marschner, 2005). A study by Goos and Johnson (2001) showed that doubling soybean seeding rate from 370,000 to 740,000 seeds ha^{-1} significantly alleviated IDC symptoms and increased grain yield. Wiersma (2007) also found that grain yield was increased with an increased seeding rate but noted that the more susceptible cultivars showed a greater response to higher plant populations than the tolerant one.

The application of chelated sources of Fe has also been effective in controlling IDC and thus contributing to yield increases in soybean grown under IDC conditions (Ferreira et al., 2019b; Wiersma, 2007; Schenkeveld et al., 2008; Gamble et al., 2014; Kaiser et al., 2014). An iron chelate is a compound that binds Fe at multiple sites, protecting it from precipitation and keeping it readily available for plant uptake (Wittwer et al., 1965; Lucena-Rodriguez and Apaolaza-Hernandez, 2010). There are different iron chelates available in the market, including Fe-DTPA, Fe-EDTA, and Fe-EDDHA. These chelated forms of iron differ in their physical and chemical components, as well as their performance in delivering Fe to the plant (Schenkeveld et al., 2008). Under high calcareous soil conditions, Fe-EDDHA has been proposed as the most stable of these chelates (Reed et al., 1988; Lucena, 2003). Wiersma (2007) attained yield increments of 15% with seed-applied Fe-EDDHA. Kaiser et al. (2014) reported significant yield increases with in-furrow application of Fe-EDDHA at a rate of 3.36 kg ha^{-1} for a susceptible variety grown under moderate to severe IDC conditions.

While producers seek management strategies that mitigate IDC, they are primarily concerned with inputs that maximize profitability while reducing economic risks. Genetic resistance is historically acknowledged as the most economical strategy for overcoming

IDC; however, not every producer has access to highly tolerant and high-yielding soybean cultivars (Heithold et al., 2003; Caliskan et al., 2008). As soybean seed and Fe-EDDHA prices have substantially increased in the last decade [soybean seed ~US$58 unit^{-1} (USDA-ERS, 2021), and 3.36 kg Fe-EDDHA ha^{-1} = US$22.50 (personal communication, 2022)], the trade-offs in cost and yield associated with higher seeding densities and the application of Fe-EDDHA rates greater than needed to maximize yield may reduce net returns (Wiersma, 2005; Wiersma, 2007).

At the present time, to our knowledge, there is only one study that specifically evaluated the effect of variety selection, plant population, and iron chelate rates combined on soybean IDC (Wiersma, 2007). Our study differs from Wiersma (2007) in that it includes two levels of IDC intensity through supplemental nitrogen to create a range of IDC symptoms within environments. Furthermore, limited literature exists regarding the cost-effectiveness of the strategies researched for IDC management. Therefore, the objectives of this research were (1) to evaluate the impact of variety selection, seeding densities, and iron chelate rates on soybean grain yield across a range of IDC levels, and (2) to define optimum combinations of these three management strategies based on profitability, risk, and expected IDC severity.

2.3 Materials and Methods

2.3.1 Research environments

On-farm paired research trials were established in Western Minnesota at three locations in 2021 and two locations in 2022. At each location, the same experiment was planted in two different areas, referred to as sites. One site was planted in the IDC "hotspot" part of the field (Hotspot Site) where IDC was expected to be most severe, and the other site was planted in the "non-hotspot" IDC part of the field (non-Hotspot Site) where symptoms were expected to be lower. The term site, herein, refers to the geographically unique position of each field trial and its IDC intensity. The term environment is used, herein, to illustrate the combination of site by year, numbered 1-10. Environments 1-6 and 7-10 refer to environments in 2021 and 2022, respectively. Soils in the area are formed by a calcium carbonate parent material that make them susceptible to IDC development. Thus, all ten research environments were expected to have some stress from Fe deficiency and

were chosen based on previous soybean IDC histories provided by farmers cooperators. Descriptions for each environment can be found in Table 2-1.

Each of the ten environments was thoroughly sampled and evaluated for soil characteristics (Supplemental Table 2-2) and weather conditions (Supplemental Table 2-1). For the 2021 growing season, weather data, including monthly air temperature and precipitation, were retrieved from the nearest weather station within a maximum of 30 km of each location from High Plains Regional Climate Center (HORCC, Lincoln, NE, https://hprcc.unl.edu/). For the 2022 growing season, remote weather stations (Hobo® U30 Station, Onset Computer Corporation, Bourne, MA) were installed at each location at the time of planting. Thirty-year normal (1984-2013) air temperatures and rainfall were collected from HORCC and were used to calculate departure from normal (DN).

Immediately after planting, multiple composite soil samples were collected within each replication by pulling 8-10 separate soil cores at 0 to 15-cm depth utilizing a manual 3.2-cm diameter soil probe. These soil samples were analyzed for Olsen P (Frank et al., 1998), ammonium acetate extractant K (Warncke and Brown, 1998), soil pH [1:1 soil/water suspension (Watson and Brown, 1998)], SOM [loss on ignition (Wang and Anderson, 1998), soluble salts [by electrical conductivity (EC) of a 1:1 soil/water suspension (Whitney, 1998b)], calcium carbonate equivalency (CCE) measured using the acetic acid dissolution method (Loeppert et al., 1984; Moore et al., 1987), and DTPA-extractable Fe (Whitney 1998a).

Weeds were controlled following the standard agronomic practices for soybean production in western Minnesota with the application of selected herbicides at rates recommended based on the specific weed species and intensities. Escapes were removed by hand weeding. Other factors that could affect soybean yield, such as insect pests and diseases, were either nonexistent or considered inconsequential. Exact emergence dates and growth stages were recorded following the soybean stage descriptions by Fehr et al. (1971).

2.3.2 Experimental design, treatments, and measurements

The experiment was designed to test 24 treatments, corresponding to the factorial combination of four main factors and their levels: two varieties (MT and HT), two seeding

rates (309,000 and 433,00 seeds ha^{-1}), three rates of Fe-EDDHA (0, 2.24, and 4.48 kg Soygreen AST® ha^{-1}), and two levels of IDC severity induced by supplemental nitrogen application (77 kg N ha^{-1} and no N). The application of supplemental N is an effective protocol developed to create a range of IDC symptoms, and it has been successfully used in previous IDC studies (Bloom et al., 2011; Dobbles, 2020). In this study, nitrogen fertilizer was manually broadcast above the row at planting as granular CH_4N_2O (46–0-0) (Loveland Products, Inc., CO). A complete description of the 24 treatments can be found in Table 2-2.

Treatment combinations were organized in a randomized complete block factorial design with split-plot treatment arrangement and four replications. Iron chelate levels were whole plots and the combination of varieties, seeding rates, and N the subplots. All 96 plots at each field site were 9 m long x 3 m wide with 4 rows spaced 76 cm apart. This experimental design was selected to facilitate the logistics involved in the application of Fe-EDDHA in-furrow as a liquid suspension while sowing the research trials.

The two soybean varieties, AG13XF0 rated as highly tolerant, and AG12XF1 rated as moderately tolerant to IDC are groups 1.3 and 1.2 relative maturity, respectively (Bayer Crop Science, MO, USA). Based on their maturity groups, the two seeding rates utilized encompass the boundaries of a practical range that growers use in the region (University of Minnesota Extension, 2018).

All ten trials were planted at a ground speed of 1.9 mph with a four-row precision research planter (Almaco Seed Pro 360, Almaco Co., Nevada, IA). Planting and emergence dates for each environment are given in Table 2-1. The Almaco Seed Pro 360 includes a high-precision single plate metering unit along with a FieldMap Software that allows for automatic adjustment of seed counts by the planter throughout the field, enabling the two different plant populations and varieties to be accurately planted. Plant population maps corresponding to each treatment's seeding rate were created in Almaco FieldMap (version 2.1) and loaded into the planter's system for use at the time of planting.

Given that Soybean Cyst Nematode (*Heterodera glycines,* SCN) causes yellowing of the leaves, stunting of the growth, and necrosis if severe, separate soil samples were evaluated for SCN infestation (egg counts) at the University of Minnesota Nematology Laboratory (Supplemental Table 2-2). Soil sampling for nematode infestation was

performed following the same method previously described for common soil chemical factors.

The chelated iron used in this study was a commercial form of ortho-ortho Fe EDDHA labeled Soygreen® AST with 1.8% of iron (CHS Inc., Inver Grove Heights, MN). Soygreen® AST contains 0.35 kg of Soygreen® per liter of product. To ensure proper application rates, all three iron chelate rates (0, 2.24, and 4.48 kg Soygreen® ha^{-1}) were mixed with water (resulting in 0, 94, and 187 L ha^{-1} mixture rates, respectively) and supplied as liquid suspension in-furrow at planting using an in-furrow tubular delivery system attached to the planter behind the seed tube that drizzles the product directly on the seed. Plant populations were estimated for each plot by counting the number of emerged plants from 1 linear meter of the inner two rows at V3-V4 developmental stages.

2.3.3 IDC symptoms assessment and grain yield data

After emergence, the two center rows of each plot were evaluated weekly for IDC symptomology using a 1 to 5 Visual Chlorosis Scoring (VCS), popularly called greenness scores (Goos and Johnson, 2000). Exact growth stages also were recorded on the same days as IDC symptom evaluation. Thus, data were collected on the following growth stages: V2, V3, V4, R1, R2, R3, R4, R5, and R5.5, except for Environments 7 and 8 (data collected at V2, R1, R2, R3, R4, R5, and R5.5).

The 1 to 5 visual severity rating has been traditionally used to evaluate IDC symptoms in soybean. In this system, a rating of “1” indicates no chlorosis, a score of “2” indicates slight yellowing most likely in the upper part of the canopy where IDC initiates, a score of “3” indicates chlorosis throughout the canopy with the majority of plants turning yellow in the plot (but no necrosis apparent), a score of “4” indicates severe chlorosis (100% of plants yellow) with stunted growth and some necrosis, and a score of “5” indicates most severe Fe-deficiency symptoms, with intense necrosis, some plants dying or entirely dead (Goos and Johnson, 2000). The ratings were completed by an experienced rater who understands IDC conditions and had no knowledge of the treatments being rated.

The center two rows of each plot were harvested with a small plot combine equipped with a scale and grain moisture sensor (Almaco SPC40, Almaco, IA, USA) at maturity (R8 according to Fehr et al., 1971) to determine yield. The weight of each

harvested sample (total grain mass plot^{-1}) was converted to yield (Mg ha^{-1}) and adjusted for a 130 g kg^{-1} moisture basis. For all measurements, the first and fourth rows were considered border rows, meant to avoid competition effect between rows of different plots, and were not used for any measurement.

2.3.4 Statistical analysis

In the present study, we included N application as a fourth factor (N was applied as a method to increase the range of chlorosis symptoms within each of the environments) and planted the same trial in two different areas within each location to test the effects of the selected agronomic practices in a wide range of IDC environments. As such, we expect that the resulting IDC environments evaluated may better represent what farmers may encounter on their farms. However, because Hotspot and non-Hotspot are not a perfect measure of IDC severity of individual site-years (that is, IDC severity varies from a non-Hotspot at Danvers to a non-Hotspot at Foxhome or from a Hotspot at Danvers in 2021 to a Hotspot at Danvers in 2022), and because N application indeed increased IDC intensity at almost all environments (Table 2-5), an Environmental Index (EI) was generated to better account for the variation in IDC symptomology within and across environments. This index was calculated as the average VCS at R5.5 for the control treatment (MT variety, 0 Fe-EDDHA, and 309,000 seeds ha^{-1}) with or without N application (Treatments 2 and 6, respectively). For example, EI calculated for Environment 1 was 3.5 with N application and 1.25 without N application. Consequently, all other treatment combinations that included N application were given an EI value of 3.5 and treatment combinations that did not include N application were given an EI value of 1.25. In other words, EI is a measure of how severe IDC was at R5.5, within environments, based on the VCS of the control treatment with or without N application. This approach allowed for the evaluation of the effects of all three management strategies based on a continuous measure of IDC severity and not only as Hotspot and non-Hotspot conditions.

All statistical analyses were performed with R statistical software version 4.1.2 (R Core Team, 2020) and considered significant at $P < 0.05$. The strength of the relationship between VCS ratings and soybean yields was determined using a Pearson correlation analysis. Mixed effects models were fitted using restricted maximum likelihood with the

lmer function from the *lme4* package [version 1.1-31, (Bates et al., 2015)] to analyze differences between factors for grain yield. All three management strategies (Fe-EDDHA rates, varieties, and plant populations) and EI were treated as fixed effects, while block, block nested within environment (to account for repeated measures), and the main-plot treatment nested within block (to account for split-plot randomization) were treated as random effects. Residual plots were examined to confirm model assumptions of homogeneity of variances and normality of residuals. For the models in which the four-way interaction term was not significant, the non-significant terms were eliminated from the model. Thus, the variation associated with non-significant factors was pooled with the error variance to assist evaluating the hypothesis of other fixed effects. Pairwise mean comparisons for the response variable grain yield were performed by calculating the Tukey's Honest Significant Difference (HSD) post-hoc test with the cld emmeans function from the *emmeans* package (Russel, 2020).

2.3.5 Economic analysis

Partial Budget Analysis (PBA), consistent with Kay et al. (2020) and Rod et al. (2021a, 2021b), was used to evaluate the net economic return of each of the treatment combinations. A PBA is commonly used for comparing the financial impact of a partial change on costs and returns and does not consider the fixed operating expenses or revenues that are left unchanged (Kay et al., 2020). Accordingly, the partial budgets performed in this study assessed the net economic return when varieties, seeding densities, Fe-EDDHA rates, and IDC intensities are changed. The MT variety at 308,000 seeds ha^{-1} with 0 Fe-EDDHA was considered the "base" treatment as this is the control treatment combination. The remaining treatments were compared to the "base" treatment to evaluate the profitability of each combination; this was done separately within each of the IDC severity conditions (EI's). Significant differences among the partial budgets were determined using the "Welch's two sample t-test with unequal variances" analysis in R. Net cost was considered the change in seed cost for each variety and seeding rate plus the change in iron chelate cost for each Fe-EDDHA rate. In western Minnesota, retail prices for a seed unit (140,000 seeds) from Bayer/Asgrow was $49.62 for AG13XF0 and $51.36 for AG12XF1 in 2022 (Bayer representative, personal communication, 2022). The average grower price

in 2022 for the Fe-EDDHA used (Soygreen® AST) was \$19.85 kg^{-1} (CHS Inc. representative, personal communication, 2022). Net revenue was considered as the change in revenue from change in grain yield and sale price. The average Minnesota soybean price for the marketing year of 2022 was \$0.558 kg^{-1} (USDA-NASS, 2022). The profitability (or net economic return) was calculated as the difference between the net cost and net revenue. A positive profitability indicates that farm income would increase due to the change, while a negative profitability indicates the change would decrease farm income (Kay et al., 2020; Tigner, 2018), within the assumptions studied here.

The results of each profitability evaluation were also used in a risk assessment analysis, adapted from Markowitz (1952), named Modern Portfolio Theory (MPT). This approach reveals how soybean growers can maximize their expected returns for a given level of risk or mitigate risk for a given level of net return by estimating an efficient frontier of varieties x Fe-EDDHA rates x seeding densities choices. As such, a soybean grower's decision of what strategies to adopt to manage IDC is like an investor's choice of what stocks to invest in a stock portfolio and is based on the variability in net economic returns. In this analysis, the standard deviation of the mean net economic return is a measurement of variability and represents the risk in the efficient frontier analysis (portfolio standard deviation = risk). The higher the standard deviation for a particular management strategy combination (portfolio), the higher the assumed risk. The main goal of constructing an efficient frontier in the present study was to determine the optimal management combinations that maximize expected returns, while keeping risk constant, or minimize risk, while holding profitability constant (Elton & Gruber, 1997). For this, the Add-In Solver was used in Microsoft Excel 2013 (www.solver.com).

2.4 Results and Discussion

2.4.1 Weather conditions

Total monthly precipitation and average monthly temperature data are summarized in Supplemental Table 2-1. Precipitation and temperature trends were generally consistent across locations within a given year. In 2021, rainfall during the first three months of the growing season (May to July) were considerably below the 30-year normal at all locations, but after this period, precipitation exceeded normal for the remainder of the growing season

(August to October). Rainfall totals during the 2021 growing season were 393.7, 622.3, and 510.5 mm for Foxhome, Danvers, and Graceville, respectively, which were greater than the normal for Danvers and Graceville (103.9 and 54.6 mm above the 30-year normal), but lower than the normal for Foxhome (81.3 mm below average). Air temperature in 2021 was higher than normal during the entire growing season for all locations, except for May at Foxhome and Graceville, which was slightly cooler than average (0.38 and 0.06 °C below normal).

In contrast, the 2022 growing season was entirely characterized by precipitation being abnormally dry (except for May at Foxhome), which was accompanied by above average temperatures during all months except for August at Danvers (0.4 °C below normal). Whole-season cumulative rainfall in 2022 was 109.5 mm for Foxhome and 125.2 mm for Danvers, resulting in 232.9 and 259 mm less precipitation, respectively, compared to the 30-year normal. Although periods of intensive drought were experienced at both locations during the whole growing season, their occurrence was especially impactful from pod formation (R3 phenological stage) until seed filling (R5.5 phenological stage). Insufficient precipitation at these locations in 2022 was associated with overall lower yields compared to the same locations in 2021.

2.4.2 Soil properties and IDC symptom severity

Soil series information for each of the research environments is summarized in Supplemental Table 2-2. According to current soybean fertilizer guidelines for Minnesota (Kaiser et al., 2022), all environments had adequate soil phosphorus [(P) ranged from 9 to 80 mg kg^{-1} by the Olsen P test] and potassium (K), except Environment 10, which had a low soil test K level (60 mg kg^{-1} by the ammonium acetate test). Soil organic matter ranged from 27 to 79.5 g kg^{-1} and SCN egg density averaged 1,880 eggs 100^{-1} CC soil (range 0 to 5,188 eggs 100^{-1} CC soil).

Although individual soil factors haven't provided perfect causal relationship with soybean yield under IDC conditions, most previous IDC studies have considered pH, calcium carbonate equivalents (CCE), soluble salts concentration [measured by electrical conductivity (EC)], and DTPA-extractable Fe (Fe-DTPA) to be determinant in identifying areas of high IDC risk (Hansen et al., 2003; Naeve & Rehm, 2006). In the present research,

all environments had pH > 7.9, calcium carbonates ranged from 10.2 to 146 mg kg^{-1}, EC levels ranged from 0.05 to 0.23 S m^{-1}, and Fe-DTPA ranged from 3 to 9 mg kg^{-1}. A predictive IDC index developed by Naeve & Rehm (2006) was utilized to forecast IDC stress severity within and across locations based on CCE, EC, and Fe-DTPA results:

$$I = 0.77 – 2.25 \times EC – 0.00572 \times CCE + 0.0615 \times \text{Fe-DTPA}$$

where I = the IDC severity index, EC is in S m^{-1}, CCE is in g kg^{-1}, and Fe-DTPA is in mg kg^{-1}. An index value greater than 1 would indicate that the environment would not likely be impacted by IDC, and a value less than 0.5 would indicate that the location is likely to elicit strong IDC symptoms. The IDC severity index (I) values calculated for all ten environments are shown in Table 2-5 and the performance of this index in estimating the severity of IDC will be discussed later.

Chlorosis developed rapidly in almost all environments and its severity varied greatly. Change in average visual chlorosis scores (VCS) calculated for treatment 6 at each growth stage indicate temporal variation in visual IDC severity, with symptoms tending to be most severe at R1 and improving thereafter (Table 2-3). Previous studies have shown that IDC is often more severe earlier in the growing season, and if environmental conditions improve as the number of days after planting increase, plants may have the ability to partially recover (Naeve and Rehm, 2006; Barker and Pilbeam, 2007). Thus, VCS recorded at R1 indicate that environments 8, 7, 3, 9, 5, and 1 were severely chlorotic (average scores > 2.5), environments 4, 6, and 10 were moderately chlorotic (average score between 1.5 and 2.5), while IDC severity was low at environment 2 (average score of 1.25) (Kaiser et al., 2014).

Pearson correlation analysis between I (IDC severity index by Naeve and Rehm, 2006) and mean VCS at R1 for treatment 6 was performed to evaluate the competence of I to predict the severity of IDC at each of the ten environments (Table 2-4). When calculated for the current study, I showed a statistically significant and negative relationship with the degree of visual chlorosis ($r = -0.695$, $P < 0.05$). Hence, the three commonly tested soil chemical properties analyzed in this study (EC, CCE, and Fe-DTPA)

delivered a good numerical estimation of future IDC intensity of individual locations when used as inputs in the index model developed by Naeve and Rehm (2006).

Pairwise correlations were also conducted between grain yield and chlorosis scores taken at each of the nine growth stages as an indicator of cumulative plant growth and development under IDC stress conditions (Table 2-4). Pearson correlation to yield was highest and highly significant at R5.5 growth stage for all environments, except for environment 2, which produced soybeans with uniformly green foliage throughout the growing season, resulting in no significant linear association between the two variables. Although the soil at environment 2 had high pH (8.0) and high concentrations of calcium carbonates expressed as $CaCO_3$ equivalent (CCE of 94.00 g kg^{-1}), it also had the highest levels of available iron (Fe-DTPA, 8.97 mg kg^{-1}), likely alleviating chlorosis symptoms.

In IDC-prone soils, excessive NO_3- concentrations have been associated with exacerbated IDC severity and decreased grain yield (Wiersma, 2010; Bloom et al., 2011b). During NO_3- acquisition from the soil, soybean roots exude bicarbonate ions into the rhizosphere to balance intracellular charge (Wiersma, 2010). These bicarbonates neutralize the acidity around the roots and limit the conversion of unavailable ferric iron to readily available ferrous iron, a necessary step in Fe uptake by soybean plants (Aktas and van Egmond, 1979; Inskeep and Bloom, 1987). Bloom et al. (2011b) showed that N fertilization, supplied in the form of urea (46–0-0), significantly reduced soybean yield. By adding urea on the furrow at planting in the present study, the level of chlorosis symptoms on treatment 6 was increased in seven of the ten environments (average increase in VCS of 0.96) and grain yield was decreased in nine of the ten environments (average yield decrease of 0.88 Mg ha^{-1} across all environments, ranging from 0.17 to 2.69 Mg ha^{-1}), although these effects were only significant in environments 1, 6, and 10 for VCS and in environments 1 and 6 for grain yield (Table 2-5).

Previous research has evaluated the effect of increases in VCS on soybean grain yield. Froechlich and Fehr (1981) reported that yield losses increased by an average of 20% for every one-point increase in chlorosis scores. To examine the relationship between VCS and grain yield in the present study, VCS at R5.5 were used to regress the relative yield of the MT variety [the grain yield of the MT variety divided by the grain yield of the HT variety under the control treatments, with or without N application (treatment 2 / treatment

1 and treatment 6 / treatment 5)]. This relationship was significant and linear (Figure 2-1). The average relationship between VCS and grain yield across environments was best determined by the equation: Relative Yield (Mg ha^{-1}) = 1.3952 – 0.2684 * X, where X is the chlorosis score of the MT variety. Thus, yield loss was found to increase by an average of 26% for each unit increase in VCS.

2.4.3 Management strategies' effects on soybean grain yield

Analysis of variance (ANOVA) was performed to examine the main effects of varieties, Fe-EDDHA rates, populations, EI, and their corresponding two-, three-, and four-way interactions. The significance of the fixed effects and their interactions for grain yield is shown in Table 2-6. The EI interacted with varieties and with Fe-EDDHA rates to affect soybean grain yield, indicating distinct responses to these two management strategies for different severities of IDC at R5.5.

As IDC severity increases at R5.5, soybean grain yield decreases at differing rates for each of the varieties tested (different slopes for each regression line with $P < 0.05$). The form of the two regression lines for the variety x EI interaction are:

$$\text{Grain Yield (Mg ha}^{-1}\text{)} \begin{cases} 3.395 + (-0.272 * \text{EI}) \ = \text{Moderately Tolerant} \\ 3.395 + (-0.00197) + (-0.272 + 0.213) * \text{EI} = \text{Highly Tolerant} \end{cases}$$

where EI is the Environmental Index calculated as the average VCS at R5.5 for the control treatment with or without N application. The results of the equations above show that, for every one-point increase in EI, yield losses of 0.27 Mg ha^{-1} and 0.06 Mg ha^{-1} are expected, on average, for the MT and HT varieties, respectively. When both varieties were grown under severe IDC conditions (EI of 4), the HT variety yielded, on average, 37% (0.85 Mg ha^{-1}) more than the MT variety. Given the genetic differences in tolerance to IDC, the HT variety was expected to exceed the MT one in grain yield as IDC severity increased. A similar soybean yield response for varieties with different levels of IDC tolerance was observed by Kaiser et al. (2014). The authors reported an average of 34% grain yield improvement with a more tolerant variety relative to a less tolerant variety when IDC was severe, and no other management strategy was used. Other studies across the US Midwest

have also reported differences in grain yield response among cultivars with varying levels of IDC tolerance (Goos and Johnson, 2000; Naeve and Rehm, 2006; Helms et al., 2010).

As shown in Figure 2-2, even when EI was 1, the HT variety tended to yield more than the MT one. This trend was consistent, with yield differences becoming larger as EI increased. In our study, a VCS of 1 at R5.5 does not indicate that IDC was not present, IDC occurred in all environments with different intensities. As noted previously, soybean plants can partially recover from IDC, and this could result in an average VCS of 1 at R5.5 (Table 2-3). Recovering, however, does not imply that plants will yield the same as they would if IDC had not occurred. Previous studies have reported that even minor IDC symptoms can significantly reduce yields and that elimination of yield loss due to IDC requires agronomic practices that prevent any chlorosis expression (Froechlich and Fehr, 1981; Niebur and Fehr, 1981). Our result supports previous research that planting a highly tolerant variety is the most important and practical strategy for IDC management (Goos and Johnson, 2000; Naeve and Rehm, 2006; Helms et al., 2010).

Although the selection of highly tolerant cultivars has long been proposed as the best option for managing IDC, previous studies have suggested the practice of planting two different varieties on different portions of the same field to maximize the yield of the entire field (Froechlich and Fehr, 1981; Helms et al., 2010; Kaiser et al., 2014). In this case, variable soybean seeding would be done by planting a less tolerant but high-yielding cultivar where IDC is low and a more tolerant but not the best-yielding cultivar in areas where IDC is moderate to severe (Kaiser et al., 2014). In the present study, the only environment in which IDC was practically non-existent was environment 2. When grain yield was compared at environment 2, it was found that both varieties yielded nearly the same [3.91 Mg ha^{-1} for the MT variety and 3.96 Mg ha^{-1} for the HT variety (data not shown)]. These findings differ from Helms et al. (2010), Liesch et al. (2011), and Kaiser et al. (2014), who found that the less tolerant genotypes yielded more than the more tolerant ones when IDC was absent or low. In fact, breeding for Fe-deficiency tolerance oftentimes selected lower-yielding genotypes for non-hotspot areas, which was previously reported as *yield drag* (Helms et al., 2010). Furthermore, although the varietal responses observed when IDC was almost absent may not be representative of all varieties available for IDC-prone areas, as we only evaluated a considerably small number of them, the lack of yield

differences between AG13XF0 and AG12XF1 may be the result of breeding efforts to select for high tolerance and high yield potential. These findings agree with those of Helms et al. (2010) in that there is evidence that some varieties have high yields in both the IDC and non-IDC areas of a field. Because a yield penalty was not observed for the HT variety in low chlorotic environments, findings from this study suggest that soybean yield can be maximized by planting a single highly tolerant and high-yielding variety across both hot and non-hot spots. From a farmer's standpoint, this approach is more practical than variable seeding of soybean because it does not require a change in cultivar as the planter proceeds across a field, and is less risky given that IDC severity can change drastically across small portions of a field and in response to several soil and environmental factors (Godsey et al., 2003; Hansen et al., 2003).

The slopes of the linear regression lines were also significantly different ($P < 0.05$) for the relationship between EI and Fe-EDDHA rates. The average relationship between grain yield and IDC severity at R5.5 for each of the Fe-EDDHA rates was best defined by the equations below:

$$\text{Yield (Mg ha}^{-1}\text{)} \begin{cases} 3.648 + (-0.494 * \text{EI}) = 0 \text{ kg ha}^{-1} \text{ FeEDDHA} \\ 3.648 + (-0.311) + (-0.494 + 0.435) * \text{EI} = 2.24 \text{ kg ha}^{-1} \text{ FeEDDHA} \\ 3.648 + (-0.338) + (-0.494 + 0.501) * \text{EI} = \ 4.48 \text{ kg ha}^{-1} \text{ FeEDDHA} \end{cases}$$

According to the equations above, for every one-point increase in EI, the yield was decreased by 16%, on average, when Fe-EDDHA was not supplied. At the same time, average yield reductions of less than 2% occurred with the application of 2.24 kg Fe-EDDHA ha^{-1}. In the present study, soybean grain yield was not negatively affected by increases in EI when Fe-EDDHA was provided at a rate of 4.48 kg ha^{-1}. Such positive grain yield responses indicate that Fe-EDDHA application was highly effective at reducing or even avoiding yield losses due to IDC (in the case of 4.48 kg Fe-EDDHA ha^{-1}). Apparently, higher Fe-EDDHA rates provide adequate iron for an extended time, satisfying the demand for a sustained supply of this micronutrient as plant development progresses and thus diminishing the chance of soybean plants developing symptoms that can negatively affect yield (Goos and Johnson, 2001; Wiersma, 2005). Compared to the untreated plots, yield improvements averaging 1.4 and 1.7 Mg ha^{-1} were observed with soil applications of 2.24

and 4.48 kg Fe-EDDHA ha^{-1}, respectively, when severe IDC conditions prevailed (EI of 4).

Although the largest yield differences among Fe-EDDHA rates were seen at high IDC intensities (Figure 2-3), our results indicate that Fe-EDDHA application, regardless of rate, also increased yield at lower EI values (at an EI of 1, yield increments of 120 and 160 kg ha^{-1} were found with the application of 2.24 and 4.48 kg Soygreen® ha^{-1}, respectively). In other words, Fe deficiency limited plant growth and grain yield even at low to moderate IDC conditions when Fe was not supplied in the soil in the form of Fe-EDDHA. This result reinforces our previous findings that, even though soybean plants can, in some cases, effectively overcome IDC towards the end of the growing season, it may only reduce the yield loss, but it will not eliminate it (Froechlich and Fehr, 1981). Niebur and Fehr (1981) evaluated the effect of iron chelate application in preventing IDC symptoms on calcareous soils. They found that a change in VCS from an average of 1 in the treated plots to an average of 1.5 in the untreated ones significantly decreased soybean yield by 130 kg ha^{-1}. As discussed previously, the lack of Fe, resulting in chlorosis symptoms, represents a more severe alteration of essential metabolic processes and this has been considered to be the reason why yield reductions occur even when the amount of yellowing is slight (Niebur and Fehr, 1981). Therefore, results from this study suggest to soybean growers that using a management strategy that eliminates IDC symptoms entirely is the key to eliminating yield losses.

Our results, however, do not indicate that Fe-EDDHA should be utilized when IDC is extremely low or absent. When Fe-EDDHA rates were compared at environment 2 (the only environment at which VCS was 1.25 at R1), it was found that Fe-EDDHA application did not result in significant yield increases (data not shown). Consequently, Fe-EDDHA application having minor to no benefit may not justify the expense of the product to the producer. Positive results with in-furrow applications of Fe-EDDHA were also reported by Kaiser et al. (2014). The authors concluded that Fe-EDDHA application in-furrow at planting presented a relatively low-cost management practice for mitigating the undesirable effects of IDC. Other studies have also shown yield increases for soybean using Fe-EDDHA as a soil application (Schenkeveld et al., 2008; Gamble et al., 2014).

While the positive results for varieties and iron chelate rates were dependent on EI, their interactive effects were similar whether utilized under low, moderate, or severe IDC conditions. Significantly greater soybean yields were found across varieties for both rates of Fe-EDDHA compared to the untreated soybeans (Figure 2-4). Applying 4.48 kg Soygreen® ha^{-1} tended to produce the highest yields (3.14 and 3.52 Mg ha^{-1} for the MT and HT varieties, respectively), but they were not statistically higher than using 2.24 kg Soygreen® ha^{-1} (2.95 Mg ha^{-1} and 3.46 Mg ha^{-1} for the MT and HT varieties, respectively). However, as illustrated by the significant variety x Fe-EDDHA interaction for yield (Table 2-8), the effect of Fe-EDDHA application was greater for the MT variety compared to the HT one (yield increases of 0.89 and 1.08 Mg ha^{-1} for the MT variety vs. 0.65 and 0.72 Mg ha^{-1} for the HT variety with 2.24 and 4.48 kg Fe-EDDHA ha^{-1}, respectively). Thus, when Fe-EDDHA was applied at a rate of 4.48 kg ha^{-1}, the average yield of the MT variety was similar to the average yield of the HT variety without Fe-EDDHA application or with 2.24 kg Fe-EDDHA ha^{-1}. Results from this research comport with those of previous studies as to the potential benefits of Fe-EDDHA as a soil application (Wiersma, 2005; Gamble et al., 2014; Kaiser et al., 2014). The larger response from the MT variety is consistent with findings from Wiersma (2005) and Kaiser et al. (2014) but is in contrast to the findings reported by Karkosh et al. (1988) where tolerant varieties alone responded to Fe-EDDHA.

Although the response to Fe-EDDHA application was greater for the MT variety compared to the HT one, the overall highest yields were achieved by providing either of the two Fe-EDDHA rates to the HT variety (3.46 and 3.52 Mg ha^{-1} with 2.24 and 4.48 kg Soygreen® ha^{-1}, respectively). Combining the HT variety with 4.48 kg Fe-EDDHA ha^{-1} produced significantly more grain than any other variety by Fe-EDDHA combination, except for the HT variety with 2.24 kg Fe-EDDHA ha^{-1} (Figure 2-4). The greatest yield levels, attained by having a HT variety with in-furrow applications of Fe-EDDHA in the current research, are consistent with the results found by Wiersma (2005), who reported that resistant cultivars exceeded susceptible cultivars in grain yield when Fe-EDDHA rates lower than 6.72 kg ha^{-1} were used.

In this study, significant differences in grain yield also were found due to the main effect of population, suggesting that the seeding rate response is not affected by Fe-EDDHA rates, varieties, and IDC intensities at R5.5 (EI) (Table 2-6). Thus, averaged

across all other fixed effects, increasing the seeding rate from 309,000 to 433,000 seeds ha^{-1} significantly and positively affected soybean grain yield by 150 kg ha^{-1} (Figure 2-5). Such consistent yield increases may be attributed to increased Fe acquisition by soybeans under Fe stress conditions with higher seeding rates. Under normal soybean production circumstances, higher yields are generally not observed with seeding rates beyond those required to establish a reasonable stand of plants (Holshouser and Whittaker, 2002; Wiersma, 2007). However, when grown under Fe-limiting conditions a higher number of plants per unit of row results in a larger exploitation of the rhizosphere, which along with the chemically reducing processes activated by Strategy I plants, increases the reductive capacity of the soil volume immediately surrounding the roots, improving Fe uptake (Rengel and Marschner, 2005). In the present study, IDC negatively affected soybean yield at all environments, except environment 2. At this environment, significant yield differences were not seen with higher seeding rates compared to lower seeding rates (data not shown).

Similar results with increased seeding rates also were observed by others (Penas et al., 1990; Goos and Johnson, 2000; Naeve, 2006; Wiersma, 2007). Goos and Johnson (2000) found that averaged across sites, cultivars, and Fe-EDDHA seed treatments, yields were 250 kg ha^{-1} higher at the higher seeding rate (370,000 vs. 740,000 seeds ha^{-1}). Similarly, Naeve (2006) reported average yield increments of 281 kg ha^{-1} across seven chlorotic environments resulting from seeding rates of 370,000 to 740,000 seeds ha^{-1} but highlighted that yield responses to greater seeding rates were relatively small and inconsistent. While positive results with increased seeding rates also were reported by Penas et al. (1990) and Wiersma (2007), responses to higher seeding densities were dependent on the varieties utilized. Penas et al. (1990) found greater responses to increased seeding rates for more tolerant varieties. Wiersma (2007) observed larger yield increases with increased seeding densities for less tolerant varieties. In our study, varieties responded similarly to increasing the seeding rate. However, as referenced above, other varieties may respond differently. Therefore, knowledge of how a specific variety may perform at different seeding rates under IDC conditions is needed to obtain maximum grain yields and reduce costs; the optimum plant density for IDC-prone soils has not been identified. This

lack of consistent recommendation may be associated with the fact that usually seeding rates being evaluated vary among studies.

In the current study, the lack of significant interactions involving seeding rates and the overall small yield enhancement found with an increased plant population may be explained by lower than desired plant stands. Averaged across all ten environments, soybean stand counts averaged 252,787 plants ha^{-1} with the 309,000 seeds ha^{-1} seeding rate, and 315,925 plants ha^{-1} with the 433,000 seeds ha^{-1} (data not shown). Thus, the population difference between the two seeding rates was only 25%, while the target difference was 40%. Contrarily, it may simply be that varieties, Fe-EDDHA rates and their combinations at varying IDC intensities are benefitted similarly by increases in plant population, preventing the occurrence of significant interactions between these factors.

2.4.4 Net economic returns and risk analysis

Although evaluating the effects of varieties, Fe-EDDHA rates, and seeding densities on soybean yield is crucial, it is critically important to determine how these management strategies, individually and collectively, impact overall economic returns. In this study, for the purpose of profitability and risk analysis, environments with or without N application were grouped into three classifications based on their EI values. As such, following an approach by Kaiser et al. (2014), an EI less than 1.5 was considered low IDC, an EI between 1.5 and 2.5 was considered moderate IDC, and an EI greater than 2.5 was severe IDC. Mean net economic returns were combined across low and moderate IDC conditions since an ANOVA for grain yield showed that management strategies responded similarly within these classes (data not shown). This grouping approach resulted in a total of 11 low-moderate and nine severe IDC environments.

When IDC was low to moderate, only four treatments had a significant ($P < 0.05$) positive net benefit compared to the control ("base") treatment [HT variety + 2.24 kg Fe-EDDHA ha^{-1} + 309,000 seeds ha^{-1} had a net benefit of $327.85; HT variety + 4.48 kg Fe-EDDHA ha^{-1} + 309,000 seeds ha^{-1} had a net benefit of $345.83; HT variety + 0 Fe-EDDHA + 433,000 seeds ha^{-1} had a net benefit of $365.45; and HT variety + 2.24 kg Fe-EDDHA ha^{-1} + 433,000 seeds ha^{-1} had a net benefit of $332.84 (Figure 2-6)]. Thus, not all

management strategies that increase yield will create a positive net benefit when Fe-stress conditions are not severe.

As described above, all four treatments with a significant positive net economic return included the HT variety with at least one of the other management strategies, either Fe-EDDHA application or increased seeding rate. This result indicates that planting a HT variety should be the first line of defense against IDC, both in terms of yield and profitability. This is because, regardless of the other management strategies used in combination, planting a MT variety never resulted in significantly higher net economic returns than the base treatment. These findings suggest that, although Fe-EDDHA application and increased seeding rates are effective at increasing the yield of the MT variety, the yield differences were not enough to significantly increase profitability when low to moderate IDC conditions prevail.

Under severe IDC conditions, all management strategies significantly increased profitability, except for the combination of a MT variety without Fe-EDDHA application, planted at a higher seeding rate, in which the net economic return was positive ($72) but not statistically significant. The greater number of treatment combinations being significantly more profitable than the control treatment may result from the need for alternatives to minimize the effects of severe Fe deficiency. Without any management treatments to restrain symptoms, severe IDC can result in a complete crop failure (Froechlich and Fehr, 1981). Thus, by adopting at least one management strategy shown to be effective in minimizing IDC losses, growers can significantly positively affect net economic returns as environments become less favorable (except by planting the MT variety at 433,000 seeds ha^{-1} without Fe-EDDHA application). Overall, the most significant net economic return under high Fe-chlorosis stress conditions was provided by the combination of a HT variety, with 2.24 kg Fe-EDDHA ha^{-1}, planted at 433,000 seeds ha^{-1} ($1,333.28). This management combination was the best option across all nine severe IDC environments because grain yield was increased by 2.54 Mg ha^{-1}, on average, compared to the base treatment, and because this management option is only number six in total input costs ($197.80, Table 2-7).

Risk Efficient Frontiers, based on the MPT, were performed to find optimum management strategy combinations that allow soybean growers to enhance profitability

while controlling the risk or reducing the risk while targeting a desired level of return (West, 2006). In the present study, this approach is proposed as a decision tool to aid soybean growers in determining what IDC management strategies to utilize given the severity of IDC, expected returns, and risk. Tables 2-10 and 2-11 illustrate the efficient frontier calculated using portfolio expected returns (mean net returns in \$ ha^{-1}) and portfolio standard deviation (risk level in \$ ha^{-1}) for low-moderate and severe IDC conditions.

One of the methods to compare efficient frontiers is through the tangency portfolio, which analyzes the most efficient or optimal portfolio available (Stevens and Bradley, 2020). In this approach, the goal is to determine which management strategy, or combination of them, provides the maximum return for a controlled risk (Optimum Portfolio) or the minimum risk for a level of return (Minimum Variance Choice). In the tangency portfolio method, the Sharpe Ratio is calculated to compare portfolios, measuring the risk-to-reward of a portfolio. Therefore, the higher the Sharpe Ratio, the higher the reward per unit of risk. As such, the Optimum Portfolio is defined as the management strategy or combination that results in the highest Sharpe Ratio. The Minimum Variance Choice is defined as the management strategy or combination that results in the lowest risk, but which may not maximize net economic returns. In the present study, the Sharpe Ratio was calculated as the portfolio expected return [mean net return for each management combination (\$ ha^{-1})] divided by the portfolio standard deviation (risk in \$ ha^{-1}).

At low-moderate IDC conditions, the optimum portfolio coincided with the combination of a HT variety with 2.24 kg Fe-EDDHA ha^{-1} planted at 309,000 seeds ha^{-1}, yielding a profit of \$1723.61 per hectare to a risk of \$579.99 ha^{-1} and a risk-to-reward of 2.97 (Table 2-8). Compared to the control treatment, this management combination provides a 58% increase in risk-to-reward. This outcome may be due to the efficacy of iron chelate application and variety selection on minimizing the effects of IDC on soybean grain yield and the relatively low cost of this management strategy combination (\$154 ha^{-1}, data not shown), resulting in mean net returns that are relatively high at all low-moderate IDC environments (lower variance, data not shown).

At the same IDC stress levels, the lowest risk (\$577.5 ha^{-1}) was achieved by having a portfolio of 50.2% HT variety + 2.24 kg Fe-EDDHA ha^{-1} + 309,000 seeds ha^{-1}; 35% HT

variety + 4.48 kg Fe-EDDHA ha^{-1} + 433,000 seeds ha^{-1}; and 14.8 % HT variety + 0 Fe-EDDHA + 309,000 seeds ha^{-1} (Table 2-9). For this level of risk, the estimated profit would be \$1676.16 ha^{-1}, with an associated Sharpe Ratio of 2.90. From these findings, portfolio theory is beneficial because it provides the lowest risk, which may be what growers prefer. However, the reduction in risk achieved with such a portfolio is only \$2 ha^{-1} less than the risk provided by the HT variety with 2.24 kg Fe-EDDHA ha^{-1} planted at 309,000 seeds ha^{-1} alone. Consequently, from a farmer's perspective, it may be more practical and profitable to plant the HT variety with 2.24 kg Fe-EDDHA ha^{-1} at 309,000 seeds ha^{-1} for a similar risk.

Under severe Fe-deficiency conditions, all management strategy combinations delivered a risk-to-reward greater than the control treatment (Table 2-9). Even though the risk was, in most cases, higher with any treatment combinations evaluated compared to the control, the expected return was increased by an average of \$1444.92 ha^{-1} (\$72.07 to 1333.29 ha^{-1} range), and this explains the greater Sharpe Ratios. However, no management combination alone coincided with either the Minimum Variance Choice or the Optimum Portfolio (Table 2-11). The efficient frontier shows that for a level of risk of \$542 ha^{-1}, a producer's profit could be \$1786 ha^{-1}, maximizing the risk-to-return to 3.29. This is achieved by planting the following portfolio: 71% of HT variety + 4.48 kg Fe-EDDHA ha^{-1} + 433,000 seeds ha^{-1}, and 29% of HT variety + 2.24 kg Fe-EDDHA ha^{-1} + 433,000 seeds ha^{-1}. The difference between the portfolio and the control treatment profit is \$1,259.6 ha^{-1}, with a risk that is \$30.16 ha^{-1} lower than the baseline. Again, if making use of a single management combination is desired by soybean growers, the single treatment combination that provided the highest profit for every unit of risk was the HT variety + 4.48 kg Fe-EDDHA ha^{-1} + 433,000 seeds ha^{-1}. The Sharpe Ratio estimated with this management combination was 3.55 times greater than the control and only 0.02 points lower than the Optimum Portfolio. The low variance and high net returns observed with the HT variety + 4.48 kg Fe-EDDHA ha^{-1} planted at 433,000 seeds ha^{-1} indicate that this treatment combination yields consistently better than the control, resulting in profits that vary less across severe IDC environments.

If a grower is risk adverse, the lowest risk (\$513.51 ha^{-1}) under severe IDC intensities was achieved by utilizing different proportions of various management strategy

combinations: 35% of HT variety + 2.24 kg Fe-EDDHA ha^{-1} + 433,000 seeds ha^{-1}; 25% of MT variety + 0 Fe-EDDHA + 309,000 seeds ha^{-1}; 24% of HT variety + 0 Fe-EDDHA + 309,000 seeds ha^{-1}; and 15% of HT variety + 4.48 kg Fe-EDDHA ha^{-1} + 433,000 seeds ha^{-1}. The lowest risk provided by this portfolio may be explained by the lower variability in mean net returns observed with the control treatment and its lower cost. The lower variability, however, does not indicate a consistently satisfactory effect of this management combination across severe IDC environments. The low variation achieved by having a MT variety + 0 Fe-EDDHA + 309,000 seeds ha^{-1} is due to this management combination providing consistently lower yields and, consequently, lower mean net returns across severe IDC environments. Therefore, when severe IDC prevails, this management strategy would not be recommended even when it is part of the optimum portfolio.

2.5 Conclusions

This study evaluated soybean grain yield response to varieties that differ in IDC tolerance, Fe-EDDHA rates applied in-furrow at planting, and seeding density under field conditions that were conducive to IDC development and with varying levels of chlorosis severity brought on by N application. Overall, N application increased Fe-deficiency symptoms and reduced yield. Thus, special attention must be given to the amount of nitrate present in the soil at the time of soybean planting. This is because of potential N carryover, which varies significantly by previous crop, N application rates, and environment during and after the previous cropping season.

Relative to a base treatment of the MT variety, no Fe-EDDHA application, and lower seeding density, soybean yield was consistently increased by planting a HT variety, applying 2.24 or 4.48 kg Fe-EDDHA ha^{-1}, and increasing the seeding density to 433,000 seeds ha^{-1}. Yield increases with the most tolerant variety and Fe-EDDHA application were greater when chlorosis symptoms were severe, but all three management strategies provided positive results even at low to moderate IDC intensities. Overall, these research results confirm those found in other studies conducted in the North Central United States that have demonstrated the effectiveness of variety selection, Fe-EDDHA application, and increased seeding rates to improve soybean yield on IDC-prone soils. Furthermore, our

results agree with previous studies that even minor IDC symptoms can significantly reduce yield. Thus, IDC symptom development needs to be suppressed for yield loss elimination.

Although greater effects from Fe-EDDHA application were found for the MT variety, combining a HT variety with Fe-EDDHA supplementation resulted in the highest yields. This result was further supported by profitability and risk analysis that showed that applying Fe-EDDHA on the HT variety provides the best Sharpe Ratio of individual management strategy combinations, regardless of IDC intensity. When IDC was low to moderate, the combination of a HT variety with 2.24 kg Fe-EDDHA ha^{-1} planted at 309,000 seeds ha^{-1} provided a 58% increase in risk-to-reward compared to the control treatment. When IDC was severe, the best option in terms of profit per unit of risk was the HT variety + 4.48 kg Fe-EDDHA ha^{-1} + 433,000 seeds ha^{-1}, with a Sharpe Ratio 3.55 times greater than the control.

All three management strategies assessed in the present study are practical from a farmer's perspective. When deciding which variety to grow, farmers should look for a cultivar with high tolerance to IDC based on public variety trial reports, seed company recommendations, or through on-farm assessment of cultivars if possible. Increasing the plant population can be efficiently done by adjusting the seeding density with a variable-rate seeder. In-furrow application of an iron chelate as liquid suspension at planting is also a practical option because many farmers possess planters equipped with such technology for similar applications on other crops or for the application of other products.

2.6 Tables

Table 2-1. Environment (Env.), Year, location/county, site, field coordinates, planting date, emergence date, and soil series for ten environments evaluated in western MN from 2021 to 2022.

Env.	Year	Location/County	Site	Field coordinates	Planting date	Emergence date	Harvest Date
1	2021	Danvers / Swift	Hotspot	45°15’25.9”N 95°42’19.9”W	11-May	23-May	19-Oct
2	2021	Danvers / Swift	Non-Hotspot	45°15’13.4”N 95°42’19.5”W	11-May	23-May	19-Oct
3	2021	Foxhome / Wilkin	Hotspot	46°12’33.9”N 96°25’01.0”W	10-May	21-May	30-Sep
4	2021	Foxhome / Wilkin	Non-Hotspot	46°12’33.5”N 96°24’50.4”W	10-May	21-May	30-Sep
5	2021	Graceville / Big Stone	Hotspot	45°34’28.9”N 96°24’32.2”W	10-May	22-May	19-Oct
6	2021	Graceville / Big Stone	Non-Hotspot	45°35’06.6”N 96°24’38.1”W	11-May	22-May	19-Oct
7	2022	Danvers / Swift	Hotspot	45°15’18.2”N 95°41’38.8”W	3-Jun	12-Jun	13-Oct
8	2022	Danvers / Swift	Non-Hotspot	45°15’28.0”N 95°41’39.1”W	3-Jun	12-Jun	13-Oct
9	2022	Foxhome / Wilkin	Hotspot	46°20’00.3”N 96°25’10.9”W	28-May	9-Jun	29-Sep
10	2022	Foxhome / Wilkin	Non-Hotspot	46°20’00.6”N 96°25’00.9”W	28-May	9-Jun	29-Sep

Table 2-2. The full set of 24 treatments arranged by the factorial combination of four factors and their levels. The IDC Highly Tolerant (AG13XF0) and IDC Moderately Tolerant [Mod. Tolerant (AG12XF1)] varieties are both extensively grown in western Minnesota (DEKALB Asgrow/Bayer Crop Science, MO, USA).

Treatment	**Fe-EDDHA (kg ha^{-1})**	**Nitrogen**	**Population (seeds ha^{-1})**	**Variety**
1	0	Nitrogen	309,000	Highly Tolerant
2	0	Nitrogen	309,000	Moderately Tolerant
3	0	Nitrogen	433,000	Highly Tolerant
4	0	Nitrogen	433,000	Moderately Tolerant
5	0	No Nitrogen	309,000	Highly Tolerant
6	0	No Nitrogen	309,000	Moderately Tolerant
7	0	No Nitrogen	433,000	Highly Tolerant
8	0	No Nitrogen	433,000	Moderately Tolerant
9	2.24	Nitrogen	309,000	Highly Tolerant
10	2.24	Nitrogen	309,000	Moderately Tolerant
11	2.24	Nitrogen	433,000	Highly Tolerant
12	2.24	Nitrogen	433,000	Moderately Tolerant
13	2.24	No Nitrogen	309,000	Highly Tolerant
14	2.24	No Nitrogen	309,000	Moderately Tolerant
15	2.24	No Nitrogen	433,000	Highly Tolerant
16	2.24	No Nitrogen	433,000	Moderately Tolerant
17	4.48	Nitrogen	309,000	Highly Tolerant
18	4.48	Nitrogen	309,000	Moderately Tolerant
19	4.48	Nitrogen	433,000	Highly Tolerant
20	4.48	Nitrogen	433,000	Moderately Tolerant
21	4.48	No Nitrogen	309,000	Highly Tolerant
22	4.48	No Nitrogen	309,000	Moderately Tolerant
23	4.48	No Nitrogen	433,000	Highly Tolerant
24	4.48	No Nitrogen	433,000	Moderately Tolerant

Table 2-3. Average visual chlorosis scores for the control treatment (MT variety, 0 Fe-EDDHA, and 309,000 plants ha^{-1}) without N application at each growth stage evaluated and IDC severity index (I) calculated for each of the ten environments utilizing the method developed by Naeve and Rehm (2006).

Environment	**V2**	**V3**	**V4**	**R1**	**R2**	**R3**	**R4**	**R5**	**R5.5**	**I**
E1	2.25	2.25	2.75	3.00	2.75	2.25	1.75	1.25	1.25	0.24
E2	1.00	1.00	1.00	1.25	1.00	1.00	1.00	1.00	1.00	0.65
E3	1.00	3.00	3.00	4.00	3.50	3.50	3.50	3.50	3.50	0.29
E4	1.00	2.25	2.00	2.25	2.00	1.75	1.75	1.75	1.50	0.55
E5	3.00	4.00	3.50	3.75	3.50	3.00	3.25	3.00	2.75	0.32
E6	2.00	1.67	1.67	1.67	1.33	1.00	1.00	1.00	1.00	0.41
E7	3.00	NA	NA	4.00	4.00	4.00	4.00	4.00	3.50	0.05
E8	3.00	NA	NA	4.00	4.00	4.00	4.00	4.00	4.00	0.15
E9	3.00	3.00	3.75	3.75	3.25	3.00	2.25	2.25	1.75	0.65
E10	1.50	2.00	2.25	1.50	1.50	1.25	1.25	1.00	1.00	1.02

Table 2-4. Pearson correlations between visual chlorosis scores collected at nine growth stages (V2 to R5.5 according to Fehr et al., 1971) and grain yield.

	Growth Stage									
Env.	V2	V3	V4	R1	R2	R3	R4	R5	R5.5	p-value†
1	-0.571	-0.651	-0.541	-0.636	-0.786	-0.846	-0.852	-0.878	-0.887	$< 2.2e^{-16}$
2	-0.155	-0.072	-0.164	-0.178	-0.162	-0.171	NA	NA	NA	NS
3	NA	-0.306	-0.410	-0.498	-0.596	-0.656	-0.633	-0.675	-0.720	$< 2.2e^{-16}$
4	NA	-0.311	-0.428	-0.451	-0.453	-0.517	-0.476	-0.583	-0.623	$1.252e^{-11}$
5	-0.764	-0.854	-0.708	-0.691	-0.723	-0.756	-0.834	-0.897	-0.930	$< 2.2e^{-16}$
6	-0.564	-0.659	-0.561	-0.500	-0.598	-0.671	-0.708	-0.732	-0.717	$1.39e^{-12}$
7	-0.631	-	-	-0.752	-0.735	-0.793	-0.843	-0.855	-0.883	$< 2.2e^{-16}$
8	-0.688	-	-	-0.834	-0.849	-0.839	-0.869	-0.892	-0.900	$< 2.2e^{-16}$
9	-0.178	-0.260	-0.461	-0.534	-0.599	-0.601	-0.614	-0.620	-0.651	$6.681e^{-13}$
10	-0.126	-0.275	-0.433	-0.523	-0.443	-0.482	-0.583	-0.586	-0.591	$2.22e^{-10}$

† *P*-value for Pearson Correlation at R5.5 growth stage

-, greenness scores not collected

NA, no linear association

Table 2-5. Environmental Index (EI) calculated as the average VCS at R5.5 and average grain yield (Mg ha^{-1}) for the control treatment (Moderately Tolerant variety + 0 Fe-EDDHA + 309,000 seeds ha^{-1}) for each of the ten environments with or without N application.

Environment	Nitrogen	EI	Average Yield (Mg ha^{-1})
1	Nitrogen	3.50b[1]	1.29b
1	No Nitrogen	1.25a	3.98a
2	Nitrogen	1.00a	3.85a
2	No Nitrogen	1.00a	4.02a
3	Nitrogen	2.75a	2.25a
3	No Nitrogen	3.50a	0.63a
4	Nitrogen	2.50a	1.73a
4	No Nitrogen	1.50a	3.21a
5	Nitrogen	2.75a	2.40a
5	No Nitrogen	2.75a	2.64a
6	Nitrogen	2.00 b	3.01b
6	No Nitrogen	1.00a	5.02a
7	Nitrogen	4.50a	0.10a
7	No Nitrogen	3.50a	0.50a
8	Nitrogen	4.25a	0.16a
8	No Nitrogen	4.00a	0.37a
9	Nitrogen	2.25a	0.73a
9	No Nitrogen	1.75a	1.02a
10	Nitrogen	2.00 b	1.38a
10	No Nitrogen	1.00a	1.82a

[1] Significance letters between N treatments within environments with alpha = 0.05.

Table 2-6. ANOVA significance of fixed effects [varieties (Variety), Fe-EDDHA rates (Fe-EDDHA), seeding rates (Population), and Environmental Index (EI)] and their interactions on soybean grain yield.

Source of Variation	**Grain Yield (Mg ha^{-1})**
	P > F
Fe-EDDHA	***
Population	**
Variety	***
EI	***
Fe-EDDHA x Population	0.0804
Fe-EDDHA x Variety	**
Population x Variety	0.1625
Fe-EDDHA x EI	***
Population x EI	0.2371
Variety x EI	***
Fe-EDDHA x Population x Variety	0.0791
Fe-EDDHA x Population x EI	0.5718
Fe-EDDHA x Variety x EI	0.9038
Population x Variety x EI	0.3842
Fe-EDDHA x Population x Variety x EI	0.4819

* Significant at the 0.05 probability level

** Significant at the 0.01 probability level

*** Significant at the 0.001 probability level

Table 2-7. Net cost ($ ha-1), Average Yield (Avg., Mg ha-1), Average Net Revenue (Avg., $ ha-1), and Average Net Benefit (Avg., $ ha-1) for each of the treatment combinations at low-moderate and severe IDC conditions.

Treatment Combination	IDC Severity	Net Cost ($ ha^{-1})	Avg. Yield (Mg ha^{-1})	Avg. Net Revenue ($ ha^{-1})	Avg. Net Benefit ($ ha^{-1})
0 - MT - 309	Low-Moderate	113.34	2.70	1509.09	1395.75
0 - MT - 309	Severe	113.34	1.15	639.78	526.44
2.24 - MT - 309	Low-Moderate	157.84	2.97	1658.37	1500.53
2.24 - MT - 309	Severe	157.84	2.79	1556.89	1399.05
4.48 - MT - 309	Low-Moderate	202.33	3.11	1732.87	1530.53
4.48 - MT - 309	Severe	202.33	3.16	1764.35	1562.02
0 - HT - 309	Low-Moderate	109.50	3.09	1721.71	1612.21
0 - HT - 309	Severe	109.50	2.00	1117.63	1008.13
2.24 - HT - 309	Low-Moderate	154.00	3.36	1877.61	1723.61
2.24 - HT - 309	Severe	154.00	3.17	1770.31	1616.31
4.48 - HT - 309	Low-Moderate	198.50	3.48	1940.08	1741.59
4.48 - HT - 309	Severe	198.50	3.64	2030.24	1831.75
0 - MT - 433	Low-Moderate	158.68	2.68	1495.66	1336.99
0 - MT - 433	Severe	158.68	1.36	757.19	598.51
2.24 - MT - 433	Low-Moderate	203.17	3.12	1740.53	1537.36
2.24 - MT - 433	Severe	203.17	3.00	1676.07	1472.90
4.48 - MT - 433	Low-Moderate	247.67	3.14	1751.05	1503.38
4.48 - MT - 433	Severe	247.67	3.20	1783.82	1536.15
0 - HT - 433	Low-Moderate	153.30	3.43	1914.50	1761.20
0 - HT - 433	Severe	153.30	2.52	1407.33	1254.03
2.24 - HT - 433	Low-Moderate	197.80	3.45	1926.39	1728.59
2.24 - HT - 433	Severe	197.80	3.69	2057.53	1859.73
4.48 - HT - 433	Low-Moderate	242.30	3.36	1877.27	1634.98
4.48 - HT - 433	Severe	242.30	3.58	1997.83	1755.54

Table 2-8. Risk ($ ha^{-1}), Expected Returns ($ ha^{-1}), and Sharpe Ratio of management strategy combinations, portfolio that minimizes risk (Minimum Variance Choice) and portfolio that maximizes the Sharpe Ratio (Optimum Portfolio) for low-moderate IDC.

Low-Moderate IDC			
Variable	RISK	EXPECTED RETURN	SHARPE RATIO
Minimum Variance Choice	577.53	1676.15	2.902
Optimum Portfolio	579.99	1723.61	2.972
0 - MT - 309,000	800.74	1395.75	1.743
2.24 - MT - 309,000	929.87	1500.53	1.614
4.48 - MT - 309,000	868.45	1530.53	1.762
0 - HT - 309,000	631.37	1612.21	2.554
2.24 - HT - 309,000	579.99	1723.61	2.972
4.48 - HT - 309,000	617.74	1741.59	2.819
0 - MT - 433,000	747.41	1336.99	1.789
2.24 - MT - 433,000	890.60	1537.36	1.726
4.48 - MT - 433,000	929.00	1503.38	1.618
0 - HT - 433,000	696.54	1761.20	2.528
2.24 - HT - 433,000	632.50	1728.59	2.733
4.48 - HT - 433,000	590.22	1634.98	2.770

Table 2-9. Risk ($ ha^{-1}), Expected Returns ($ ha^{-1}), and Sharpe Ratio of management strategy combinations, portfolio that minimizes risk (Minimum Variance Choice) and portfolio that maximizes the Sharpe Ratio (Optimum Portfolio) for severe IDC.

Severe IDC			
Variable	RISK	EXPECTED RETURN	SHARPE RATIO
Minimum Variance Choice	513.51	1308.30	2.548
Optimum Portfolio	541.99	1786.05	3.295
0 - MT - 309,000	572.15	526.44	0.920
2.24 - MT - 309,000	797.84	1399.05	1.754
4.48 - MT - 309,000	875.31	1562.02	1.785
0 - HT - 309,000	623.56	1008.13	1.617
2.24 - HT - 309,000	663.38	1616.31	2.436
4.48 - HT - 309,000	575.72	1831.75	3.182
0 - MT - 433,000	635.63	598.51	0.942
2.24 - MT - 433,000	919.44	1472.90	1.602
4.48 - MT - 433,000	886.85	1536.15	1.732
0 - HT - 433,000	729.68	1254.03	1.719
2.24 - HT - 433,000	583.88	1859.73	3.185
4.48 - HT - 433,000	536.33	1755.54	3.273

Table 2-10. Tangency Portfolio Weights, Expected Returns and Risk for Minimum Variance Choice and Optimum Portfolio for low-moderate IDC severity.

Efficient Frontier	Risk	Expected Return	Sharpe Ratio	Portfolio											
				0 - MT - 125	2 - MT - 125	4 - MT - 125	0 - HT - 125	2 - HT - 125	4 - HT - 125	0 - MT - 175	2 - MT - 175	4 - MT - 175	0 - HT - 175	2 - HT - 175	4 - HT - 175
Minimum Variance Choice	577.52	1676.14	2.902	0	0	0	0.147	0.502	0	0	0	0	0	0	0.350
Optimum Portfolio	579.99	1723.61	2.972	0	0	0	0	1	0	0	0	0	0	0	0

Table 2-11. Tangency Portfolio Weights, Expected Returns and Risk for Minimum Variance Choice and Optimum Portfolio for severe IDC conditions.

Efficient Frontier	Risk	Expected Return	Sharpe Ratio	Portfolio											
				0 - MT - 125	2 - MT - 125	4 - MT - 125	0 - HT - 125	2 - HT - 125	4 - HT - 125	0 - MT - 175	2 - MT - 175	4 - MT - 175	0 - HT - 175	2 - HT - 175	4 - HT - 175
Minimum Variance Choice	513.51	1308.30	2.54	0.245	0	0	0.244	0	0	0	0	0	0	0.353	0.158
Optimum Portfolio	541.99	1786.05	3.29	0	0	0	0	0	0	0	0	0	0	0.293	0.707

Supplemental Table 2-1. Monthly total precipitation and average temperature data at the five location-years studied.

	Precipitation data (mm)											
	May		June		July		August		September		October	
Location-Year	Tot.	DN	Tot.	DN	Tot.	DN	Tot.	DN	Tot.	DN	Tot.	DN
Foxhome-2021	45.72	-27.94	48.26	-55.88	35.56	-63.50	109.22	45.72	71.12	7.62	83.82	12.70
Foxhome-2022	33.53	21.34	32.77	-71.37	27.94	-71.12	9.65	-53.85	5.57	-57.93	-	-
Danvers-2021	35.56	-49.28	68.58	-35.56	83.82	-17.78	165.10	69.34	132.08	62.23	137.16	74.93
Danvers-2022	-	-	31.24	-57.15	24.13	-77.47	49.28	-46.48	19.81	-50.04	0.76	-27.94
Graceville-2021	38.10	-33.53	15.24	-80.01	71.12	-29.72	172.72	104.90	91.44	29.72	121.92	63.25

	Temperature data (°C)											
	May		June		July		August		September		October	
Location-Year	Avg.	DN	Avg.	DN	Avg.	DN	Avg.	DN	Avg.	DN	Avg.	DN
Foxhome-2021	13.15	-0.38	21.87	2.53	23.21	1.40	20.88	0.33	17.33	1.60	10.47	2.78
Foxhome-2022	20.63	3.82	22.10	2.77	22.79	0.99	20.75	0.20	16.69	0.97	-	-
Danvers-2021	15.33	1.11	23.61	3.56	23.44	1.11	21.50	0.56	17.83	1.39	12.00	3.78
Danvers-2022	-	-	23.35	2.84	23.03	0.70	20.54	-0.40	16.84	0.40	18.20	7.09
Graceville-2021	13.44	-0.06	21.83	2.67	23.17	1.44	21.61	1.22	17.22	1.78	10.78	2.94

† Tot., total monthly precipitation; DN, departure from normal.
‡ Avg., average monthly temperature, DN, departure from normal.

Supplemental Table 2-2. Soil average Olsen soil test P, ammonium acetate K, soil/water pH, DTPA-extractable Fe, electrical conductivity (EC), calcium carbonate equivalency (CCE), and nematodes (eggs per 100 CC soil) for each of the ten environments studied. Soil samples were composed of 6 soil cores per replication (4 replications = 24 cores per site) taken at a depth of 0 to 15 cm.

Environment	P	K	Fe	SOM	CCE	EC†	pH	Nematodes
	(mg kg^{-1})			(g kg^{-1})		(S m^{-1})		Eggs/100 CC
1	29	325	7	79.5	118.7	0.13	7.9	2,525
2	28	290	9	76.0	94.0	0.06	8.0	1,125
3	11	173	3	47.0	72.0	0.12	8.2	50
4	9	173	4	47.0	49.0	0.08	8.1	13
5	67	346	7	63.5	115.7	0.11	8.0	0
6	80	394	8	66.2	60.7	0.23	7.9	13
7	16	181	5	57.5	114.0	0.18	7.9	3,931
8	13	146	5	53.2	146.0	0.05	8.2	2,094
9	14	161	4	51.0	26.2	0.10	8.2	3,856
10	12	60	6	27.0	10.2	0.04	8.3	5,188

2.7 Figures

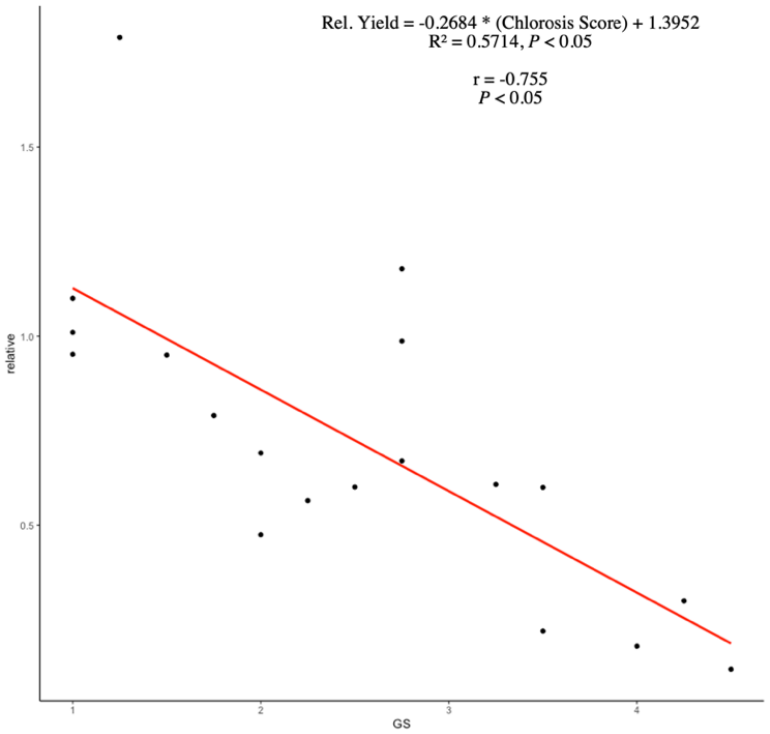

Figure 2-1. Relationship between the relative yield of the MT variety by the yield of the HT variety without any other management treatment vs visual IDC scores taken at R5.5 growth stage. The red line represents the linear regression with the best fit.

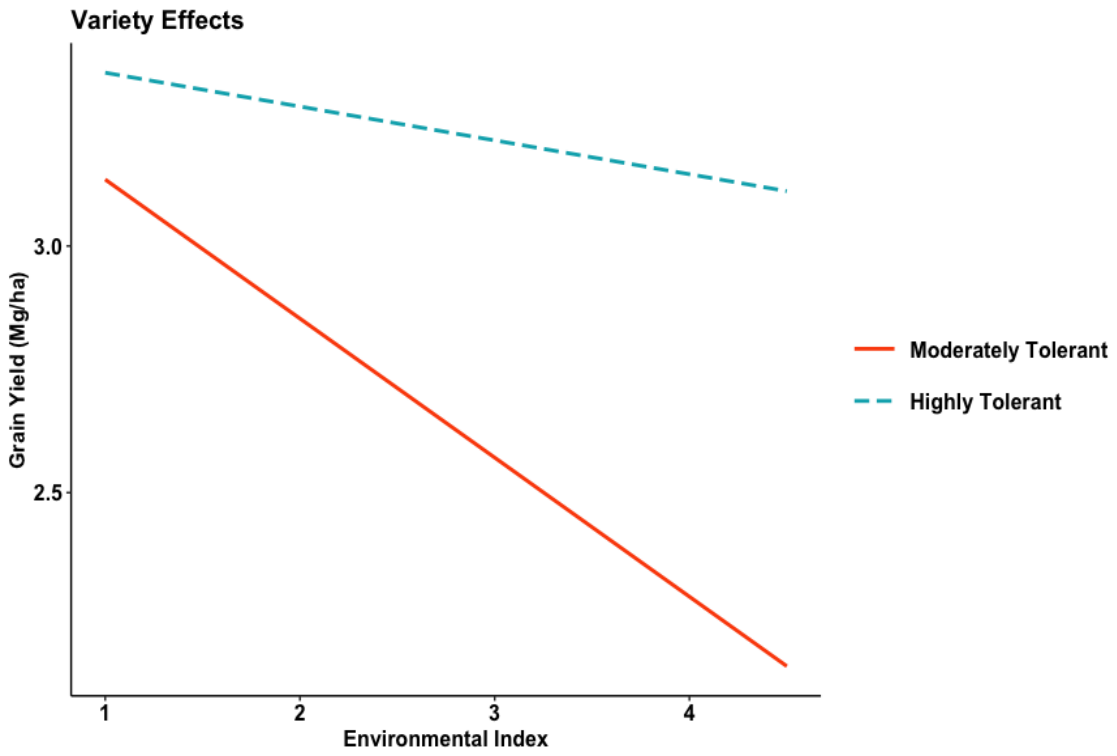

Figure 2-2. Decline in soybean grain yield in response to the interaction between varieties (MT and HT) and IDC severity measured by EI.

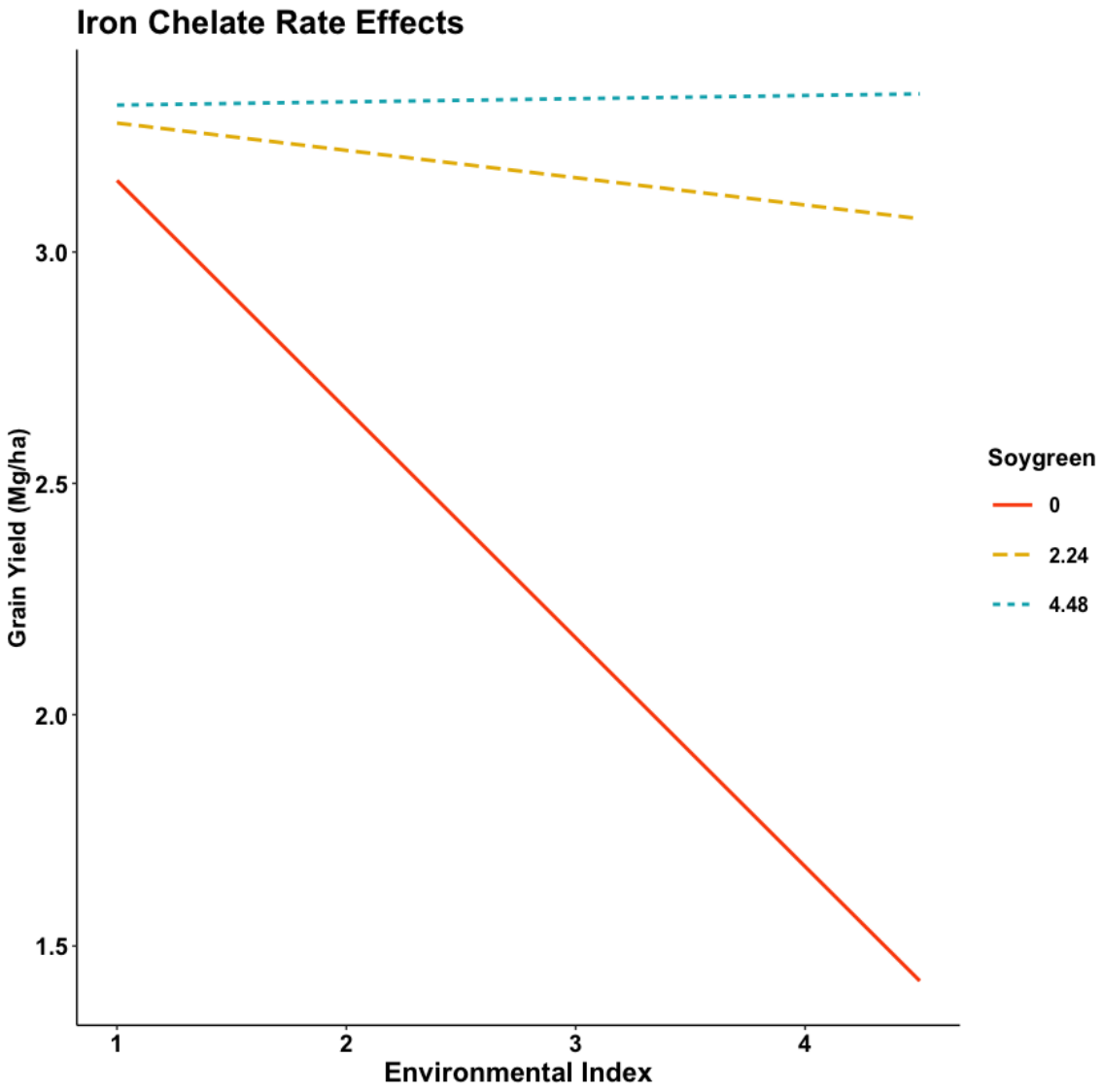

Figure 2-3. Soybean grain yield in response to the interaction between Fe-EDDHA rates (0, 2.24, and 4.48 kg Soygreen® ha^{-1}) and IDC severity measured by EI.

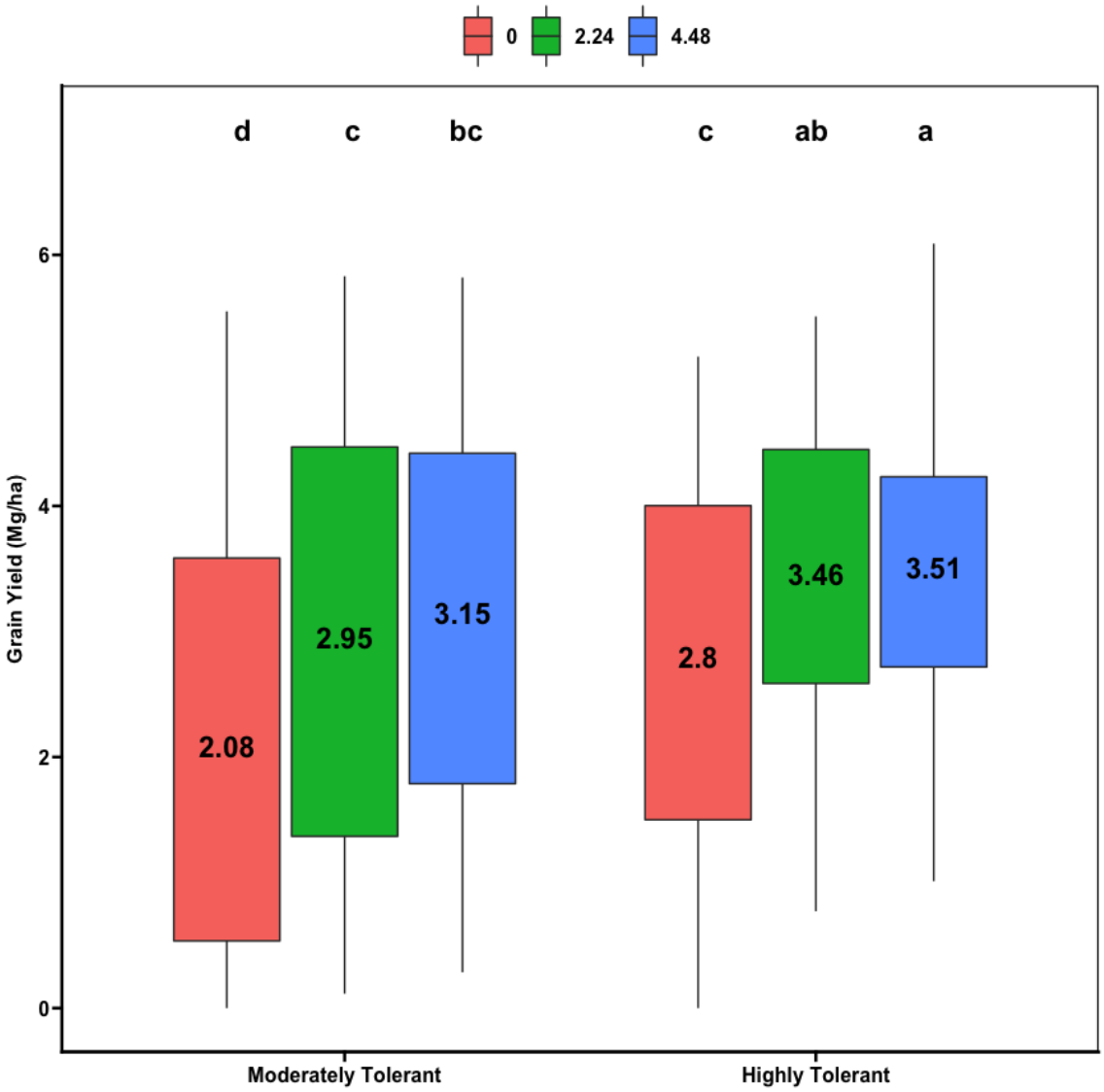

Figure 2-4 Distribution of grain yield as related to Fe-EDDHA rates for both varieties. Numbers inside the boxplots indicate the average grain yield. Black letters on top denote significant differences in grain yield ($P < 0.05$) across varieties and Fe-EDDHA rates.

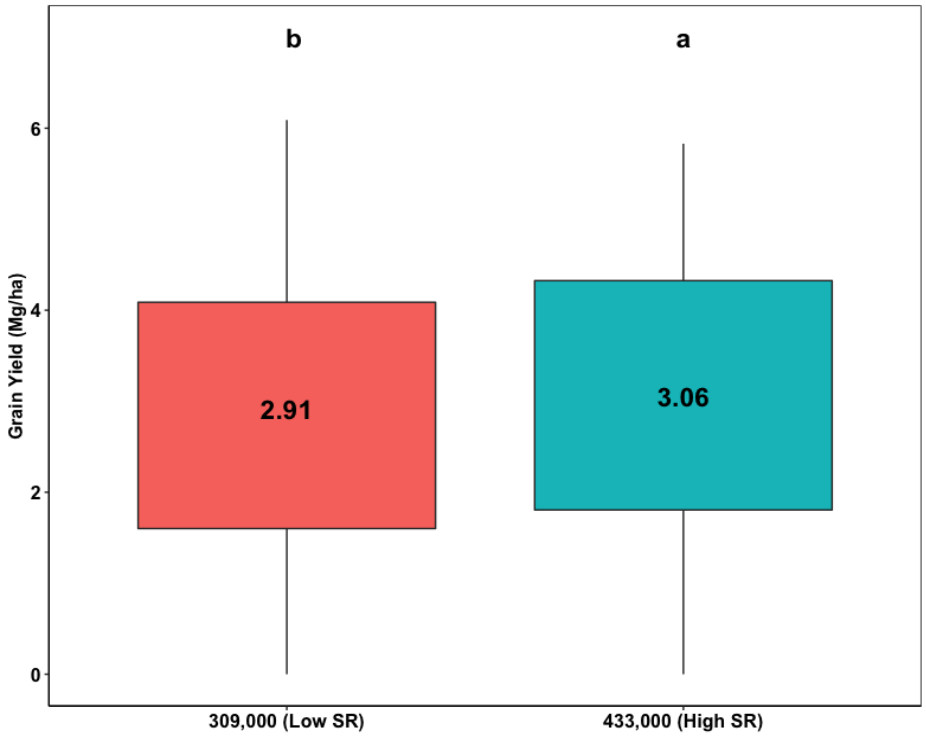

Figure 2-5. Distribution of grain yield as related to seeding rates. Numbers inside the boxplots indicate the average grain yield. Black letters on top denote significant differences in grain yield ($P < 0.05$) between seeding rates tested.

Figure 2-6. Mean net economic returns of varieties [Moderately Tolerant (MT) and Highly Tolerant (HT)], Fe-EDDHA rates [0, 2.24 (2) and 4.48 (4) kg Soygreen® ha^{-1}] and seeding rate [309,000 (125) and 433,000 (175) seeds ha^{-1}) combinations compared to the control treatment of (MT variety with 0 Fe-EDDHA at 309,000 seeds ha^{-1}).

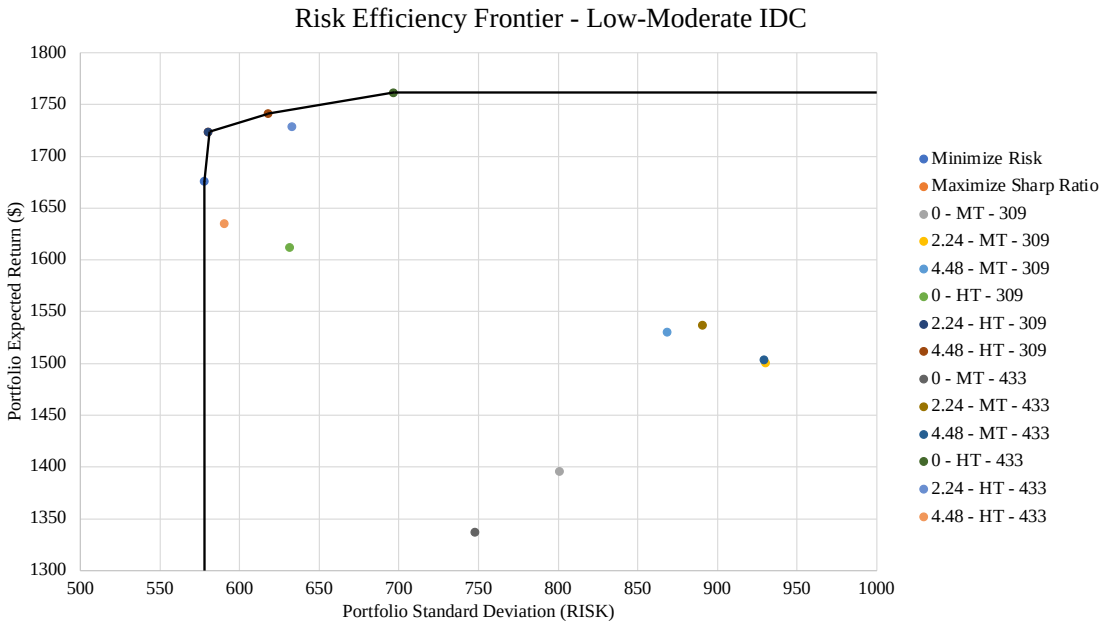

Figure 2-7. Portfolio Net Return ($ ha^{-1}) vs. Portfolio Standard Deviation (Risk, $ ha^{-1}) for each of the management strategy combinations (0, 2.24 and 4.48 represent all three iron chelate rates in kg ha^{-1}, and 309 and 433 represent both seeding rates in thousand seeds ha^{-1}) under low-moderate IDC conditions. Risk Efficient Frontier is represented by the black line. Minimize risk represents the Minimum Variance Choice (or lowest risk) and Maximize Sharpe Ratio represents the Optimum Portfolio (or highest net return).

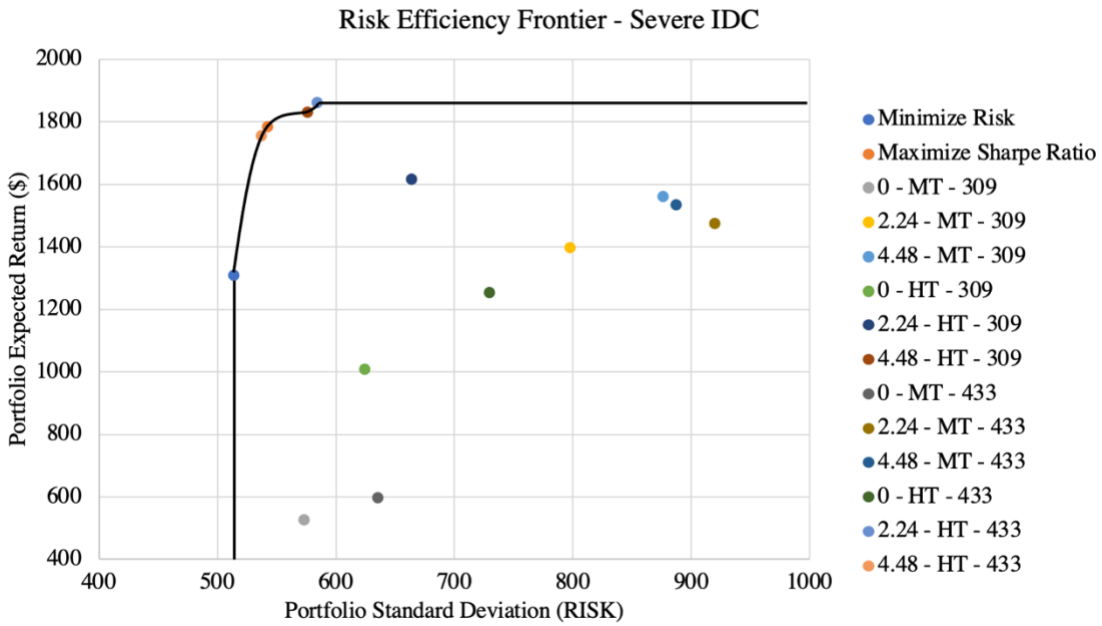

Figure 2-8. Portfolio Net Return ($ ha^{-1}) vs. Portfolio Standard Deviation (Risk, $ ha^{-1}) for each of the management strategy combinations (0, 2.24 and 4.48 represent all three iron chelate rates in kg ha^{-1}, and 309 and 433 represent both seeding rates in thousand seeds ha^{-1}) under severe IDC conditions. Risk Efficient Frontier is represented by the black line. Minimize risk represents the Minimum Variance Choice (or lowest risk) and Maximize Sharpe Ratio represents the Optimum Portfolio (or highest net return).

Chapter 3. Application of UAV Imagery-Derived Vegetation Indices for Estimating Soybean Yield Grown Under IDC Stress Conditions

3.1 Summary

Iron deficiency chlorosis (IDC) can significantly limit soybean yield, especially on calcareous soils, where it usually occurs in complex, discontinuous, and unpredictable patterns. Given that IDC is a serious management issue for soybean growers in the US Upper Midwest, accurate yield predictions of soybean cultivated under such stress conditions could serve as a management, marketing, and policy making tool for farmers, soybean-related industries, and governmental agencies. The goal of this study was to develop a model to predict the yield of soybean affected by IDC using UAV-based vegetation indices as explanatory variables. Five vegetation indices were generated from UAV-imagery collected at R1 and R5.5 phenological stages from five experiments carried out at three locations during the 2021 and 2022 growing seasons. Canopy reflectance measurements were collected using a MicaSense multispectral sensor, mounted on a DJI Inspire 2 UAV. Main outcomes from this research were: (i) UAV-based VI's provide a more precise, objective and efficient assessment of IDC symptom severity compared to traditional visual scores and ground-based active sensors; (ii) NDVI at R1 and NDRE at R5.5 are the best VI's for grain yield forecasting in soybean grown under IDC stress conditions; (iii) the linear regression model generated with NDRE measurements collected at R5.5 resulted in better prediction accuracies compared to the model developed with NDVI data collected at R1, but the overall performance of both models were not satisfactory when validated with testing data; and (iv) a decision tree using VI's indicated through a path analysis as most prominent for yield estimation provided an accurate (RMSE and MAE of 0.53 and 0.45 Mg ha^{-1}, respectively) and intuitive prediction model that explained 93.5% of the yield variability. Results from this study are promising and provide a simple and practical tool for soybean yield estimation at the farm level, but which could be refined and used in a broader scale (e.g., region, country).

Abbreviations: IDC, iron deficiency chlorosis; VI, vegetation index; UAV, unmanned aerial vehicle; DN, departure from normal; VCS, visual chlorosis scoring; GCP, ground control point; CRP, calibrated reflectance panel; DLS, downwelling light sensor; AIC, Akaike Information Criteria; RMSE, root mean square error; MAE, mean absolute error;

NDVI, normalized difference vegetation index; NDRE, normalized difference red-edge index; ENDVI, enhanced normalized difference vegetation index; OSAVI, optimized soil adjusted vegetation index; SAVI, soil adjusted vegetation index; EMS, electromagnetic spectrum; MSE, mean squared error.

3.2 Introduction

Iron (Fe) is an essential micronutrient required for chlorophyll biosynthesis and functioning of the photosynthetic apparatus of plants (Yadavalli et al., 2012). Despite being relatively abundant in agricultural soils, Fe is often present in the oxidized (Fe^{3+}) state that soybean plants cannot take up (Souri, 2016). In soybean, iron deficiency leads to interveinal chlorosis and stunting of the growth, both of which severely affect yield (Inskeep and Bloom, 1987). This nutrient stress is termed Iron Deficiency Chlorosis (IDC). In the US alone, IDC is estimated to cause yield reductions totaling $260 million annually (Peiffer et al., 2012).

Selection of varieties with improved tolerance remains the most effective and most practical strategy to manage IDC (Niebur and Fehr, 1981; Goos and Johnson, 2000; Naeve and Rehm, 2006; Helms et al., 2010). Consequently, the use of IDC-tolerant varieties is considered fundamental for profitable production in chlorosis-prone fields (Wiersma, 2005). Increased seeding rates and soil applications of iron chelates also have been studied and shown to be effective in improving the overall health and final yields of soybean grown in iron-deficient soils (Penas et al., 1990; Goos and Johnson, 2000; Kaiser et al., 2014).

In the US Upper Midwest, soils formed by a calcium carbonate parent material are often highly conducive to IDC development (Goos and Johnson, 2001). These soils commonly have a pH in the range of 7.0 to 8.5, with elevated calcium carbonate and soluble salt concentrations (Hansen et al., 2003). Although calcareous soils are prone to IDC, the severity of symptoms is highly dependent on various environmental and edaphic factors, such as soil moisture and nitrate levels (Godsey et al., 2003; Bloom et al., 2011). The spatial and temporal variability of these set of variables controlling Fe-chlorosis expression creates severe, moderate, and low IDC areas interspersed in a landscape (Gamble et al., 2014). Given that IDC most frequently occurs in complex and discontinuous patterns, soybean growers often do not know the extent of these areas and amount of yield loss being caused by this abiotic stress (Rogovska and Blackmer, 2008).

Considering the importance of soybean as a source of protein and oil and the escalating demand for food and energy, monitoring and forecasting soybean yield is essential for food security worldwide (Holzman et al., 2014). Accordingly, early prediction of soybean yield is of great interest because early information on potential yield reductions can be a useful instrument to aid crop management and crop marketing planning, project market behavior, and to support governmental policies (Schwalbert et al., 2020; Zhao et al., 2020).

Canopy sensing technologies have been proposed as a tool to predict the yield of various crops (Rehman et al., 2019; Hassan et al., 2019; Dong et al., 2015; Christenson et al., 2016), as well as to map the distribution of IDC throughout a field (Kyaw and Ferguson, 2008; Rogovska and Blackmer, 2008). Because IDC impacts chlorophyll synthesis, affecting leaf color, such technologies have been used to quantify plant greenness, an indirect measure of IDC severity (Hassanijalilian, 2020).

Plant greenness can be quantitatively measured by calculating a series of vegetation indices (VI's), which are based on reflectance measurements from optical sensor (Rasmussen et al., 2015). Vegetation indices can be defined as mathematical models on light reflected at two or more spectral wavebands and have been recognized as a reliable way to relate canopy reflectance with crop yield (Christenson, et al., 2016; Schwalbert et al., 2020; da Silva, et al., 2020). Previous research has shown that VI's are advantageous for mapping spatial variability within and across plots and fields (Govaerts et al., 2007; Mulla, 2013; Merotto et al., 2012; Portz et al., 2012), but selection of the best VI protocol for a specific crop and issue is critical for the successful development of a yield prediction algorithm (Samborski et al., 2009, Liu et al., 2017, Bushong et al., 2018).

The NDVI is the most widely used vegetation index, and it is derived by the combination of reflectance from the red and near-infrared bands (Rouse et al., 1974). The downside of NDVI is that this index reaches saturation levels when the crop canopy is fully developed, deriving unreliable measurements (Schepers, 2008; Sharma et al., 2015). To overcome this problem, several modifications of NDVI have been proposed, such as the NDRE and ENDVI. The NDRE and ENDVI are indices based on the red edge and green spectral bands, respectively, which are more sensitive to moderate to high chlorophyll content, avoiding saturation as leaves completely cover the row (Kanke et al., 2012). Other

modifications of NDVI also have been proposed, such as SAVI and OSAVI, but these indices attempt to minimize the soil background effect. Most ratio-based VI's that account for soil background include coefficients that were derived from empirical studies (Hatfield et al., 2008). The SAVI index includes a constant "L", which is an adjustment factor for soil reflectance, and is set based on the vegetation density (Huete, 1988). OSAVI is an extension of SAVI, having a more specific constant (0.16). In vegetation cover that is higher than 50%, OSAVI is expected to perform better in decreasing the effect of soil noise (Rondeaux, 1996).

Studies showing the benefits of remote sensing technologies and VI's utilization for yield estimation in soybean are abundant, but there is limited reporting of the use of UAV-based VI's in yield prediction of soybean grown under IDC stress conditions. For growers, mapping the extent and severity of IDC-prone fields and early prediction of grain yield in these areas could provide an advantage in terms of on-farm management, such as crop marketing planning. Considering the importance of soybean and IDC in the North Central United States, soybean yield prediction could support policy decision-making, such as insurance and other financial decisions. Therefore, the goal of the current research was to develop a model to predict soybean yield using UAV-based VI's measurements that is simple and practical and that could be used by growers, researchers, and industry. The specific objectives were: 1) compare the performance of different in-field methods of IDC symptom assessment; 2) identify which UAV-based VI is best for estimating grain yield of soybean affected by IDC; and 3) test the performance of the best VI's in forecasting yield using different prediction approaches.

3.3 Materials and Methods

3.3.1 Research environments

Five of the ten research environments described in Chapter 2 were used in this study (environments 1, 3, 5, 7, and 9). Environments 1, 3, 5, 7 and 9 will be identified hereafter as environments 1, 2, 3, 4, and 5, respectively. All five field sites were established in the "hotspot" IDC part of commercial farmer's fields, where IDC was expected to be severe. General soil properties and additional environment and agronomic information for each of the five environments are presented in Tables 3-1 and 3-2, respectively. All field sites were

in a corn-soybean rotation, expect for environment 3 that was in a corn-soybean-sugar beet rotation. At all environments, plots were 9 x 3 meters with four rows spaced 76 cm apart from each other.

For the 2021 growing season, weather data were retrieved from the nearest weather station no more than 30 km from a given site from High Plains Regional Climate Center (HPRCC, Lincoln, NE, https://hprcc.unl.edu/). For the 2022 growing season, remote weather stations (Hobo® U30 Station, Onset Computer Corporation, Bourne, MA) installed at each location at the time of planting provided monthly air temperature and precipitation information. Thirty-year normal (1984-2013) air temperatures and rainfall also were collected from HORCC and were used to calculate departure from normal (DN).

3.3.2 In-field evaluations of IDC severity and grain yield data

IDC symptom assessment was performed using a 1 to 5 visual chlorosis scoring (VCS based on Goos and Johnson, 2000), Crop Circle™ model ACS-430 (Holland Scientific Inc., NE, USA), and high-resolution drone imagery at R1 and R5.5 growth stages. All in-field evaluations of IDC severity were carried out on the same day between 10:00 and 14:00 h local time to limit shading effects.

The 1 to 5 visual chlorosis scoring, popularly called greenness scores, has been traditionally used to evaluate IDC symptoms. In this system, 1 = no chlorosis, 2 = slight chlorosis on the upper leaves, 3 = distinct chlorosis throughout the canopy, 4 = distinct chlorosis throughout the canopy with stunted growth and some leaf necrosis, and 5 = severe necrosis with plants dying or dead (Goos and Johnson, 2000). The visual ratings were performed by the same experienced rater at all dates of data collection. Only the two inner rows of each plot were rated.

The Crop Circle™ is a ground-based active crop canopy sensor that measures crop/soil reflectance at 670 nm, 730 nm, and 780 nm, providing NDVI and NDRE vegetation indices data as well as basic reflectance information. This sensor was manually carried at walking speed above the second row of each plot (sensor distance above the canopy was around 1 meter), positioned on a 0° angle relative to the canopy (nadir position), collecting approximately 50 spectral measurements per experimental unit. Average NDVI and NDRE readings were calculated for further analysis.

Drone imagery was acquired with a RedEdge-MX sensor (MicaSense Inc., Seattle, WA, USA) mounted on a DJI Inspire 2 (DJI Technology Co. Ltd., Shen Zhen, China). This sensor captures the five following spectral bands at the same time: blue (475 nm x 32 nm), green (560 nm x 27 nm), red (668 nm x 14 nm), red-edge (717 nm x 12 nm) and near-infrared (842 nm x 57 nm). The drone was programmed to fly each field autonomously with the assistance of Pix4D Capture, which remotely controls the Unmanned Aerial Vehicle (UAV) flight path, desired flight altitude, and image overlap. Thus, the UAV was flown at a ground speed of 1 m s^{-1} and at 23m AGL (above ground level). This altitude was defined to obtain proper ground sample distance (GSD = 1.6 cm pixel-1), and consequently, high spatial resolution. All images were captured from nadir view with 75% front and 75% side overlap. On average, approximately 200 images were captured per flight. A pipeline was created from image capture to image analysis and is shown in Figure 1.

Considering that ambient light conditions may change in the middle of a flight, images of the RedEdge-MX Calibrated Reflectance Panel (CRP) were obtained before and after each flight to provide accurate representation of light conditions at each time point of data collection. The CRP has unique known reflectance values across the visible and near-infrared light spectrum and are provided by MicaSense to convert the raw pixel values of an orthomosaic into reflectance. Additionally, a DLS (downwelling light sensor) was also integrated with the camera onto the drone (the DLS was installed on top of the aircraft, facing up towards the sky), measuring the solar irradiance throughout each mission. The irradiance information is embedded within the metadata of each image for each band. In summary, the CRP and DLS are used in conjunction in post processing to correct for changing illumination conditions, enabling improved reflectance calibration. Detailed information about the conversion of raw pixel values to reflectance with the use of CRP and DLS can be found in the MicaSense Knowledge Base (https:// support.micasense.com/hc/en-us/articles/115000765514-Use- of-Calibrated-Reflectance-Panels-For-RedEdge-Data).

A total of six ground control points (GCPs, orange bucket lids of 30.5 cm in diameter with a painted black circle in the center) were placed at the four corners and in the center of each research trial and remained there for the duration of the growing season.

A Trimble® GPS unit (Catalyst™ DA2 GNSS receiver, Trimble®, Westminster, CO, USA) mounted on a survey pole and connect to a smartphone was used to record the coordinates (known location) of the center of each GCP before the first flight. The positioning derived had an estimated accuracy averaging 2 cm and was used for geometric calibration.

Final yields were recorded for every single plot. Yield data was collected by harvesting the center two rows of each plot with a small plot combine (Almaco SPC40, Almaco, IA, USA) at maturity stage (R8 according to Caviness and Fehr, 1977). The first and fourth rows were considered border rows and were not harvested to avoid competition effect between rows of different plots. The weight of each sample (total grain mass plot^{-1}) was converted to yield (Mg ha^{-1}) and adjusted for a 13% moisture basis (130 g kg^{-1}).

3.3.3 Image processing

The main goal in image processing is to produce a map where the value of each pixel faithfully indicates the reflectance of the target object. Thus, after image acquisition, the raw imagery (16-bit TIF format) was processed, mosaicked and orthorectified using Pix4D mapper (Pix4D SA, Lausanne, Switzerland). Pix4D mapper uses an advanced structure from motion (SfM) workflow to derive accurate orthomosaics in absolute reflectance values. The default processing option template, "Ag Multispectral" was selected for generating the geo-referenced reflectance maps. Although the processing speed of this template is slow, it provides outputs with high quality and reliability (Pix4D Support, 2022). The three key steps of reflectance map generation in Pix4D mapper comprise initial processing (in which geometric and radiometric calibration are performed), point cloud densification and mesh generation, and creation of a digital surface model, orthomosaic, and reflectance map. In step 1, the WGS 84 datum was used with a projected coordinate system of UTM zone 15 N. In addition, all six GCPs were input into each of the Pix4D projects directly following the initial processing step using the ray cloud editor. In step 3, the derivation of absolute reflectance values was achieved by Pix4D using both the CRP images with known reflectance values and the readings from the DLS stored in the image EXIF. The known reflectance values for each spectral band of the CRP equal to 0.47

(46.98%), 0.47 (47.19%), 0.47 (47.21%), 0.47 (47.21%) and 0.47 (47.12%) for blue, green, red, red-edge, and near-infrared bands, respectively.

3.3.4 Vegetation Index (VI) Calculation

QGIS software (QGIS Geographic Information System, http://qgis.osgeo.org) was used for plot segmentation, index calculation, thresholding, soil-plant masking, and VI values extraction. The "Create Grid" tool was used to generate polygon shapefile to delineate each plot and segment the rows of interest (two center rows).

Five vegetation indices were created from the generated reflectance maps using the "Raster Calculator" plugin in QGIS and were based on the reflectance in the near infrared, red, red-edge, green, and blue portions of the electromagnetic spectrum: NDVI (Normalized Difference Vegetation Index), NDRE (Normalized Difference Red Edge Index), ENDVI (Enhanced Normalized Different Vegetation Index), OSAVI (Optimized Soil Adjusted Vegetation Index), and SAVI (Soil Adjusted Vegetation Index) (Table 3-4). Since IDC causes yellowing of the leaves, which is associated with a decrease in chlorophyll content, these indices were chosen based on their ability to estimate greenness and chlorophyll levels in leaves (Rasmussen et al., 2013, Gago et al., 2015, Hansen and Schjoerring, 2003; Jannoura et al., 2014; Huete, 1988; Rondeaux, 1996). As described previously, the SAVI index includes a soil adjustment constant "L", defined based on the vegetation density (Huete, 1988). In the current project, L = 1 was used, which is meant for very low vegetation.

Thresholding was performed in QGIS using the "raster calculator" tool to separate the soybean pixels from the soil background due to their simplicity and applicability (Zepp et al., 2021). The threshold value was created by observing the image's histogram and selecting the pixel value that included the maximum number of soybean pixels without soil pixels (Duddu, et al., 2019). Although thresholding was done to eliminate background noise, SAVI and OSAVI were generated in an attempt to remove the contribution of soil noise, specifically in the leaf edge pixels, where soil and vegetation information may be mixed (Barzin, et al., 2020). The masked soybean canopy for each vegetation index was then used to extract the mean index values of each plot using the "Zonal Statistics" tool in QGIS.

3.3.5 Statistical analysis

Statistical analyses were conducted using R project for statistical computing in combination with R Studio version 4.1.2 (R Core Team, 2020) and considered significant at $P < 0.05$. Pearson correlation was calculated to evaluate the strength of the relationship between in-field evaluations of IDC severity (VCS, Crop Circle NDVI and NDRE, and UAV-based VI's) and soybean grain yield. The Pearson's correlation coefficient (R) was computed at R1 and R5.5 for every one of the five environments.

To identify which UAV-based VI is best for predicting grain yield of soybean affected by IDC, restricted maximum likelihood (REML) linear mixed models were performed using the lme4 package (Bates et al, 2014) across all five environments. For R5.5 estimations, the data was log-transformed to provide a greater goodness of fit with the exponential response of grain yield and VI's values. For each growth stage and VI, models were fitted with mean index values as fixed effect and combinations of independent intercept and/or slopes for environments and blocks nested within environments as random effects. For this analysis, 70% of the data was used to fit and 30% of the data was used to test each of the models. For each of the growth stages, the best VI to predict soybean yield was chosen based on the Akaike Information Criteria (AIC), where lower values indicate better fit (Weisberg, 2014). Although the coefficient of determination (R^2) is routinely used to assess goodness of fit, it was calculated to describe the proportion of variance explained by each of the models only (Weisberg, 2014). The AIC number was preferred over R^2 to determine the best VI for yield prediction because it provides a greater test of relative model fit (is more robust) for comparing mixed effects models. The root mean square error (RMSE) also was calculated to check the goodness of each of VI in estimating grain yield. Residual plots were examined to confirm model assumptions of homogeneity of variances and normality of residuals.

Linear regression model fit was employed to develop a yield prediction model for each growth stage using the best VI as features. Different training and validation datasets were used for model generation and performance evaluation. During the training phase, data from environments 1, 2, 4, and 5 were used to fit each of the models, while data from the environment 3 was used to test the model during the validation phase. The same

procedure was done for R1 and R5.5 development stages. The coefficient of determination (R^2) was used to assess each model's explanatory abilities for soybean yield variances. In addition, two metrics were computed to examine the predictive accuracy of each model: the root mean square error (RMSE), and the mean absolute error (MAE). The formulas for calculating each of these parameters are expressed as follows:

$$R^2 = 1 - \frac{\sum(y_i - \hat{y})^2}{\sum(y_i - \bar{y})^2} \;\; ; \; RMSE = \sqrt{\frac{1}{n}\sum_{i=1}^{n}(y_i - \hat{y}_i)^2} \;\; ; \; MAE = \frac{1}{n}\sum_{i=1}^{n}|y_i - \hat{y}_i|$$

where n denotes the number of samples, y_i the observed yield of sample i, and $\hat{y}_i$ the predicted yield of sample i.

3.4 Results and Discussion

This study presents a novel approach to estimate yield of soybean grown under IDC stress conditions using UAV-derived vegetation indices. Four major steps included the development of a model that can accurately forecast soybean yield: (1) correlation analysis between different in-field methods of IDC symptom assessment for validation purposes; (2) linear mixed effects model to evaluate the goodness of fit of each of the VI's as in-season soybean yield estimators; (3) use of the indices identified as best in Step 2 in linear regression algorithms to assess their performance in predicting grain yield; (4) development of a regression tree using VI's selected as having the strongest cause-and-effect relationship with grain yield as an alternative methodology to provide a more accurate yield prediction model.

3.4.1 Performance of different in-field methods of IDC symptom assessment

In soybean, IDC symptom severity is traditionally accomplished using a 1-5 visual rating system (VCS) with a score of 1 given to plots showing no symptoms and a score of 5 given to plots displaying severe necrosis, plants dying or even dead (Goos and Johnson, 2000). A visual scorecard of this method is presented in Supplemental Figure 3-1. Although

the VCS is a simple method, there are two major problems associated with its utilization. First, human inconsistencies arising from variations in color perception, physical conditions of the researcher, or even the fluctuation in field illumination conditions can result in less accurate measurements (Bai et al., 2018). Second, the visual rating system is laborious and time consuming, which can be a limitation when several plots are to be evaluated (De Cianzio et al., 1979). The speed of IDC visual rating has been the reason why symptoms are typically assessed only at one time point during the growing season (Dobbels and Lorenz, 2019).

Portable crop canopy sensors such as the Crop Circle™ (Crop Circle) represent another tool to produce information about crop health. The Crop Circle uses a modulated polychromatic LED array light source and three photodetection channels that simultaneously measure crop/soil reflectance. Although the Crop Circle provides a less subjective measurement of IDC symptom severity compared to visual ratings, it is also somewhat laborious and time consuming. In addition, the reliability of NDVI and NDRE values generated with the Crop Circle can be negatively affected by soil background interference when low canopy cover is apparent (Hong et al., 2007). Besides interveinal chlorosis, IDC causes stunting of the growth, and therefore, soybean plants very often do not fully close the canopy. Given that the Crop Circle is usually run approximately 1m above the crop canopy, it may not always only collect information from the crop canopy but also soil reflectance. Gamble et al. (2014) utilized another active crop canopy sensor named Greenseeker (Trimble Navigation Limited, Sunnyvale, CA) to generate NDVI values from soybean fields affected by IDC and the authors reported that NDVI values were not able to detect differences from untreated soybean most likely due to the minimal ground cover provided by the soybean crop. Therefore, if VI's values generated in a more high-throughput manner using UAV imagery are as good/reliable as the ones obtained with the crop circle and visual scores, logistics for in-season data collection could be significantly improved.

Pearson correlation analysis was performed between grain yield and data collected from each of the three IDC symptom severity assessment methods at R1 and R5.5 (Table 3-5). Highly significant ($P < 0.001$) negative (for VCS) and positive (for the Crop Circle and UAV-based VI's) correlations were observed between IDC symptom severity

measurements and grain yield at all environments and dates of data collection. The UAV-based measurements provided the highest correlation coefficient in four of five environments at R1 and in all environments at R5.5. At R1, changes in grain yield could be best predicted by changes in UAV-based NDVI at environments 1, 2, 3, and 5 (R = 0.935, 0.678, 0.941, and 0.579, respectively). At R1 in environment 4, NDRE derived from the Crop Circle resulted in the highest correlation coefficient (R = 0.898). At R5.5, UAV-based NDRE showed the highest correlation coefficient at three out of five environments (environments 1, 2, and 5, with R = 0.963, 0.945, 0.895, respectively). At R5.5 in environments 3 and 4, the strongest correlation with yield was achieved with UAV-based OSAVI and SAVI, respectively (R = 0.965, and 0.943, respectively). Averaged across all environments, the highest correlation coefficient was obtained with UAV-based NDVI at R1 (0.801) and UAV-based NDRE at R5.5 (0.934). Compared to measurements acquired with VCS and the Crop Circle, the correlation coefficient was increased by an average of 0.18- and 0.04-points with UAV-based NDVI at R1 and 0.12- and 0.05-points with UAV-based NDRE at R5.5. This overall increase in R indicates that the UAV-based VI's were more precise than VCS and the Crop Circle. These findings may be explained by the fact that UAV measurements are less subjective than the visual rating system and contain less soil background interference caused by the field of view and distance from canopy of the Crop Circle. Further, relative to both, VCS and Crop Circle, UAV-based measurements are more efficient and less laborious, which could facilitate logistics for in-season data collection over larger areas and at a higher frequency in a growing season.

Results from the current study agree with those of Rasmussen et al., (2015) and Dobbels (2020). Rasmussen, et al. (2015) used two different UAVs and two different consumer-grade sensors to determine whether UAV-based VI's were reliable for assessing experimental plots and found that UAV-acquired VI's had the same capability to quantify crop responses to different abiotic and biotic stress as ground-based methods. Dobbels (2020) collected IDC symptom severity data for ten weeks during the growing season of nine environments and reported Pearson correlation to yield averaging 0.72 for UAV-based NDVI, 0.57 for Crop Circle NDVI, and 0.59 for VCS, across all environments and dates of data collection. Overall, the general stronger correlation between UAV-derived VI's and

grain yield was expected, as this was the first hypothesis to be validated towards the use of VI's values for yield prediction in soybean affected by IDC.

3.4.2 Evaluating the ability of different VI's in estimating soybean yield

In this study, we explored five vegetation indices generated from multispectral UAV imagery to compare their ability to estimate grain yield. All five VI's evaluated are indicators of plant greenness and have been previously used by researchers for estimating grain yield of several crops (Sharma et al., 2015; Hassan et al., 2019; Shen et al., 2022; Johnson et al., 2014; Da Silva et al., 2020; Santana et al., 2022; Schwalbert et al., 2020).

At R1, all vegetation indices showed a highly significant positive linear relationship with grain yield ($P < 0.001$, Table 3-6). At this growth stage, NDVI measurements provided the highest predictive power for grain yield estimation (AIC = 592.84), followed by OSAVI (AIC = 655.61), NDRE (AIC = 698.16), ENDVI (AIC = 712.72), and SAVI (AIC = 727.83). When unseen data was used for validation, the NDVI model at R1 explained 89.3% of the variation, with predictions resulting in a RMSE of 0.545 Mg ha^{-1}. The strong relationship observed between NDVI and grain yield at R1 is not surprising as a sensitivity analysis has demonstrated that NDVI has the highest sensitivity to estimate biophysical parameters of vegetation when the canopy is not fully closed (Ji and Peters, 2007). This increased sensitivity shown by NDVI before canopy closure is mainly due to a sharp absorption of the red band caused by chlorophyll during photosynthesis and a peak of reflectance in the near infra-red caused by the cellular structure of the leaves (Silva Junior et al., 2018). Da Silva et al. (2020) used a path analysis to evaluate the direct relationship of several VI's generated from UAV-imagery collected at V4 with soybean grain yield and reported that NDVI was the most relevant vegetation index for yield estimation. Kyaw et al. (2008) evaluated vegetation indices derived from aerial imagery and soil properties such as pH and electrical conductivity as to their potential to delineate chlorosis management zones in soybean. The authors reported that across five chlorosis-prone sites, NDVI was the parameter most related to grain yield.

A highly significant positive exponential relationship with soybean yield also was observed for all VI's at R5.5 ($P < 0.001$, Table 3-6). However, contrarily to what was found at R1, NDRE was the VI with the best performance at the seed filling stage (AIC = 321.49),

delivering a R^2 of 0.939 and a RMSE of 0.413 Mg ha^{-1} when validating the model with testing data. At R5.5, the inferior performance of NDVI (AIC = 577.67, R^2 testing = 0.886, RMSE testing = 0.564 Mg ha^{-1}) is likely due to saturation at high amounts of green biomass (i.e., NDVI loses sensitivity at greater values of leaf area index) (Asner et al., 2003; Chen et al., 2006). Saturation of NDVI occurs when the NIR band continues to increase at the latest stages of crop development and the red band exhibits a nearly flat response (when leaf coverage approaches 100%, the amount of red light that can be absorbed by leaves reaches a peak (Tucker, 1979; Thenkabail et al., 2000). The imbalance between these two spectral bands results in a change in the NDVI ratio (the denominator has a much larger impact on the ratio than the numerator), lowering the sensitivity of NDVI to chlorophyll concentrations (only small changes in NDVI measurements occur at full canopy), and thus yielding a poorer relationship with biomass (Gitelson et al., 1996). The red edge region of the electromagnetic spectrum (EMS) is defined as a transition zone between absorption by pigments and scattering by leaves and canopies (Gitelson and Merzlyak, 1994). Relative to the red band, the red edge portion of the EMS can penetrate deeper into high biomass canopies due to a reduced absorption coefficient (Nguy-Robertson et al., 2012). For this reason, higher values of chlorophyll content and leaf area index are needed to reduce the sensitivity of red edge at advanced development stages. As such, red-edge-based vegetation indices can usually overcome the saturation problems reported with NDVI (Van Niel and McVicar, 2004). Similar findings were reported by Kanke et al. (2012), who compared NDRE and NDVI for detecting differences in winter wheat N status. Their study showed that NDVI performed better in detecting plant growth differences at the same N rates at early growth stages, while REP (Red-Edge Position index) was better at advanced growth stages and increased N rates, highlighting the potential of red-edge-based VI's in overcoming saturation. Results from our study are also in agreement with those of Sharma et al. (2015), who reported better late-season corn yield predictions with NDRE compared to NDVI.

The lower predictive power of OSAVI and SAVI (AIC = 655.51 and 727.83 for OSAVI and SAVI, respectively) compared to NDVI at R1 indicates that thresholding was performed well enough to minimize soil background interference, and that the soil-brightness-dependent correction factors included in the mathematical equations of OSAVI,

and SAVI ended up reducing their ability to capture the changes in leaf reflectance caused by IDC. The ENDVI measurements had the second lowest predictive power at both growth stages evaluated (AIC of 712.72 and 524.03 at R1 and R5.5, respectively), indicating that the inclusion of the green and blue bands didn't improve grain yield estimation of soybean affected by IDC.

3.4.3 Prediction model development using the best VI's and linear regression

The best VI at each growth stage (NDVI at R1 and NDRE at R5.5) was used in a linear regression model to predict soybean grain yield. Model fit was evaluated by calculating the coefficient of determination (R^2), the root mean square error (RMSE), and the mean absolute error (MAE). These parameters also were used to evaluate prediction accuracies of each of the models when testing data was used for validation. Further, in yield prediction model development using linear regression, the use of data from multiple years and locations is essential because it ensures that spatial and temporal variability due environmental conditions (soil and weather) will reflect the predictive boundaries of the model (Mourtzinis, et al., 2014). In the present research, there was substantial environmental variation among all four environments used for model fitting (Tables 3-1 and 3-2).

Although both linear regression models were significant ($P < 0.05$, data not shown), soybean yield predictability improved as the phenological stage progressed from R1 to R5.5 (Table 3-7). When each model was validated with testing data, the calculated R^2, RMSE and MAE were 0.88, 1.72 Mg ha^{-1}, and 1.63 Mg ha^{-1}, respectively, for the R1 model, while the model using measurements from R5.5 resulted in a R^2 of 0.91, a RMSE of 0.92 Mg ha^{-1}, and a MAE of 0.82 Mg ha^{-1}. This is likely because at R5.5, soybeans have integrated a greater portion of the growing season conditions impacting grain yield, such as weather conditions and recovery from IDC, if any. Ma et al. (2001) used a hand-held multispectral radiometer to collect canopy reflectance measurements at multiple growth stages in soybean and determine optimum development stage at which yield could be predicted. The authors found that the yield-NDVI relationship was linear at R2 and R4 but exponential at R5, with NDVI measurements at R2 explaining 29% of the variation in yield, 59% at R4 and 80% at R5. Both the relationships between VI's measurements and

yield and the R^2 values were similar to what was observed in our study. According to the same authors, soybean yield potential is set at later phenological stages for varieties that show indeterminate growth habit, such as the ones grown in shorter grown seasons like in the US Upper Midwest. As shown in Table 3-2, the 2022 growing season was especially dry from pod formation (R3) to seed filling (R5.5), and IDC symptoms (data not shown) tended to improve after R1 at all five environments. Thus, NDVI at R1 solely does not account for these factors contributing to final yields, which may explain why the fitted model at R1 only explained 28% of the yield variability compared to 78% with the fitted model at R5.5, and why predictions using R1 measurements were less precise than predictions using data from R5.5. Findings from the current study also agree with those of Schwalbert et al. (2020), who reported that soybean yield prediction models tended to become less accurate as yield forecasts were performed earlier in the growing season and tended to become more assertive towards the end of the growing season. This is unfortunate because the earliest the predictions, the broader the options these yield estimations could be used to support agricultural decisions. However, R5.5 occurred 55 days before harvest, on average across all five environments, which indicates that soybean yield could be forecasted more than a month ahead of harvesting time.

Even though the model developed using NDRE measurements collected at R5.5 presented better performance than the R1 model using NDVI values, the accuracy of predictions was still not satisfactory as other studies have reported better performance metrics for soybean yield estimation (Mourtzinis et al., 2014; Kross et al., 2020; Schwalbert et al., 2020; Christenson et al., 2016). The relatively poor performance of the regression-based models could be associated with a small number of environments used for model calibration (environmental variability encountered in environment 3 was not well reflected in the predictive boundaries of the model) or with the existence of non-linear relationships between VI's and yield that simple linear regressions cannot integrate during model development (Barzin et al., 2020). Further, our findings could also indicate that the use of NDVI at R1 and NDRE at R5.5 alone did not provide adequate information for accurate soybean yield prediction. Perhaps the inclusion of ancillary variables would be necessary for the development of a model with improved predictive performance (Mourtzinis et al., 2014).

3.4.4 Improving predictive performance using an alternative approach

Because the linear regression algorithms developed with NDVI at R1 and NDRE at R5.5 solely did not provide satisfactory yield prediction results, we evaluated an alternative approach using results from a path analysis as explanatory variables in a decision tree algorithm, as it has been done by Da Silva et al. (2020). A path analysis aims to provide estimates of the magnitude and significance of assumed causal relationships between a set of variables and it has been previously used to partition the relative contribution of yield components in soybean (Kang, 1994; Board et al., 1997; Shukla et al., 1999). A path coefficient measures the direct effect of a variable hypothesized to be a cause on another variable hypothesized to be an effect (Dewey and Lu, 1959). Although a path coefficient is derived from correlations, it is deemed as more informative and useful than a simple correlation coefficient (Kang et al., 1983; Gravois and McNew, 1993). In the present study, a path analysis was used to identify which VI's were most relevant for estimating soybean yield. In R Studio, the path analysis was performed using the "cfa" function from the lavaan package version 0.6-12 (Rosseel, 2012) and the path diagram was created using the "semPaths" function from the semPlot package version 1.1.6 (Epskamp, 2015). Data from environments 1, 2, 4 and 5 were used in the path analysis and in the development of the path diagram (Figure 3-4).

Results from the path analysis revealed that NDRE at R5.5 had the strongest positive direct effect on grain yield (path coefficient = 0.92), followed by OSAVI at R5.5, and NDVI at R1 (path coefficient = 0.8 and 0.42, respectively) (Figure 3-4). NDRE, ENDVI, OSAVI and SAVI at R1 and NDVI, ENDVI, and SAVI at R5.5 were not found to have a prominent positive direct contribution to grain yield (i.e., their direct effects on yield were either weak when positive or negative). Da Silva et al., (2020) and Santana et al., (2022) used VI's derived from UAV-imagery as explanatory variables and grain yield as the dependent variable in a path analysis and observed that NDVI had the highest direct effect on soybean yield. In their studies, VI's were generated from images captured at V4 (Da Silva et al., 2020) and R1 (Santana et al., 2022), which is similar to our findings that NDVI had the highest direct effect on soybean yield among all VI's generated at the earlier growth stage (R1).

The three VI's indicated by the path analysis as the most important for yield estimation were used as independent explanatory variables in a regression tree algorithm with grain yield as the principal dependent variable. The decision tree is an inverse tree-like graph with the root node (the variable that best splits the data) on top and terminal nodes (where the predictions, in this case numerical, are made) at the bottom and is built by recursively evaluating different features and using, at each decision node, the feature that best splits the data (Géron, 2017). A decision tree algorithm was selected over other machine learning models because they are fairly intuitive (not considered a black box) and are easy to interpret (Hassanijalilian et al., 2020). The decision tree was generated using the "ctree" function from the partykit package version 1.2-16 (Hothorn et al., 2006). The decision tree was trained with data from environments 1, 2, 4, and 5 and was validated with data from environment 3. The performance of the decision tree in predicting soybean yield also was evaluated by computing the R^2, RMSE, and MAE.

Although the path analysis indicated that OSAVI at R5.5 had a stronger direct effect on yield compared to NDVI at R1, results from the regression tree (Figure 3-5) show that NDVI at R1 provided a smaller mean squared error (MSE) compared to OSAVI at R5.5 during attribute selection, and this is the reason why NDVI was used as decision nodes instead of OSAVI (the classification and regression tree algorithm uses MSE-based node splitting criteria to split nodes and minimize the MSE of the whole tree). The resulting regression tree is composed of 10 inner nodes and 11 terminal nodes, with NDRE at R5.5 as the most important variable for the prediction model. The regression tree shows that, if NDRE at R5.5 is lower or equal to 0.521, grain yield is predicted to be lower than 2 Mg ha^{-1} (average of 1.7 Mg ha^{-1}). If NDRE values at R5.5 are greater than 0.521, soybean yield is estimated to range from an average of 2.6 Mg ha^{-1} to 4.6 Mg ha^{-1}, depending on other NDRE values at R5.5 and NDVI values at R1.

The training step of the decision tree used training data from environments 1, 2, 4, and 5, and provided a R^2 of 0.91, a RMSE of 0.43 Mg ha^{-1}, and a MAE of 0.33 Mg ha^{-1}. The validation step used testing data from environment 3, and highlights that the decision tree was able to predict grain yield of soybean grown under IDC stress conditions with a relatively high accuracy (RMSE of 0.53 and MAE of 0.45 Mg ha^{-1}), accounting for 93.5% of the yield variability (Figure 3-6). These results are of great value because they

demonstrate that the VI's indicated by the path analysis and used in the regression tree were able to accurately predict soybean yield. Using a similar approach, Da Silva et al. (2020) reported soybean yield predictions with a RMSE of 196 kg ha^{-1}, and a R^2 of 0.85. Similar findings were also reported by Jonshon (2014), who used NDVI and daytime land surface temperature information as explanatory variables in a decision tree algorithm to forecast soybean yield in the United States on a county level. Likewise, the average difference between the predicted and observed yield in the validation phase was 0.42 Mg ha^{-1}, presenting a R^2 of 0.71. Decision tree models have also been used for crop yield estimation in other studies (Fernandes et al., 2011; Marinkovć et al., 2009; and Veenadhari et al., 2014).

Compared to the linear regression models for R1 and R5.5 using NDVI and NDRE measurements alone, combining results from a path analysis and a regression tree algorithm provided yield predictions that are 3.25 and 1.73 times more accurate in terms of RMSE for R1 and R5.5, respectively, and 3.62 and 1.81 times more accurate considering MAE at R1 and R5.5, respectively. The yield prediction improvement observed with the decision tree relative to the simple linear regression could be explained by two things. First, the fusion of VI's measurements from two growth stages that are critical stages of crop development can better capture cumulative greenness and biomass conditions, providing improved metrics for soybean yield estimation in comparison with models using NDVI at R1 and NDRE at R5.5 solely. Johnson et al. (2016) reported that complementing NDVI with EVI (enhanced vegetation index) led to a significant improvement in crop yield forecasting in Canada relative to models utilizing NDVI alone. Second, it could be that machine learning models are simply more accurate than conventional empirical models such as linear regression due to their ability to overcome issues related to the spatial and temporal nonlinear properties of crop yields (Kamir et al., 2020). Advantage of machine learning models such as decision tree, random forest, and support vector machine over linear regression models has already been reported (Jiang et al., 2004; Uno et al., 2005). However, it is important to note that the performance of an algorithm depends on multiple factors, such as the crop of interest, the predictor variables being used, the environment, and the quality of the training data, and as such, making assumptions about the performance of a specific algorithm is extremely difficult (Kamir et al., 2020).

3.5 Conclusions

This study compared different UAV-based vegetation indices generated from imagery collected at R1 and R5.5 growth stages in their ability to estimate grain yield of soybean grown under IDC stress conditions and evaluated the performance of different models for yield prediction. Knowing which VI and growth stage is best for yield estimation is important for precision agriculture applications, such as mapping the extent and severity of IDC areas. Developing a model that can accurately predict yield has a practical value as it can be used by growers, researchers, industry, and policy makers to support agricultural decisions.

Our results show that in-season measurements of IDC using a UAV had the advantages of objectiveness, efficiency, and precision over ground-based methods. Our study also revealed that NDVI and NDRE at R1 and R5.5, respectively, provided the highest predictive power for yield estimation of soybean affected by IDC compared to ENDVI, OSAVI, and SAVI. Performance of linear regression models using the best VI's at each growth stage for grain yield estimation were not as good as hoped, which could be attributed to a small number of environments used for model fitting, the inability of simple linear regression in integrating a potential non-linear relationship between VI's and grain yield, or the need of ancillary variables to provide other important information associated with grain yield. Moreover, combining VI's indicated through a path analysis as most prominent for yield estimation in a regression tree algorithm suggests that soybean yield can be predicted with reasonable accuracy (RMSE of 0.53 and MAE of 0.45 Mg ha^{-1}), while explaining more than 93% of the yield variability. As such, this model has the potential to be a useful tool to guide soybean management and marketing at the farm level, as well as aid the projection of market behavior, and provide information to support governmental policies. Inclusion of data from additional environments, especially from soybean grown under IDC stress conditions outside of the specified boundaries of the training dataset used in this study could refine model performance and allow its usage in a broader scale.

3.6 Tables

Table 3-1. Soil average Olsen soil test P, ammonium acetate K, soil/water pH, DTPA-extractable Fe, electrical conductivity (EC), calcium carbonate equivalency (CCE), and nematodes (eggs per 100 CC soil) for each of the ten environments studied. Soil samples were composed of 6 soil cores per replication (4 replications = 24 cores per site) taken at a depth of 0 to 15 cm.

Environment	P	K	Fe	SOM	CCE	EC†	pH	Nematodes
	(mg kg^{-1})			(g kg^{-1})		(S m^{-1})		Eggs/100 CC
1	29	325	7	79.5	118.7	0.13	7.9	2,525
2	11	173	3	47.0	72.0	0.12	8.2	50
3	67	346	7	63.5	115.7	0.11	8.0	0
4	16	181	5	57.5	114.0	0.18	7.9	3,931
5	14	161	4	51.0	26.2	0.10	8.2	3,856

Table 3-2. Monthly total precipitation and average temperature data at the five environments studied.

	Precipitation data (mm) †											
	May		June		July		August		September		October	
Location-Year	Tot.	DN	Tot.	DN	Tot.	DN	Tot.	DN	Tot.	DN	Tot.	DN
Danvers-2021	35.56	-49.28	68.58	-35.56	83.82	-17.78	165.10	69.34	132.08	62.23	137.16	74.93
Danvers-2022	-	-	31.24	-57.15	24.13	-77.47	49.28	-46.48	19.81	-50.04	0.76	-27.94
Foxhome-2021	45.72	-27.94	48.26	-55.88	35.56	-63.50	109.22	45.72	71.12	7.62	83.82	12.70
Foxhome-2022	33.53	21.34	32.77	-71.37	27.94	-71.12	9.65	-53.85	5.57	-57.93	-	-
Graceville-2021	38.10	-33.53	15.24	-80.01	71.12	-29.72	172.72	104.90	91.44	29.72	121.92	63.25

	Temperature data (°C) ‡											
	May		June		July		August		September		October	
Location-Year	Avg.	DN	Avg.	DN	Avg.	DN	Avg.	DN	Avg.	DN	Avg.	DN
Danvers-2021	15.33	1.11	23.61	3.56	23.44	1.11	21.50	0.56	17.83	1.39	12.00	3.78
Danvers-2022	-	-	23.35	2.84	23.03	0.70	20.54	-0.40	16.84	0.40	18.20	7.09
Foxhome-2021	13.15	-0.38	21.87	2.53	23.21	1.40	20.88	0.33	17.33	1.60	10.47	2.78
Foxhome-2022	20.63	3.82	22.10	2.77	22.79	0.99	20.75	0.20	16.69	0.97	-	-
Graceville-2021	13.44	-0.06	21.83	2.67	23.17	1.44	21.61	1.22	17.22	1.78	10.78	2.94

† Tot., total monthly precipitation; DN, departure from normal.
‡ Avg., average monthly temperature, DN, departure from normal.

Table 3-3. Environment (Env.), year, location/county, site, field coordinates, planting date, emergence date, and soil series for ten environments evaluated in western MN from 2021 to 2022.

Env.	Year	Location/County	Site	Field coordinates	Planting date	Emergence date	Harvest Date
1	2021	Danvers / Swift	Hotspot	45°15'25.9"N 95°42'19.9"W	11-May	23-May	19-Oct
2	2021	Foxhome / Wilkin	Hotspot	46°12'33.9"N 96°25'01.0"W	10-May	21-May	30-Sep
3	2021	Graceville / Big Stone	Hotspot	45°34'28.9"N 96°24'32.2"W	10-May	22-May	19-Oct
4	2022	Danvers / Swift	Hotspot	45°15'18.2"N 95°41'38.8"W	3-Jun	12-Jun	13-Oct
5	2022	Foxhome / Wilkin	Hotspot	46°20'00.3"N 96°25'10.9"W	28-May	9-Jun	29-Sep

Table 3-4. Mathematical representation of vegetation indices calculated from spectral reflectance.

Vegetation Index	Equation	Reference
NDVI (Normalized Difference Vegetation Index)	(NIR - Red) / (NIR + Red)	Rouse et al., 1974
NDRE (Normalized Difference RedEdge Index)	(NIR - RedEdge) / (NIR + RedEdge)	Li et al., 2014
ENDVI (Enhanced Normalized Difference Vegetation Index)	((NIR + Green) - (2 x Blue)) / ((NIR + Green) + (2 x Blue))	Rasmussen et al., 2015
OSAVI (Optimized Soil Adjusted Vegetation Index)	(NIR - Red) / (NIR + Red + 0.16)	Rondeaux et al., 1996
SAVI (Soil Adjusted Vegetation Index)	((NIR - Red) / (NIR + Red + L)) * (1 + L), where L set to 1	Huete, 1988

Table 3-5. Pearson correlations between grain yield and IDC symptom severity measurements collected with a 1-5 visual rating system (VCS), an active crop canopy sensor named Crop CircleTM, and with an unmanned aircraft vehicle (UAV) at R1 and R5.5.

Environment	Method/Sensor-Index	*R* (R1)	*P* (R1)	*R* (R5.5)	*P* (R5.5)
1	VCS	-0.635	3.616e-12	-0.887	< 2.2e-16
	Crop Circle - NDVI	0.893	< 2.2e-16	0.790	< 2.2e-16
	Crop Circle - NDRE	0.829	< 2.2e-16	0.917	< 2.2e-16
	UAV - NDVI	0.935	< 2.2e-16	0.917	< 2.2e-16
	UAV - NDRE	0.861	< 2.2e-16	0.963	< 2.2e-16
	UAV - ENDVI	0.865	< 2.2e-16	0.919	< 2.2e-16
	UAV - OSAVI	0.893	< 2.2e-16	0.937	< 2.2e-16
	UAV - SAVI	0.838	< 2.2e-16	0.933	< 2.2e-16
2	VCS	-0.498	2.47e-07	-0.720	< 2.2e-16
	Crop Circle - NDVI	0.610	4.34e-11	0.757	< 2.2e-16
	Crop Circle - NDRE	0.603	8.19e-11	0.797	< 2.2e-16
	UAV - NDVI	0.678	3.24e-14	0.932	< 2.2e-16
	UAV - NDRE	0.602	8.52e-11	0.945	< 2.2e-16
	UAV - ENDVI	0.545	9.12e-09	0.936	< 2.2e-16
	UAV - OSAVI	0.586	3.46e-10	0.943	< 2.2e-16
	UAV - SAVI	0.507	1.38e-07	0.941	< 2.2e-16
3	VCS	-0.691	6.82e-15	-0.930	< 2.2e-16
	Crop Circle - NDVI	0.901	< 2.2e-16	0.858	< 2.2e-16
	Crop Circle - NDRE	0.795	< 2.2e-16	0.937	< 2.2e-16
	UAV - NDVI	0.941	< 2.2e-16	0.938	< 2.2e-16
	UAV - NDRE	0.832	< 2.2e-16	0.957	< 2.2e-16
	UAV - ENDVI	0.915	< 2.2e-16	0.940	< 2.2e-16
	UAV - OSAVI	0.929	< 2.2e-16	0.965	< 2.2e-16
	UAV - SAVI	0.908	< 2.2e-16	0.958	< 2.2e-16
4	VCS	-0.752	< 2.2e-16	-0.883	< 2.2e-16
	Crop Circle - NDVI	0.858	< 2.2e-16	0.874	< 2.2e-16
	Crop Circle - NDRE	0.898	< 2.2e-16	0.921	< 2.2e-16
	UAV - NDVI	0.871	< 2.2e-16	0.848	< 2.2e-16
	UAV - NDRE	0.896	< 2.2e-16	0.910	< 2.2e-16
	UAV - ENDVI	0.808	< 2.2e-16	0.885	< 2.2e-16
	UAV - OSAVI	0.862	< 2.2e-16	0.922	< 2.2e-16
	UAV - SAVI	0.827	< 2.2e-16	0.943	< 2.2e-16
5	VCS	-0.533	2.19e-08	-0.651	6.677e-13
	Crop Circle - NDVI	0.530	2.71e-08	0.712	4.074e-16
	Crop Circle - NDRE	0.567	1.72e-09	0.832	< 2.2e-16
	UAV - NDVI	0.579	6.30e-10	0.889	< 2.2e-16
	UAV - NDRE	0.566	1.82e-09	0.895	< 2.2e-16
	UAV - ENDVI	0.496	2.68e-07	0.865	< 2.2e-16
	UAV - OSAVI	0.545	9.48e-09	0.816	< 2.2e-16
	UAV - SAVI	0.529	3.12e-08	0.795	< 2.2e-16

Table 3-6. Five site-year mean regression parameters of soybean yield [y (Mg ha^{-1})] and vegetation index values (x) for various vegetation indices at R1 and R5.5 growth stages.

Stage	Vegetation Index	Regression Model	AIC†	P	R^2 fitted	RMSE fitted	R^2 testing	RMSE testing
R1	NDVI	y = -10.133 + 17.508x	592.84	< 0.001	0.915	0.477	0.893	0.545
	NDRE	y = -1.772 + 14.577x	698.16	< 0.001	0.889	0.546	0.849	0.649
	ENDVI	y = -17.879 + 28.008x	712.72	< 0.001	0.870	0.588	0.850	0.645
	OSAVI	y = -7.557 + 21.041x	655.61	< 0.001	0.898	0.522	0.873	0.593
	SAVI	y = -4.853 + 20.207x	727.83	< 0.001	0.875	0.578	0.844	0.658
R5.5	NDVI	y = (-0.920 + 2.359x)^(1/0.184)	577.67	< 0.001	0.926	0.445	0.886	0.564
	NDRE	y = (-0.543 + 3.596x)^(1/0.368)	321.49	< 0.001	0.963	0.316	0.939	0.413
	ENDVI	y = (-1.941 + 3.792x)^(1/0.259)	524.03	< 0.001	0.936	0.414	0.907	0.508
	OSAVI	y = (-0.432 + 2.719x)^(1/0.223)	363.56	< 0.001	0.959	0.332	0.935	0.429
	SAVI	y = (-0.613 + 4.377x)^(1/0.435)	381.07	< 0.001	0.957	0.338	0.931	0.434

† Akaike Information Criterion. Lower AIC values indicate better fit.

Table 3-7. Performance metrics (R^2 = coefficient of determination, RMSE = root mean square error, MAE = mean absolute error) for soybean grain yield estimation using linear regression models with different training and testing datasets. RMSE and MAE are reported in Mg ha^{-1}. Data from environments 1, 2, 4, and 5 were used to fit the models and data from environment 3 was used to validate the model.

Growth Stage	VI	Equation	Training			Testing		
			R^2	RMSE	MAE	R^2	RMSE	MAE
R1	NDVI	y = -5.53 + 10.83x	0.28	1.20	1.03	0.88	1.72	1.63
R5.5	NDRE	y = (-0.57 + 3.51*x)^(1/0.317)	0.78	0.68	0.55	0.91	0.92	0.82

3.7 Figures

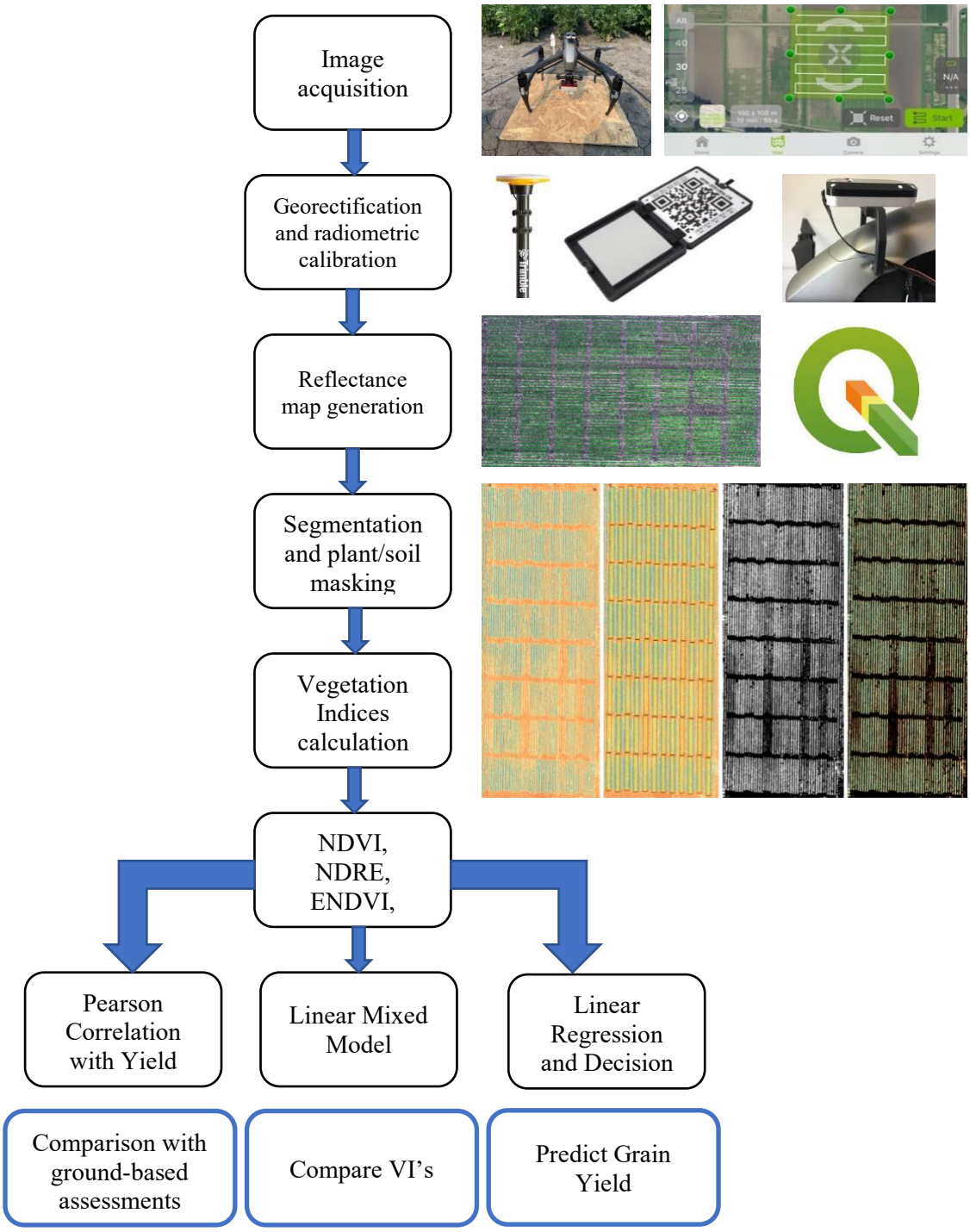

Figure 3-1. Pipeline for image capture and analysis for iron deficiency chlorosis symptomology assessment and use in yield prediction models.

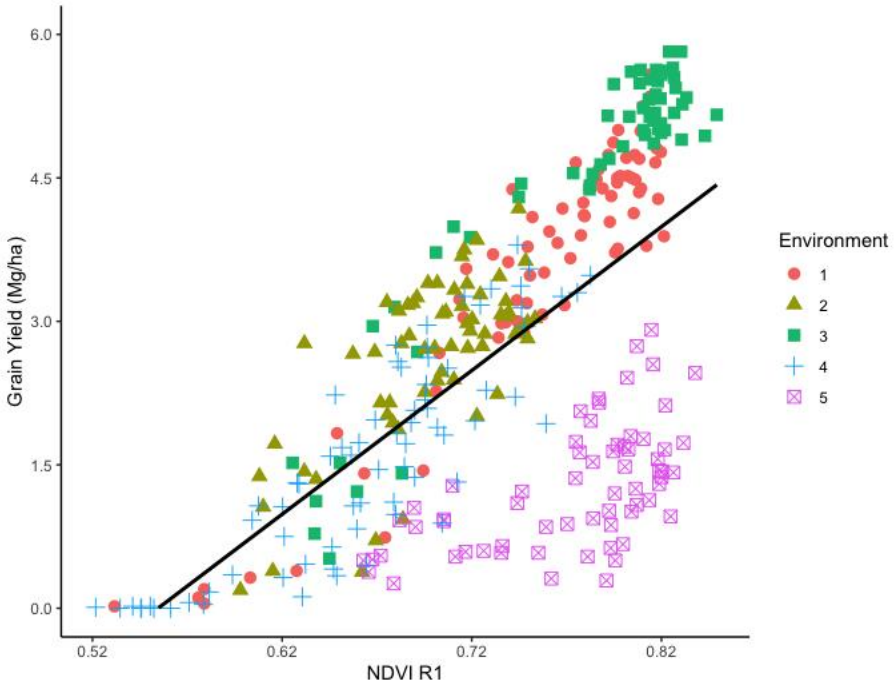

Figure 3-2. Fitted line for the regression of soybean yield in relation to UAV-based NDVI at R1 growth stage.

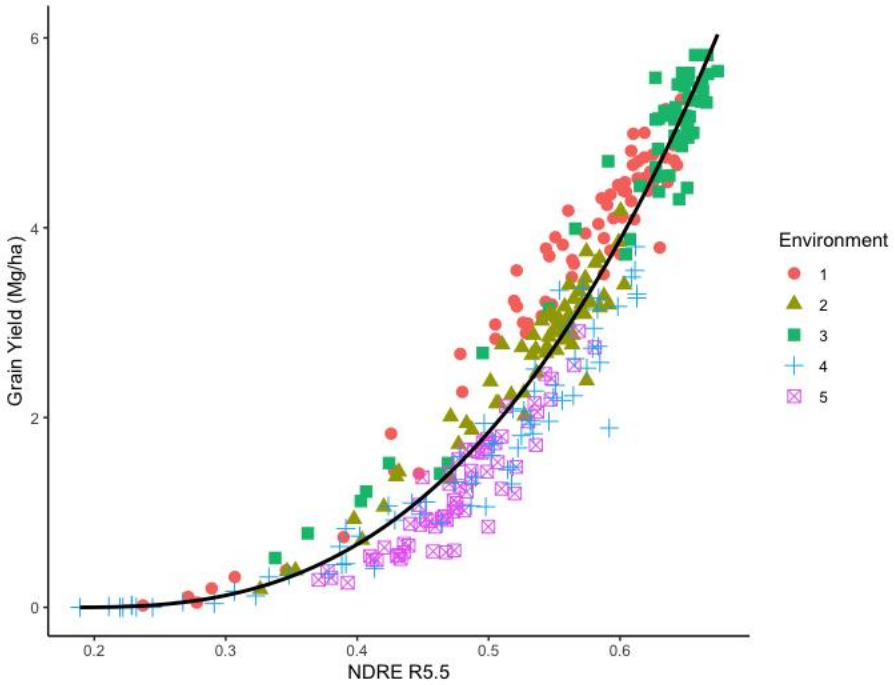

Figure 3-3. Fitted line for the regression of soybean yield in relation to UAV-based NDRE at R5.5 growth stage.

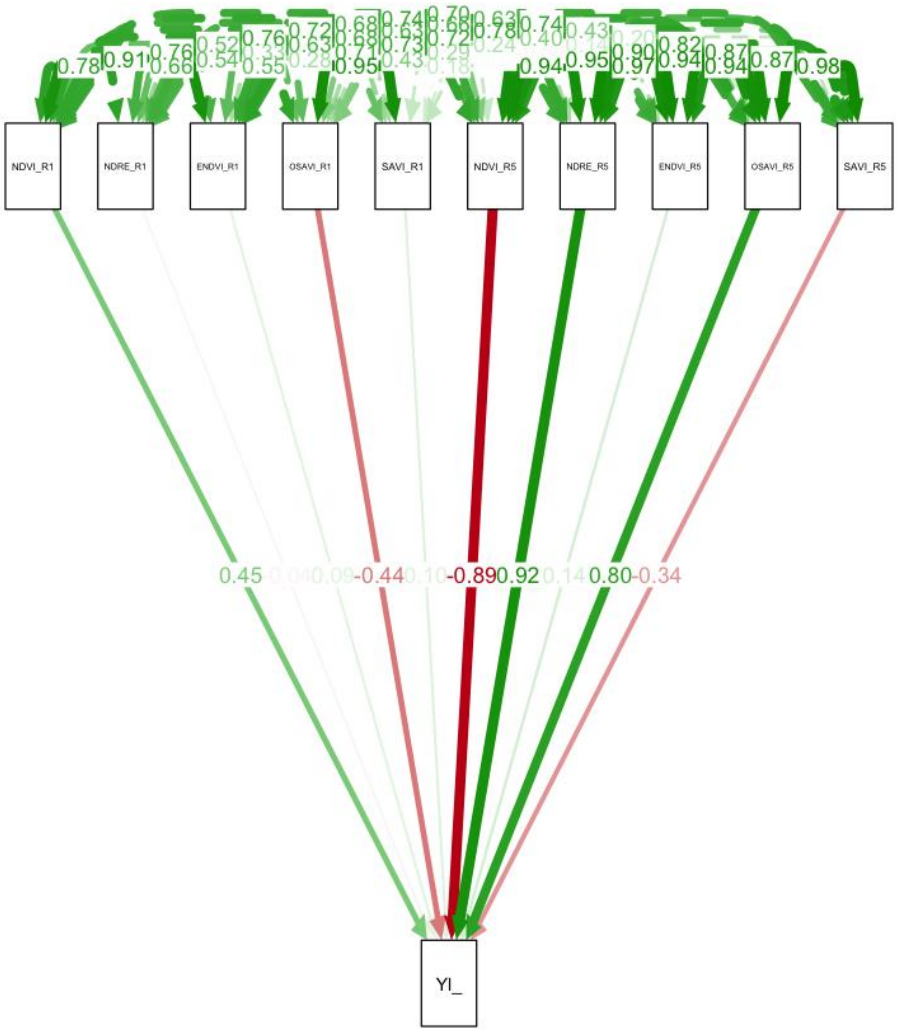

Figure 3-4. Path diagram from a path analysis for soybean grain yield (YI_) as a function of vegetation indices. One directional arrows represent direct paths and two directional arrows represent correlations. Path coefficients are represented by the numbers in th e middle of the one directional arrows and correspond to assumed direct effects of each of the vegetation indices on yield.

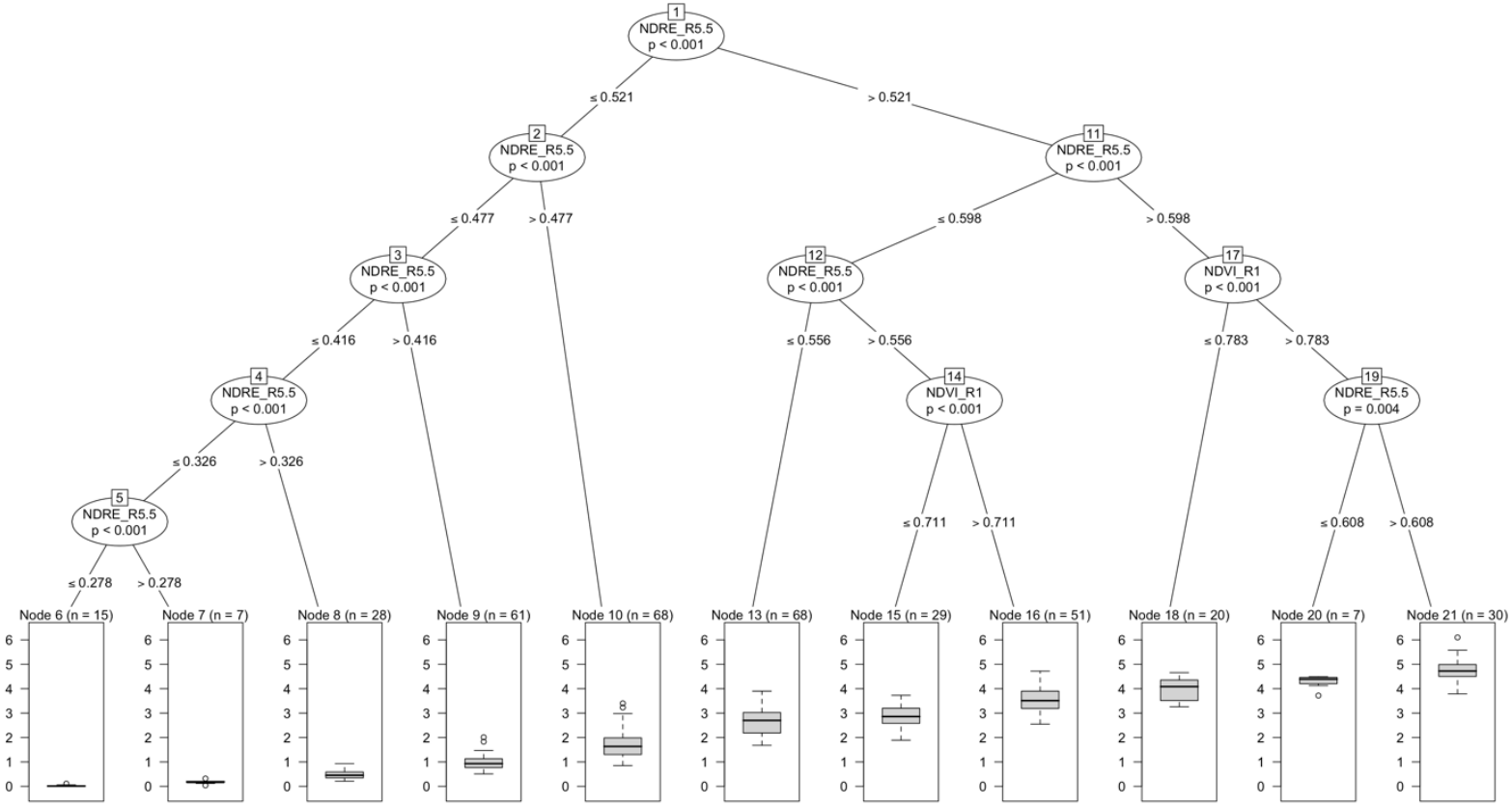

Figure 3-5. Decision criteria of the regression tree algorithm generated with NDRE at R5.5 and NDVI at R1 selected by a path analysis. Two sub-nodes are derived from each node, and the one that is derived to the left of the node represents the true evaluation of the parent node's condition.

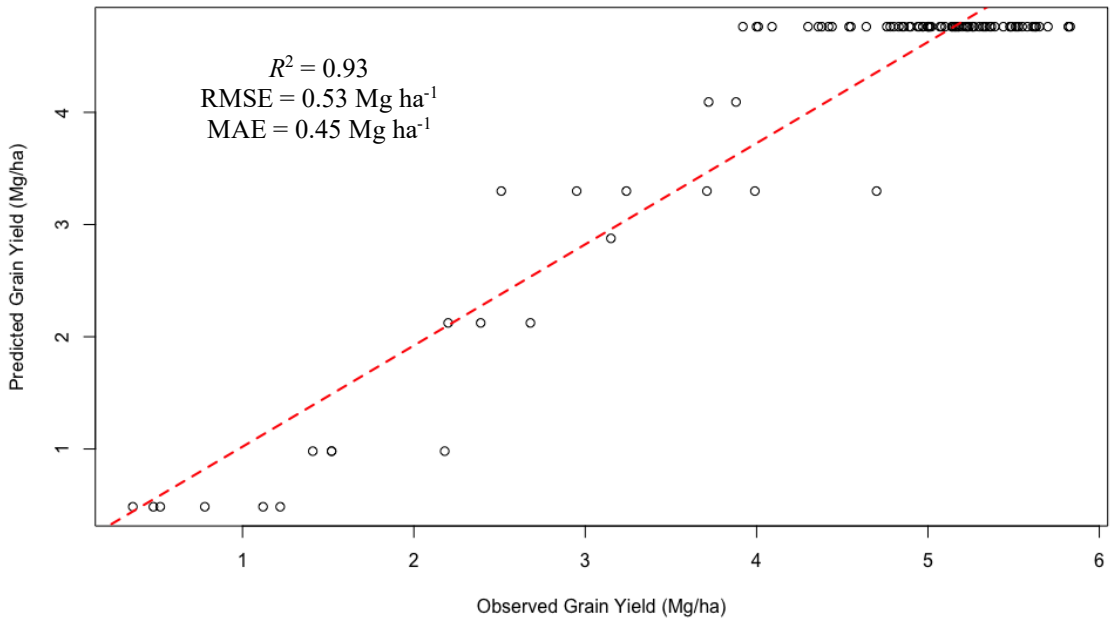

Figure 3-6. Relationship between the observed and predicted grain yield by the regression tree.

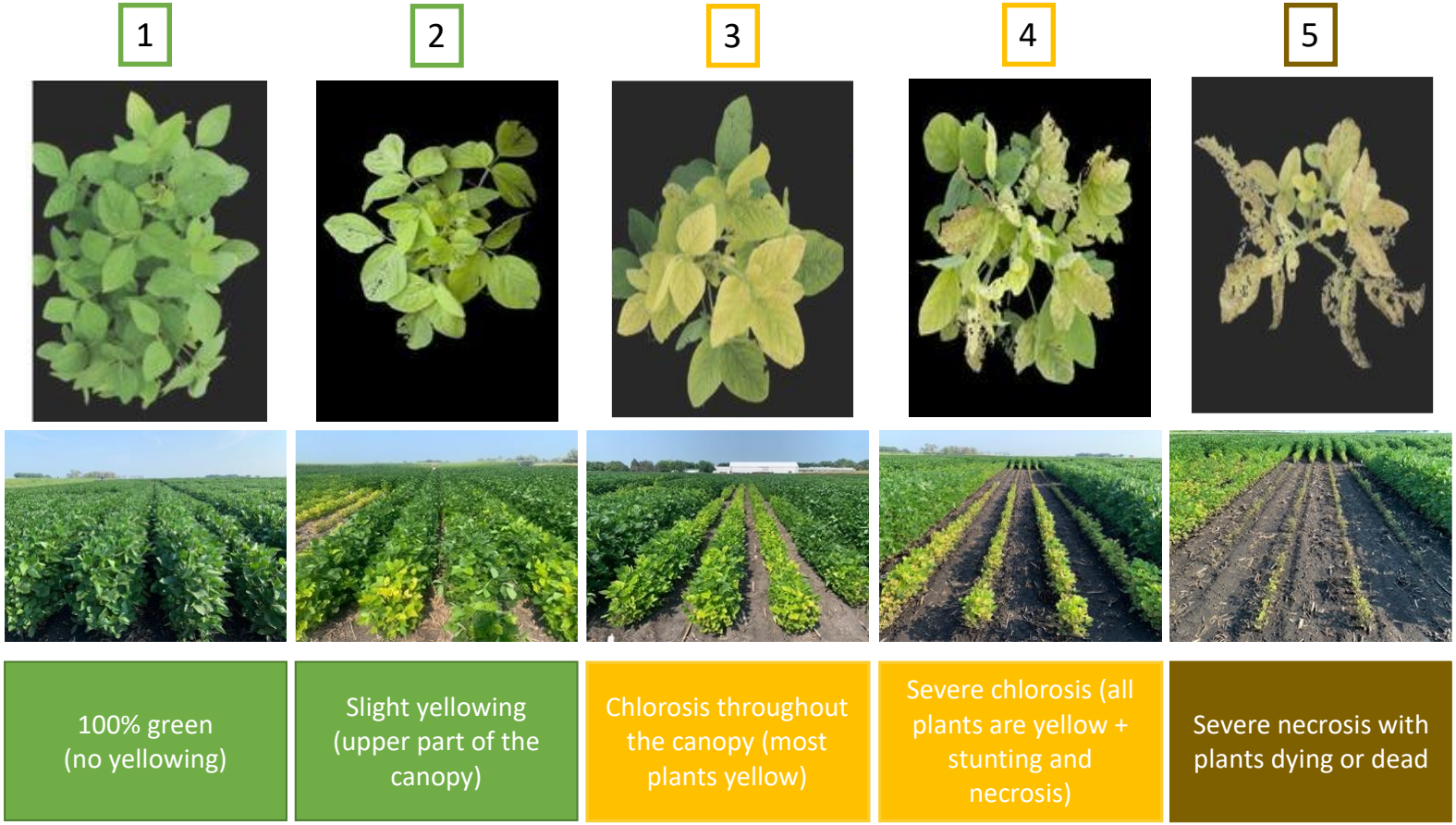

Supplemental Figure 3-1. IDC symptom severity rating protocol, popularly termed "greenness scores".

Literature cited

Aktas, M., & Van Egmond, F. (1979). Effect of nitrate nutrition on iron utilization by an Fe-efficient and an Fe-inefficient soybean cultivar. *Plant Soil*, *51*, 257-274.

Asner, G. P., Scurlock, J. M. O., & Hicke, J. A. (2003). Global synthesis of leaf area index observations: implications for ecological and remote sensing studies. *Global Ecology and Biogeography*, *12*, 191–205.

Atencio, L., Salazar, J., Lauter, A. N. M., Gonzales, M. D., O'Rourke, J. A., & Graham, M. A. (2021). Characterizing short and long term iron stress responses in iron deficiency tolerant and susceptible soybean (*Glycine max* L. Merr.) *Plant Stress 2*, 100012. https://doi.org/10.1016/j.stress.2021.100012

Barker, A. V., & Pilbeam, D. J. (2007). Handbook of plant nutrition. CRC Press, Boca Raton, FL.

Barzin, R., Pathak, R., Lofti, H., Varco, J., & Bora, G. C. (2020). Use of UAS multispectral imagery at different physiological stages for yield prediction and input resource optimization in corn. *Remote Sensing*, *12*, 2392. https://doi.org/ 10.3390/rs12152392

Bates, D., Maechler, M., Bolker, B., & Walker, S. (2014). lme4: Linear mixed-effects models using Eigen and S4. R package version 1.1–7. 2014. Institute for Statistics and Mathematics of WU.

Bloom, P. R., Rehm, G. W., Lamb, J. A., & Scobbie, A. J. (2011). Soil Nitrate is a causative factor in iron deficiency chlorosis in soybeans. *Soil Fertility & Plant* Nutrition, *75*, 2233–2241. https://doi.org/10.2136/sssaj2010.0391

Board, J. E., Kang, M. S., & Harville, B. G. (1997). Path analysis identify indirect selection criteria for yield of late-planted soybean. *Crop Science*, *27*, 879-884.

Bushong, J. T., Mullock, J. L., Arnall, D. B., & Raun, W. R. (2018). Effect of nitrogen fertilizer source on corn (*Zea mays* L.) optical sensor response index values in a rain-fed environment. *Journal of Plant Nutrition*, *41*, 1172–1183. https://doi.org/10.1080/01904167.2018.1434202

Caliskan, S., Ozkaya, I., Caliskan, M. E., & Arslan, M. (2008). The effects of nitrogen and iron fertilization on growth, yield and fertilizer use efficiency of soybean in a Mediterranean-type soil. *Field Crops Research*, *108*, 126-132. https://doi.org/10.1016/j.fcr.2008.04.005

Chatterjee, A., Lovas, S., Rasmussena, H., & Goos, R. J. (2017). Foliar application of iron fertilizers to control iron deficiency chlorosis of soybean. *Crop Forage Turfgrass Management*, *3*, 2017-05-0037. https://doi.org/10.2134/ cftm2017.05.0037

Chen, P. Y., Fedosejevs, G., Tiscareño-López, M., & Arnold, J. G. (2006). Assessment of MODIS-EVI, MODIS-NDVI and VEGETATION-NDVI composite data using agricultural measurements: an example at corn fields in western Mexico. *Environmental Monitoring and Assessment*, *119*, 69–82.

Christenson, B. S., Schapaugh, W. T., An, N., Price, K. P., Prasad, V., & Fritz, A. K. (2016). Predicting soybean relative maturity and seed yield using canopy reflectance. *Crop Science*, *56*, 625–643.

Da Silva Junior, C. A., Nanni, M. R., Shakir, M., Teodoro, P. E., Oliveira-Junior de, J. F., Cezar, E., Gois de, G., Lima, M., Wojciechowski, J. C., & Shiratsuchi, L. S. (2018). Soybean varieties discrimination using non-imaging hyperspectral sensor. *Infrared physics and Technology*, 338-350. https://doi.org/10.1016/j.infrared.2018.01.027

Da Silva, E. D., Baio, F. H. R., Teodoro, L. P. R., da Silva Junior, C. A., Borges, R. S., & Teodoro, P. E. (2020). UAV-multispectral and vegetation indices in soybean grain yield prediction based on in situ observation. *Remote Sensing Applications: Society and Environment*, *18*, 100318.

De Cianzio, S. R., Fehr, W. R., & Anderson, I. C. (1979). Genotypic evaluation for iron deficiency chlorosis in soybeans by visual scores and chlorophyll concentration. *Crop Science*, *19*, 644–646.

Dewey, D. R., & Lu, K. H. (1959). A correlation and path-coefficient analysis of components of crested wheatgrass seed production. *Agronomy Journal*, *51*, 515–518.

Dobbels, A. A. (2020). High-Throughput Phenotyping for Soybean Iron Deficiency Chlorosis Using an Unmanned Aircraft System: Applications in Breeding, Agronomy, and Genetics. Dissertation (PhD), University of Minnesota.

Dobbels, A. A., & Lorenz, A. J. (2019). Soybean iron deficiency chlorosis high-throughput phenotyping using an unmanned aircraft system. *Plant Methods*, *2019*, 15:97.

Dong, J., Xiao, X., Wagle, P., Zhang, G., Zhou, Y., Jin, C., Torn, M. S., Meyers, T. P., Suyker, A. E., Wang, J., Yan, H., Biradar, C., Moore, B. (2015). Comparison of four EVI-based models for estimating gross primary production of maize and soybean croplands and tallgrass prairie under severe drought. *Remote Sensing of Environment*, *162*, 154–168.

Duddu, H. S. N., Johnson, E. N., Willenborg, C. J., & Shirtliffe, S. J. (2019). High-Throughput UAV Image-Based Method Is More Precise Than Manual Rating of Herbicide Tolerance. *Plant Phenomics*, *2019*, 1-9. https://doi.org/10.34133/2019/6036453

Ellsworth, J.W., Jolley, V.D., Nuland, D.S., & Blaylock, A. D. (1998). Use of hydrogen release or a combination of hydrogen release and iron reduction for selecting iron-efficient dry bean and soybean cultivars. *Journal of Plant Nutrition*, *21*, 2639–2651.

Epskamp, S. (2015). semPlot: Unified visualizations of structural equation models. *Structural Equation Modeling*, *22(3)*, 474–483. https://doi.org/10.1080/10705511.2014.937847

Fehr, W. R., Caviness, C. E., Burmood, D. T., & Pennington, J. S. (1971). Stage of development descriptions for soybeans *Glycine max* (L.) Merrill. *Crop Science*, *11*, 929–931

Fernandes, J. L., Rocha, J. V., & Lamparelli, R. A. C. (2011). Sugarcane yield estimates using time series analysis of spot vegetation images. *Scientia Agricola*, *68(2)*, 139–146.

Ferreira, C. M., Sousa, C. A., Sanchis-Pérez, I., López-Rayo, S., Barros, M. T., Soares, H. M., & Lucena, J. J. (2019). Calcareous soil interactions of the iron (iii) chelates of dph and azotochelin and its application on amending iron chlorosis in soybean (Glycine max). *Science of the Total Environment*, *647*, 1586–1593.

Franzen D. W., & Richardson, J. L. (2008). Soil factors affecting iron chlorosis of soybean in the red river valley of North Dakota and Minnesota. *Journal of Plant Nutrition*, *23*, 67–78. https://doi.org/10.1080/01904160009381998

Frank, K., Beegle, D., & Denning, J. (1998). Phosphorus. In: J.R. Brown, editor, Recommended chemical soil test procedures for the North Central Region. North Central Regional Research Publication 221 (rev.). *University of Missouri*, Columbia. p. 21–30.

Froechlich D. M., & W. R. Fehr. (1981). Agronomic Performance of Soybeans with Differing Levels of Iron Deficiency Chlorosis on Calcareous Soil. *Crop Science*, *21*, 438–441. https://doi.org/10.2135/cropsci1981.0011183x002100030021x

Gago, J., Douthe, C., Coopman, R. E., Gallego, P.P., Ribas-Carbo, M., Flexas, J., Escalona, J., & Medrano, H. (2015). UAVs challenge to assess water stress for sustainable agriculture. *Agricultural Water Management*, *153*, 9-19.

Gamble A. V., Howe, J. A., Delaney, D., Van Santen, E., & Yates, R. (2014). Iron chelates alleviate iron chlorosis in soybean on high pH soils. *Agronomy Journal*, *106*, 1251–1257. https://doi.org/10.2134/agronj13.0474

Géron, A. (2017). Hands-On Machine Learning with Scikit-Learn and TensorFlow: Concepts, Tools, and Techniques to Build Intelligent Systems. O' Reilly Media, Inc.: Sebastopol, CA, USA, 2017.

Gitelson, A. A. & Merzlyak, M.N. (1994). Quantitative Estimation of Chlorophyll-a Using Reflectance Spectra: Experiments with Autumn Chestnut and Maple Leaves. *Journal of Photochemistry and Photobiology*, *22*, 247-252.

Gitelson, A. A., Kaufman, Y. J., & Merzlyak, M. N. (1996). Use of a Green Channel in Remote Sensing of Global Vegetation from EOS-MODIS. *Remote Sensing of Environment*, *58*, 289-298.

Godsey, C.B., Schmidt, J. P., Schlegel, A. J., Taylor, R. K., Thompson, C. R., & Gehl, R. J. (2003). Correcting iron deficiency in corn with seed row-applied iron sulfate. *Agronomy Journal*, *95*, 160–166.

Goos R. J., & Johnson, B. E. (2000). A comparison of three methods for reducing iron deficiency chlorosis in soybean. *Agronomy Journal*, *92*, 1135–1139. https://doi.org/10.2134/agronj2000.9261135x

Goos, R. J., & Johnson, B. E. (2001). Seed treatment, seeding rate, and cultivar effects on iron deficiency chlorosis of soybean. *Journal of Plant Nutrition*, *24*, 1255–1268. https://doi.org/10.1081/ PLN-100106980

Govaerts, B., Verhulst, N., Sayre, K. D., de Corte, P., Goudeseune, B., Lichter, K., Crossa, J., Deckers, J., & Dendooven, L. (2007). Evaluating spatial within plot crop

variability for different management practices with an optical sensor? *Plant and Soil*, *9*, 29–42.

Gravois, K. A., & McNew, R. W. (1993). Genetics relationships among and selection for rice yield and yield components. *Crop Science*, *33*, 249-252.

Hansen, N. C., Schmitt, M. A., Anderson, J., & Strock, J. S. (2003). Iron Deficiency of Soybean in the Upper Midwest and Associated Soil Properties. *Agronomy Journal*, *95*, 1595-1601. https://doi.org/10.2134/agronj2003.1595

Hansen, N.C., Jolley, V. D., Naeve, S. L., & Goos, R. J. (2004). Iron deficiency of soybean in the North Central U.S. and associated soil properties. *Soil Science and Plant Nutrition*, *50*, 983–987.

Hansen, P.M., & Schjoerring, J.K. (2003). Reflectance measurement of canopy biomass and nitrogen status in wheat crops using normalized difference vegetation indices and partial least squares regression. *Remote Sensing of Environment*, *86*, 542-533.

Hassan, M. A., Yang, M., Rasheed, A., Yang, G., Reynolds, M., Xia, X., Xiao, Y., & He, Z. (2019). A rapid monitoring of NDVI across the wheat growth cycle for grain yield prediction using a multi-spectral UAV platform. *Plant Science*, *282*, 95–103.

Hassanijalilian, O. (2020). Soybean leaf chlorophyll estimation and iron deficiency field rating determination at plot and field scales through image processing and machine learning. Dissertation (PhD), North Dakota State University, Fargo, ND.

Hassanijalilian, O., Igathinathane, C., Bajwa, S., & Nowatzki, J. (2020). Rating iron deficiency in soybean using image processing and decision-tree based models. *Remote Sensing*, *12*, 4143. https://doi.org/ 10.3390/rs12244143

Hatfield, J.L., Gitelson, A.A., Schepers, J.S., & Walthall, C.L. (2008). Application of spectral remote sensing for agronomic decisions. *Agronomy Journal*, *100*, 117–131.

Heithold, J.J., Sloan, J.J., MacKown, C.T., & Cabrera, R.I., 2003. Soybean growth on calcerous soil as affected by three iron sources. *Journal of Plant* Nutrition, *26*, 935–948.

Helms T. C., Scott, R. A., Schapaugh, W. T., Goos, R. J., & Franzen, D. W. (2010). Soybean iron-deficiency chlorosis tolerance and yield decrease on calcareous soils. *Agronomy Journal*, *102*, 492–498. https://doi.org/10.2134/agronj2009.0317

Holshouser, D.L., & Whittaker, J. P. (2002). Plant population and row-spacing effects on early soybean production systems in the Mid-Atlantic USA. *Agronomy Journal*, *94*, 603–611.

Holzman, M. E., Rivas, R., & Piccolo, M. C. (2014). Estimating soil moisture and the relationship with crop yield using surface temperature and vegetation index. *International Journal of Applied Earth Observation and Geoinformation*, *28*, 181–192.

Hothorn, T., Hornik, K., & Zeileis, A. (2006). Unbiased recursive partitioning: A conditional inference framework. *Journal of Computational and Graphical Statistics*, *15(3)*, 651-674. https://doi.org/10.1198/106186006X133933.

Huete, A. R. (1988). A soil-adjusted vegetation index (SAVI). *Remote Sensing of Environment*, *25*, 295–309.

Inskeep, W. P., & Bloom, P. R. (1987). Soil chemical factors associated with soybean chlorosis in Calciaquolls of Western Minnesota. *Agronomy Journal*, *79*, 779–86.

Jannoura, R., Brinkmann, K., Uteau, D., Bruns, C., & Joergensen, R. G. (2014). Monitoring of crop biomass using true colour aerial photographs taken from a remote controlled hexacopter. *Biosystems* Engineering, *129*, 341-351.

Jeong, J., Merkovich, A., Clyne, M. & Connolly, E. L. (2017). Directing iron transport in dicots: regulation of iron acquisition and translocation. *Current Opinion in Plant Biology*, *39*, 106–113. https://doi.org/10.1016/j.pbi.2017.06.014

Ji, L., & Peters, A. J. (2007). Performance evaluation of spectral vegetation indices using a statistical sensitivity function. *Remote Sensing of Environment*, *106*, 59–65.

Jiang, D., Yang, X., Clinton, N., & Wang, N. (2004). An artificial neural network model for estimating crop yields using remotely sensed information. *International Journal of Remote Sensing*, *25(9)*, 1723–1732.

Johnson, D. M. (2014). An assessment of pre- and within-season remotely sensed variables for forecasting corn and soybean yields in the United States. *Remote Sensing of Environment*, *141*, 116–128.

Johnson, D. M. (2016). A comprehensive assessment of the correlations between field crop yields and commonly used MODIS products. *International Journal of Applied Earth Observation and Geoinformation*, *52*, 65–81.

Johnson, M. D., Hsieh, W. W., Cannon, A. J., Davidson, A., & Bédard, F. (2016). Crop Yield forecasting on the canadian prairies by remotely sensed vegetation indices and machine learning methods. *Agricultural and Forest Meteorology*, *218–219*, 74–84. https://doi.org/10.1016/j.agrformet.2015.11.003.

Kaiser D. E., Lamb, J. A., & Bloom, P. R. (2011). Managing Iron Deficiency Chlorosis in Soybean. University of Minnesota Extension.

Kaiser D. E., Lamb, J. A., Bloom, P. R., & Hernandez, J. A. (2014). Comparison of field management strategies for preventing iron deficiency chlorosis in soybean. *Agronomy Journal*, *106*, 1963–1974. https://doi.org/10.2134/agronj13.0296

Kaiser, D. E., Fernande, F., & Wilson, M. (2022). Soybean fertilizer guidelines. University of Minnesota Extension. https://extension.umn.edu/crop-specific-needs/soybean-fertilizer-guidelines (accessed on 22 Nov 2022).

Kamir, E., Waldner, F., & Hochman, Z. (2020). Estimating wheat yields in Australia using climate records, satellite image time series and machine learning methods. *ISPRS Journal of Photogrammetry and Remote Sensing*, *160*, 124–135.

Kang, M. S. (1994). Applied quantitative genetics. M. S. Kang Publisher, Baton Rouge, LA.

Kang, M. S., Miller, J. D., & Tai, P. Y. P. (1983). Genetic and phenotypic path analyses and heritability in sugarcane. *Crop Science*, *23*, 643-647.

Kanke, Y., Raun, W., Solie, J., Stone, M., & Taylor, R. (2012). Red edge as a potential index for detecting differences in plant nitrogen status in winter wheat. *Journal of Plant Nutrition, 35,* 1526–541.

Karkosh, A.E., Walker, A. K., & Simmons, J. J. (1988). Seed treatment for control of iron-deficiency chlorosis of soybean. *Crop Science, 28,* 369–370.

Kay, R., Edwards, W., & Duffy, P. A. (2020). *Farm management* (9th ed.). McGraw-Hill.

Kross, A., Znoj, E., Callegari, D., Kaur, G., Sunohara, M., Lapen, D. R., & McNairn, H. (2020). Using artificial neural networks and remotely sensed data to evaluate the relative importance of variables for prediction of within-field corn and soybean yields. *Remote Sensing, 12,* 2230. https://doi.org/ 10.3390/rs12142230

Kyaw, T., Ferguson, R. B., Adamchuk, V. I., Marx, D., Tarkalson, D., & McCallister, D. (2008). Delineating site-specific management zones for pH-induced iron chlorosis. *Precision Agriculture, 9(1-2),* 71–84.

Liesch, A. M., Ruiz Diaz, D. A., Martin, K. L., Olson, B. L., Mengel, D. B., & Roozeboom, K. L. (2011). Management strategies for increasing soybean yield on soils susceptible to iron deficiency. *Agronomy Journal, 103,* 1870–1877. https://doi.org/10.2134/agronj2011.0191

Lindsay, W.L., 1979. Chemical Equilibria in Soils. *John Willey and Sons,* New York, 129-449.

Lingenfelser, J. E., Schapaugh, W. T., Jr., Schmidt, J. P., & Higgins, J. J. (2005). Comparison of genotype and cultural practices to control iron deficiency chlorosis in soybean. *Communications in Soil Science and Plant Analysis, 36,* 1047–1062.

Liu, H., Zhu, H., & Wang, P. (2017). Quantitative modelling for leaf nitrogen content of winter wheat using UAV-based hyperspectral data. *International Journal of Remote Sensing, 38(8-10),* 2117–2134.

Loeppert, R. H., Hallmark, C. T., & Koshy, M. M. (1984). Routine procedure for rapid determination of soil carbonates. *Soil Science Society of America Journal, 48,*1030-1033.

Lucena, J. J. (2000). Effects of bicarbonate, nitrate and other environmental factors on iron deficiency chlorosis. A review, *Journal of Plant Nutrition, 23,*11-12, 1591-1606. https://doi.org/10.1080/01904160009382126

Lucena, J. J. (2003). Fe chelates for remediation of Fe chlorosis in strategy I plants. *Journal of Plant Nutrition,* 26, 1969-1984. https://doi.org/10.1081/PLN-120024257

Ma, B. L., Dwyer, L. M., Costa, C., Cober, E. R., & Morrison, M. J. (2001). Early prediction of soybean yield from canopy reflectance measurements. *Agronomy Journal, 93,* 1227-1234.

Marinković, B., Crnobarac, J., Brdar, S., Antić, B., Jaćimović, G., & Crnojević, V. (2009). Data mining approach for predictive modeling of agricultural yield data. In: Proc. First Int Workshop on Sensing Technologies in Agriculture, Forestry and Environment (BioSense09). Serbia. Novi Sad, pp. 1–5.

Markowitz, H. (1952). Portfolio selection. *Journal of* Finance, *7*, 77–91.

Marschner, H., & Römheld, V. (1994). Strategies of plants for acquisition of iron. *Plant and Soil*, *165*, 261–274.

Marschner, H., Römheld, V., & Kissel, M. (1986). Different strategies in higher plants in mobilization and uptake of iron. *Journal of Plant Nutrition*, *9*, 3–7.

Merotto, A., Bredemeier, C., Vidal, R. A., Goulart, I. C. G. R., Bortoli, E. D., & Anderson, N. L. (2012). Reflectance indices as a diagnostic tool for weed control performed by multipurpose equipment in precision agriculture. *Planta Daninha*, *30*, 437–447.

Moore, J. J., Loeppert, R. H., West, L. T., & Hallmark, C. T. (1987). A routine method for calcium carbonate equivalent of soils. *Communications in Soil Science and Plant Analysis*, *18*, 265-277.

Mourtzinis, S., Rowntree, S. C., Suhre, J. J., Weidenbenner, N. H., Wilson, E. W., Davis, V. M., Naeve, S. L., Casteel, S. N., Diers, B. W., Esker, P. D., Specht, J. E., & Conley, S. P. (2014). The use of reflectance data for in-season soybean yield prediction. *Biometry, Modeling & Statistics*, *106*, 1159-1168.

Mulla, D. J. (2013). Twenty-five years of remote sensing in precision agriculture: key advances and remaining knowledge gaps. *Biosystems Engineering*, *114*, 358–371.

Naeve, S. L. (2004). Iron Deficiency Chlorosis: Management for hot spots and whole fields. 2004 Integrated Crop Management Conference, Iowa State University.

Naeve, S. L. (2006). Iron deficiency in soybean: Soybean seeding rate and companion crop effects. *Agronomy Journal*, *98*, 1575–1581. https://doi.org/10.2134/agronj2006.0096

Naeve, S. L., & Rehm, G. W. (2006). Genotype x environment interactions within iron deficiency chlorosis-tolerant soybean genotypes. *Agronomy* Journal, *98*, 808–814. https://doi.org/10.2134/agronj2005.0281

Nguy-Robertson, A., Gitelson, A., Peng, Y., Viña, A., Arkebauer, T., & Rundquist, D. (2012). Green leaf area index estimation in maize and soybean: combining vegetation indices to achieve maximal sensitivity. *Agronomy Journal*, *104*, 1336–1347.

Niebur, W. S., & Fehr, W. R. (1981). Agronomic evaluation of soybean genotypes resistant to iron deficiency chlorosis. *Crop Science*, *21*, 551–554. https://doi.org/10.2135/cropsci1981.0011183X002100040019x

O'Rourke, J. A., Charlson, D. V., Gonzalez, D. O., Vodkin, L. O., & Graham, M. A. (2007). Microarray analysis of iron deficiency chlorosis in near-isogenic soybean lines. *BMC Genomics*, 8: 1–13. https://doi.org/10.1186/1471-2164-8-476

Peiffer, G. A., King, K. E., Severin, A. J., May, G. D., & Cianzio, S. R. (2012). Identification of candidate genes underlying an iron efficiency quantitative trait locus in soybean. *Plant Physiology*, *158*, 1745–1754. https://doi.org/10.1104/pp.111.189860

Penas, E.J., Wiese, R.A., Elmore, R.W., Hergert, G.W., & Moomaw, R.S. (1990). Soybean chlorosis studies on high pH bottomland soils. Univ. Nebraska Inst. Agric. Nat. Resour. Bull. 312; University of Nebraska: Lincoln, NE.

Pinheiro J., D. Bates, S. DebRoy, & D. Sarkar, R Core Team. (2020). nlme: Linear and Nonlinear Mixed Effects Models. R package version 3.1-152, <URL: https://CRAN.R-project.org/package=nlme>

Pix4D. (2022). Processing options default templates. - Support. Available online at: https://support.pix4d.com/hc/en-us/articles/205319155-Processing-Options-Default-Templates (accessed December 21, 2022).

Portz, G., Molin, J. P., & Jasper, J. (2012). Active crop sensor to detect variability of nitrogen supply and biomass on sugarcane fields. *Precision Agriculture*, *13*, 33–44.

R Core Team. R: A Language and Environment for STATISTICAL computing; R Foundation for Statistical Computing: Vienna, Austria, 2020. Available online: https://www.R-project.org/ (accessed on 16 Nov 2022).

Rasmussen, J., Georgios, N., Jon, N., Svensgaard, J., Poulsen, R. N., & Christensen, S. (2015). Are vegetation indices derived from consumer-grade cameras mounted on UAVs sufficiently reliable for assessing experimental plots? *European Journal of Agronomy*, *29*, 75-92.

Rasmussen, J., Nielsen, J., Garcia-Ruiz, F., Christensen, S., & Streibig, J. C. (2013). Potential uses of small unmanned aircraft systems (UAS) in weed research. *Weed Research*, *53*, 242–248.

Reed, D., Lyons, C., & Eachern, G. Mc. (1988). Field evaluation of inorganic and chelated iron fertilizers as foliar sprays and soil application. *Journal of Plant Nutrition*, *11*, 1369–1378.

Rehman, T. H., Reis, B., Froes, A., Akbar, N., & Linquist, B. A. (2019). Use of normalized difference vegetation index to assess N status and predict grain yield in rice. *Agronomy Journal*, *111*, 2889–2898.

Rengel, Z., & Marschner, P. (2005). Nutrient availability and management in the rhizosphere: Exploiting genotypic differences. *New Phytologist*, *168*, 305–312.

Rod, K. S., Bradley, C. A., Shockley, J., & Knott, C. A. (2021). Double-crop soybean management practices for high yield and profitability. *Crop, Forage & Turfgrass Management*, *7:e20119*. https://doi.org/10.1002/cft2.20119

Rod, K. S., Shockley, J., & Knott, C. A. (2021). Seed yield, seed quality, profitability, and risk analysis among double crop soybean maturity groups and seeding rates. *Agronomy Journal*, *113*(2), 1792–1802. https://doi.org/10.1002/agj2.20626

Rodriguez-Lucena, P., Hernandez-Apaolaza, L., & Lucena, J. J. (2010). Comparison of iron chelates and complexes supplied as foliar sprays and in nutrient solution to correct iron chlorosis of soybean. *Journal of Plant Nutrition and Soil Science*, *173*, 120–126. https://doi.org/10. 1002/jpln.200800256

Rogovska, N., & Blackmer, A. M. (2009). Remote sensing of soybean canopy as a tool to map high pH, calcareous soils at field scale. *Precision Agriculture*, *10(2)*, 175.

Rondeaux, G., Steven, M., & Baret, F. (1996). Optimization of soil-adjusted vegetation indices. *Remote Sensing of Environment*, 55, 95–107.

Rosseel, Y. (2012). lavaan: An R Package for Structural Equation Modeling. *Journal of Statistical Software*, *48(2)*, 1–36. https://doi.org/10.18637/jss.v048.i02.

Rouse, J. W., Haas, R. H., Schell, J. A., & Deering, D. W. (1974). Monitoring vegetation systems in the Great Plains with ERTS. Third ERTS-1 Symposium. pp. 309–317. Washington, DC: NASA.

Russell, L. (2020). Emmeans: Estimated Marginal Means, Aka Least-Squares Means. R Package Version 1.5.2-1. Available online: https://CRAN.R-project.org/package=emmeans (accessed on 16 Nov 2022).

Samborski, S. M., Tremblay, N., & Fallon, E. (2009). Strategies to make use of plant sensors-based diagnostic information for nitrogen recommendations. *Agronomy Journal*, *101(4)*, 800–816. https://doi.org/10.2134/ agronj2008.0162Rx

Santana, D. C., Cunha, M. P. de O., Santos, R. G. dos, Cotrim, M. F., Teodoro, L. P. R., Junior, C. A. Silva da, Baio, F. H. R., & Teodoro, P. E. (2022). High-throughput phenotyping allows
the selection of soybean genotypes for earliness and high grain yield. *Plant Methods*, 18:13. https://doi.org/10.1186/s13007-022-00848-4

Schenkeveld, W. D. C., Dijcker, R., Reichwein, A. M., Temminghoff, E. J. M., & Van Riemsdijk, W. H. (2008). The effectiveness of soil-applied FeEDDHA treatments in preventing iron chlorosis in soybean as a function of the *o,o*-FeEDDHA content. *Plant Soil*, *303*, 161–176. https://doi.org/10.1007/s11104-007-9496-x

Schepers, J. S. (2008). Active sensor tidbits. Available at http://www.isafarmnet.com/2008OFNConf/Nitrogen/Nitrogen_Sensors_Handout.pdf (verified 21 Dec. 2022).

Schwalbert, R. A., Amado, T., Corassa, G., Pott, L. P., Prasad, P. V., & Ciampitti, I. A. (2020). Satellite-based soybean yield forecast: integrating machine learning and weather data for improving crop yield prediction in southern Brazil. *Agricultural and Forest Meteorology*, *284*, 107886.

Sharma, L. K., Bu, H., Denton, A., & Franzen, D. W. (2015). Active-optical sensors using red NDVI compared to red edge NDVI for prediction of corn grain yield in North Dakota, U.S.A. *Sensors*, *15*, 27832–27853.

Shen, Y., Mercatoris, B., Cao, Z. Kwan, P., Guo, L., Yao, H., & Cheng, Q. (2022). Improving Wheat Yield Prediction Accuracy Using LSTM-RF Framework Based on UAV Thermal Infrared and Multispectral Imagery. *Agriculture*, *12*, 892. https://doi.org/10.3390/agriculture12060892

Shukla, S., Singh, K., & Pushpendra. (1999). Correlation and path coefficient analysis of yield and its components in soybean (*Glycine max* L. Merrill.). *Soybean Genetics Newsletter*, *25*, 67–70.

Silva J., & R. Uchida. (2000). Essential nutrients for plant growth: nutrient functions and deficiency symptoms. *Plant Nutrient Management in Hawaii's Soils, Approaches for Tropical and Subtropical Agriculture*, 31–55.

Stevens, A. W., & Bradley, W. B. (2020). Crop rotation and risk management in Mississippi delta agriculture. *2020 Agricultural & Applied Economics Association Annual Meeting.*

Stucki, J. W. (1988). Structural iron in smectites: in *Iron in Soils and Clay Minerals*, J. W. Stucki, B. A. Goodman, & U. Schwertmann, eds. D. Reidel, Dordrecht, The Netherlands, 625–675.

Thenkabail, P. S., Smith, R. B., & Pauw De, E. (2000). Hyperspectral vegetation indices and their relationships with agricultural crop characteristics. *Remote Sensing of Environment*, *71*, 158-182.

Tigner, R. (2018). *Partial budgeting: A tool to analyze farm business changes* (Vol. C1-50). Ames, IA: Iowa State University Extension and Outreach.

Tucker, C. J. (1979). Red and photographic infrared linear combinations for monitoring vegetation. *Remote Sensing of Environment*, *8*, 127–150.

Uno, Y., Prasher, S. O., Lacroix, R., Goel, P. K., Karimi, Y., Viau, A., & Patel, R.M. (2005). Artificial neural networks to predict corn yield from Compact Airborne Spectrographic Imager data. *Computers and Electronics in Agriculture*, *47(2)*, 149–161.

USDA-ERS (2021). United States Department of Agriculture (USDA), Economic Research Service. Recent costs and returns:soybeans. https://www.ers.usda.gov/data-products/commodity-costs-and-returns/commodity-costs-and-returns/#Recent%20Cost%20and%20Returns (accessed on 16 Nov 2022).

USDA-NASS (2022). United States Department of Agriculture (USDA), National Agricultural Statistics Service. Quick Stats: Soybeans – Price Received in Minnesota. https://quickstats.nass.usda.gov/#5CFDF6CC-25FB-3160-A921-F01A4F8DE743

Van Niel, T. G., & McVicar, T. R. (2004). Current and potential uses of optical remote sensing in rice-based irrigation systems: a review. *Australian Journal of Agricultural Research*, *55(2)*, 155–185.

Veenadhari, S., Misra, B., & Singh, C. (2014). In: 2014 International Conference on Computer Communication and Informatics. IEEE, pp. 1–5.

Wang, D., & Anderson, D. W. (1998). Direct measurement of organic carbon content in soils by the Leco CR-12 carbon analyzer. *Communications in Soil Science and Plant Analysis*, *29*, 15–21. doi:10.1080/00103629809369925

Warncke, D., & Brown, J. R. (1998). Potassium and other basic cations. In: J.R. Brown, editor, Recommended chemical soil test procedures for the North Central Region. North Central Regional Research Publication 221 (rev.). *University of Missouri*, Columbia. p. 31–33.

Watson, M. E., & Brown, J. R. (1998). pH and lime requirement. In: J.R. Brown, editor, Recommended chemical soil test procedures for the North Central Region. North Central Regional Research Publication 221 (rev.). *University of Missouri*, Columbia. p. 13–16.

Weisberg, S. (2014). Variable selection. In: Balding, D. J., Cressie, N. A. C., Fitzmaurice, G. M., Goldstein, H., Johnstone, I. M., Molenberghs, G., Scott, D. W.,

Smith, A. F. M., Tsay, R. S., & Weisberg, S. editors, Applied Linear Regression, 4th Edition. John Wiley & Sons, Minneapolis, MN. p. 234-251

West, G. (2006). An introduction to modern portfolio theory: Markowitz, CAP-M, APT and Black-Litterman. *Financial Modelling Agency*.

Wiersma, J. V. (2005). High rates of Fe-EDDHA and seed iron concentration suggest partial solutions to iron deficiency in soybean. *Agronomy Journal*, *97*, 924–934. https://doi.org/10.2134/agronj2004.0309

Wiersma, J. V. (2007). Iron acquisition of three soybean varieties grown at five seeding densities and five rates of Fe-EDDHA. *Agronomy Journal*, *99*, 1018–1028. https://doi.org/10.2134/agronj2006.0271

Wiersma, J. V. (2010). Nitrate-induced iron deficiency in soybean varieties with varying iron-stress responses. *Agronomy Journal*, *102*, 1738-1744. https://doi.org/ 10.2134/agronj2010.0240

Wittwer, S. H., Jyung, W. H., Yamada, Y., Bukovac, M. J., Kannan, R. De S., Rasmussen, H. P., & Haile-Mariam, S. N. (1965). Pathways and mechanisms for foliar absorption of mineral nutrients as revealed by radioisotopes. p. 387– 403. *In* Isotopes and radiation in soil plant nutrition studies. Proc. Symp. IAEA (Vienna), Ankara, Turkey. 28–2 July. Int. Atomic Energy Agency, Vienna, Austria.

Whitney, D. A. (1998a). Micronutrients: Zinc, iron, manganese, and copper. In: J.R. Brown, editor, Recommended chemical soil test procedures for the North Central Region. North Central Regional Research Publication. 221 (rev.). *University of Missouri*, Columbia. p. 41–44.

Whitney, D. A. (1998b). Soil salinity. In: J.R. Brown, editor, Recommended chemical soil test procedures for the North Central Region. North Central Regional Research Publication 221 (rev.). *University of Missouri*, Columbia. p. 59–60.

Yadavalli, V., Neelam, S., Rao, A. S. V. C., Reddy, A. R., & Subramanyam, R. (2012). Differential degradation of photosystem I subunits under iron deficiency in rice. *Journal of Plant Physiology*, *169(8)*, 753–759.

Zepp, S., Jilge, M., Metz-Marconcini, A., & Heiden, U. (2021). The influence of vegetation index thresholding on EO-based assessments of exposed soil masks in Germany between 1984 and 2019. *ISPRS Journal of Photogrammetry and Remote Sensing*, *178*, 366-381.

Zhao, Y., Potgieter, A. B., Zhang, M., Wu, B., & Hammer, G. L. (2020). Predicting wheat yield at the field scale by combining high-resolution sentinel-2 satellite imagery and crop modelling. *Remote Sensing*, *12*, 1024.